Supplementary data

Design, synthesis and pharmacological evaluation of novel 2-chloro-3-(1H-benzo[d]imidazol-2-yl)quinoline derivatives as antitumor agents: *in vitro* and *in vivo* antitumor activity, cell cycle arrest and apoptotic response

Wen-Bin Kuang[a,b], Ri-Zhen Huang[c], Yi-Lin Fang[b], Gui-Bin Liang[b], Chen- Hui Yang[a], Xian-Li Ma[a,*], Ye Zhang[a,b,d*]

[a] *School of Pharmacy, Guilin Medical University, Guilin 541004, China.*

[b] *State Key Laboratory for the Chemistry and Molecular Engineering of Medicinal Resources (Ministry of Education of China), School of Chemistry and Pharmaceutical Sciences of Guangxi Normal University, Guilin 541004, PR China*

[c] *Department of Pharmaceutical Engineering, School of Chemistry and Chemical Engineering, Southeast University, Nanjing 211189, PR China*

[d] *Department of Chemistry & Pharmaceutical Science, Guilin Normal College, Xinyi Road 15, Guangxi 541001, PR China*

* Corresponding author. School of Pharmacy, Guilin Medical University, North Ring 2rd Road 109, Guilin 541004, PR China.

Tel./Fax.: +86-773-5895132.

E-mail addresses: zhangye81@126.com (Y. Zhang); mxl78@glmc.edu.cn (Xian-Li Ma)

Part 1. Experimental methods

1.1. *In vitro* Antiproliferation Activity

HepG2 human liver hepatocellular carcinoma cells, SK-OV-3 human ovarian carcinoma cells, NCI-H460 human large cell lung carcinoma cell, HL 7702 human liver hepatocellular cells and BEL-7404 human liver cancer cell were all obtained from the Institute of Biochemistry and Cell Biology, China Academy of Sciences. They were cultured in a humidified, 5% CO_2 atmosphere at 37°C and maintained in monolayer culture in Dulbecco's modified Eagle's medium (DMEM) supplemented with 10% fetal bovine serum (FBS), 100 mg/mL streptomycin and 100 mg/mL penicillin. Chemosensitivity was assessed with a 3-(4,5-dimethylthiazol-2-yl)-2,5-diphenyl tetrazolium bromide (MTT) assay. Briefly, exponentially growing cells were seeded into 96-well plates and treated with the indicated concentrations of compounds (**3**) for 48 h, and then 10 mL of MTT (10 mg/mL) was added. After incubation for 4 h at 37°C, the purple formazan crystals (a reduced form of MTT) generated in viable cells were dissolved by adding 100 μL DMSO to each well. The plates were swirled gently for 10 min to dissolve the precipitate, and quantified by measuring the optical density of the plates at 490 nm using a plate reader (TECAN infinite M1000). Each concentration was repeated in three wells and the same experimental conditions were maintained for all testing procedures. The MTT assays were repeated three times for each cell line.

1.2. Hoechst 333258 Staining

Cells grown on a sterile cover slips in six-well tissue culture plates were treated with test compounds for the indicated time. The culture medium containing the compounds was removed, and the cells were fixed in 4% paraformaldehyde for 10 min. After washing twice with phosphate buffered saline (PBS), the cells were stained with 0.5 mL of Hoechst 33258 (Beyotime) for 5 min and again washed twice with PBS. Nuclear staining was observed with a Nikon ECLIPSETE2000-S fluorescence microscope at 350 nm excitation and 460 nm emission wavelengths.

1.3. AO/EB Staining

Cells were seeded at a concentration of 5×10^4 cell/mL in a volume of 2 mL on sterile cover slips in six-well tissue culture plates. Following incubation, the medium was removed and replaced with fresh medium plus 10% FBS and supplemented with compound**s**. After treatment, cover slips with cell monolayers were inverted on a glass slide with 20 μL of AO/EB stain (100 mg/mL). Fluorescence was read on a Nikon ECLIPSETE2000-S fluorescence microscope (OLYMPUS Co., Japan).

1.4. Apoptosis Analysis

Apoptosis was assayed by annexin V-FITC and PI. Cells were seeded at 2×10^6/well in 10% FBS–DMEM into six-well plates and treated with test compounds for 24 h. The cells

were then washed twice with cold PBS and resuspended in 1×binding buffer (0.1 M pH 7.4 Hepes/NaOH, 1.4 M NaCl, 25 mM $CaCl_2$) at a concentration of 1×10^6 cells/mL. A 100 µL volume of the solution (1×10^5 cells) was transferred to a 5 mL culture tube; 5 µL of FITC Annexin V (BD, Pharmingen) and 5 µL PI were added to each tube. The cell suspension was gently vortexed and incubated for 30 minutes at room temperature (25°C) in the dark, and then 200 µl PBS was added to each tube. The apoptosis assay was carried out by flow cytometry (FACSVerse, BD, USA) at 488 nm excitation. The lower left quadrant included viable cells (annexin V^-PI^-); lower right quadrant included early apoptotic cells (annexin V^+/PI^-); upper right quadrant included late apoptotic cells (annexin V^+/PI^+); and the upper left quadrant included necrotic cells (annexin V^-/PI^+). The percentage of PI^+ and/or Annexin V-$FITC^+$ cells inside the quadrants was reported.

1.5. Cell Cycle Analysis

Cell cultures were treated with the indicated concentrations of compounds and after 48 h incubation, the cells were washed twice with ice-cold PBS, fixed and permeabilized with ice-cold 70% ethanol at −20°C overnight. The cells were treated with 100 µg/mL RNase A at 37°C for 30 min after washing with ice-cold PBS, and finally stained with 1 mg/mL PI in the dark at 4°C for 30 min. Cell cycle analysis was performed by flow cytometry (FACSVerse, BD, USA) at an excitation of 488 nm and an emission of 620 nm.

1.6. ROS Assay

Tumour cells were seeded into six-well plates, and following treatment, were incubated with 10 mM DCFH-DA (Beyotime, Haimen, China) dissolved in cell-free medium for 30 min at 37°C and in the dark. They were then washed three times with PBS. Cellular fluorescence was measured with a Nikon ECLIPSETE2000-S fluorescence microscope at 485 nm excitation and 538 nm emission.

1.7. Calcium Analysis

To monitor the effect of compounds on calcium release, tumour cells were seeded into six-well plates, and loaded with 5 mM of the membrane-permeable calcium indicator Fluo-3 acetoxymethyl ester (Beyotime, Haimen, China) in PBS buffer for 40 min at 37°C. After loading with the Fluo-3 dye, cells were washed with PBS and suspended in Ca-free PBS containing 5 mM EGTA. Fluo-3 was excited by argon laser light at 488 nm; fluorescence was measured at 515 nm, and quantified with a Nikon ECLIPSETE2000-S fluorescence microscope.

1.8. Western Blot Assay

Tumour cells were collected after treatment with compound (10 µM) for 12 h and then lysed in ice-cold lysis buffer (1% sodium dodecyl sulfate in 25 mM pH 7.5 Tris–HCl, 4 mM EDTA, 100 mM NaCl, 1 mM phenylmethylsulfonyl fluoride, 10 mg/mL leupeptin and 10 mg/mL soybean trypsin inhibitor). Whole-cell lysates were centrifuged at 12,000×*g* for

5 min. Thereafter, the protein concentration was determined with a bicinchoninic acid protein assay kit (Beyotime Co, China). An aliquot of cell lysate (40–50 μg) was fractionated by SDS-PAGE on 12% polyacrylamide gels for 2 h and transferred to polyvinylidene difluoride membranes. After blocking with 5% non-fat dry milk in PBS-t for 1 h at room temperature, the membranes were incubated with β-actin, cytochrome c, caspase-9, caspase-3, Bax or Bcl-2 antibodies (Bioworld Technology Inc, USA) overnight at 4^{o}C, washed with tris-buffered saline and Tween 20, and then incubated with horseradish peroxidase-conjugated secondary antibodies for 1 h at room temperature. Proteins were detected by electrochemiluminescence, Thermo Fisher Scientific, USA) and analysed by Image J software.

1.9. Animal Used

Kunming (KM) mice (both male and female, 20−22 g, 5−6 week old) and BALB/c nude mice (male, 20−22 g, 6−7 weeks old) were supplied by Beijing HFK Bioscience Co., Ltd. (Beijing, China) and used for the human large cell lung cancer cell (NCI-460) and the human hepatocarcinoma (BEL-7402) xenograft. The in vivo antitumor studies were carried out at the Institute of Radiation Medicine, Chinese Academy of Medical Sciences (Tian Jin, China). The handling of animals and the experimental design were approved by the Ethnics Committee and Animal Care Committee of the Institute. Nude mice were housed in an individual ventilated caging system (IVC Rack) with sterile environment with conditions at a constant photoperiod (12 h light/12 h dark at 25−28 °C and 45−65% relative humidity).

1.10. Acute Toxicity Studies

Six-week old male and female KM mice (weight 20−22 g) were randomly divided into 3 groups (n = 6) and used to study the in vivo safety of 6. The highest solubility of 6 in solvent (5% v/v DMSO/saline) was used as the solution, and a good practice volume (0.6 mL/20 g) by intraperitoneal injection was used. Two groups of KM mice were treated with 6 at a dose of 16 mg/kg twice a day (bid) or once a day (qd) for 10 day, respectively, and one group received the same volume of solvent and used as the control. The signs of toxicity were observed, and body weight was recorded daily.

1.11. The *in Vivo* Antitumor Activity

Nude mice received subcutaneous injection of 5×10^7 tumor cells in the right flank. When the xenograft tumor growth to the volume about 1000 mm^3, the mice were killed and the tumor tissue were cut into small pieces at about 1.5 mm^3 and then transplanted into the right flank of male nude mice. When the average tumors reached the volumes of 100−150 mm^3, the mice were randomly divided into solvent control and treatment groups (n = 7/group). Compouds at doses of 50 and 25 mg/kg (5% v/v DMSO/saline) were given twice a day for 13 or 20 days (ip). Cisplatin was given to mice by ip administration at a dosage of 2 mg/kg/per 2 days and used as a positive reference for comparison, 5-FU was given to mice by ip administration at a dosage of 25 mg/kg/per 2 days, while control mice received the solvent (5% v/v DMSO/saline). Tumor size and body weight were

monitored every 2 days. On day 14 or 21, the animals were sacrificed for humane reasons, and the tumors were weighted and recorded. The tumor volumes were determined every 2 days by measuring length (l) and width (w) and calculating with the formula of V = lw2/2 as described elsewhere. Meanwhile, body weight of mice was measured and taken as a parameter of systemic toxicity. All mice were sacrificed on day 14 or 21 after treatment (grouping), and tumor weight was recorded. The rate of tumor growth was calculated using a formula of (1 − TWt/TWc) × 100, where TWt is the tumor weight of compounds treated mice and the TWc is the tumor weight of vehicle-treated animals.

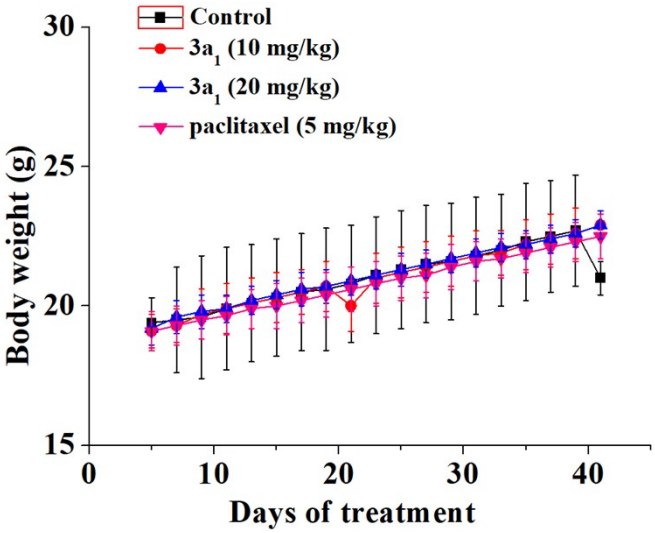

Fig. S1-1. Body weight change of the mice treated with **5a$_3$**.

1.12. Statistical Analysis

Data are expressed as mean ± SD for three different determinations. Statistical significance was analyzed by one-way ANOVA. Mean separations were performed using the least significant difference method. P<0.05was defined as statistically significant.

Part 2. ^{1}H NMR, ^{13}CNMR and HRMS of compounds 3a$_1$-3d$_6$

3a$_1$: Yield, 64.8%; ^{1}H NMR (500 MHz, DMSO-d$_6$) δ 12.68 (s, 1H, NH), 8.97 (s, 1H, HC=C), 8.20 (s, 1H, H-Ar), 8.06 (s, 1H, H-Ar), 7.92 (d, J = 8.4 Hz, 1H, H-Ar), 7.75 (d, J = 8.1 Hz, 1H, H-Ar), 7.45 (s, 2H, H-Ar), 2.36 (s, 6H, -CH$_3$); ^{13}C NMR (126 MHz, DMSO-d$_6$) δ 147.68, 147.21, 141.58, 132.36, 129.01, 128.44, 128.16, 126.87, 125.14, 20.50; ESI-HRMS, calculated *m/z* for $C_{18}H_{14}ClN_3$ $[M+H]^+$: 308.0955, found: 308.0972.

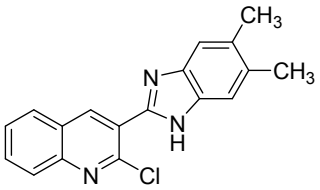

Fig. S2-1. Chemical structure of compound 3a$_1$

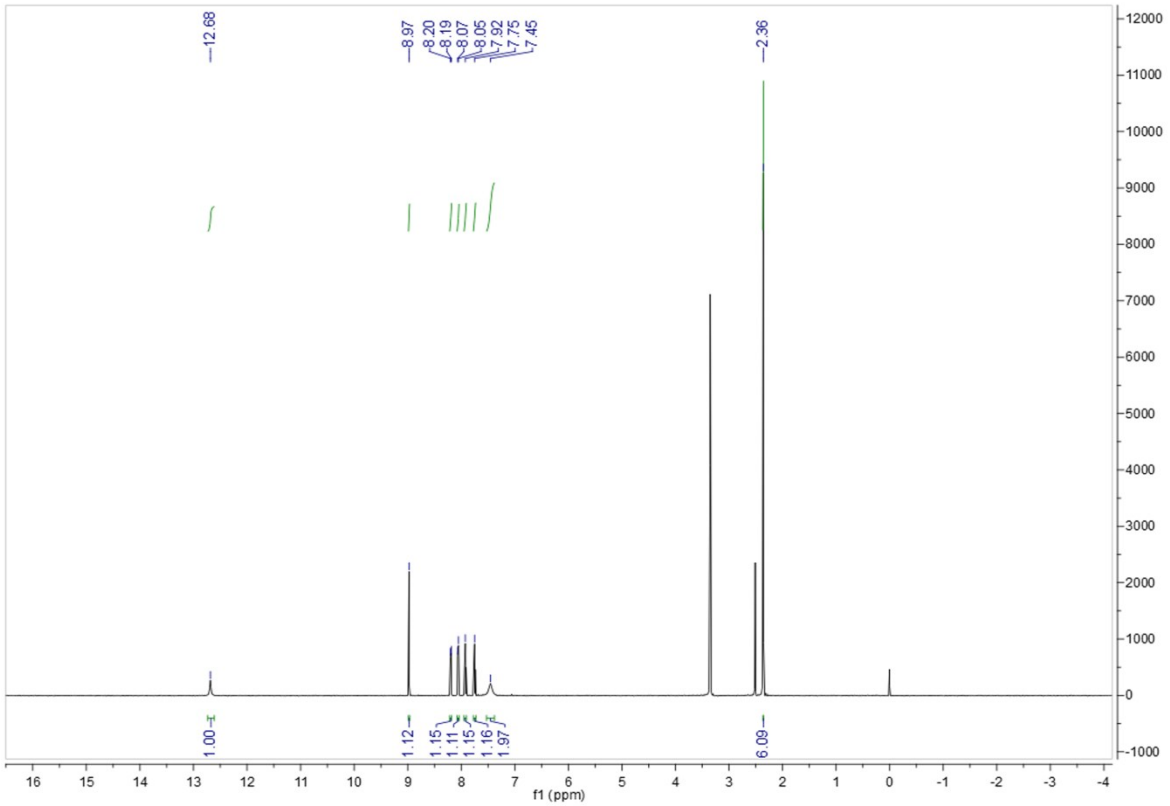

Fig. S2-2. ^{1}H NMR of compound 3a$_1$

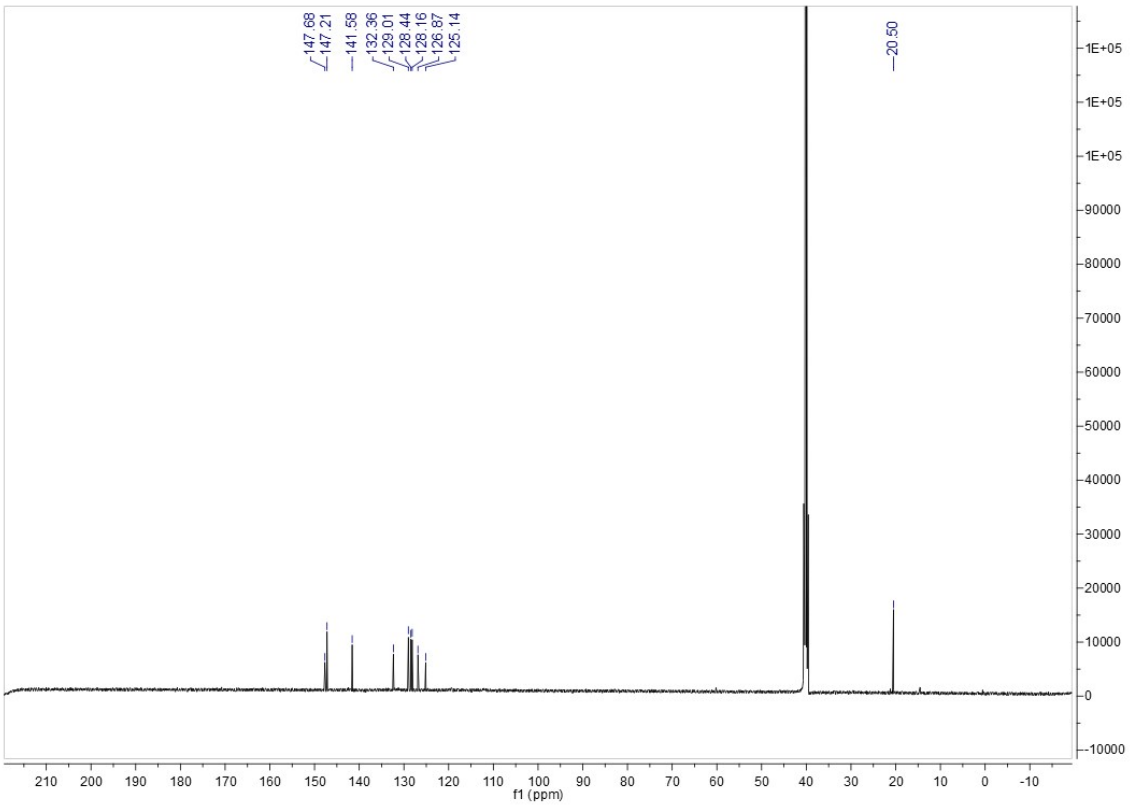

Fig. S2-3. ^{13}C NMR of compound 3a$_1$

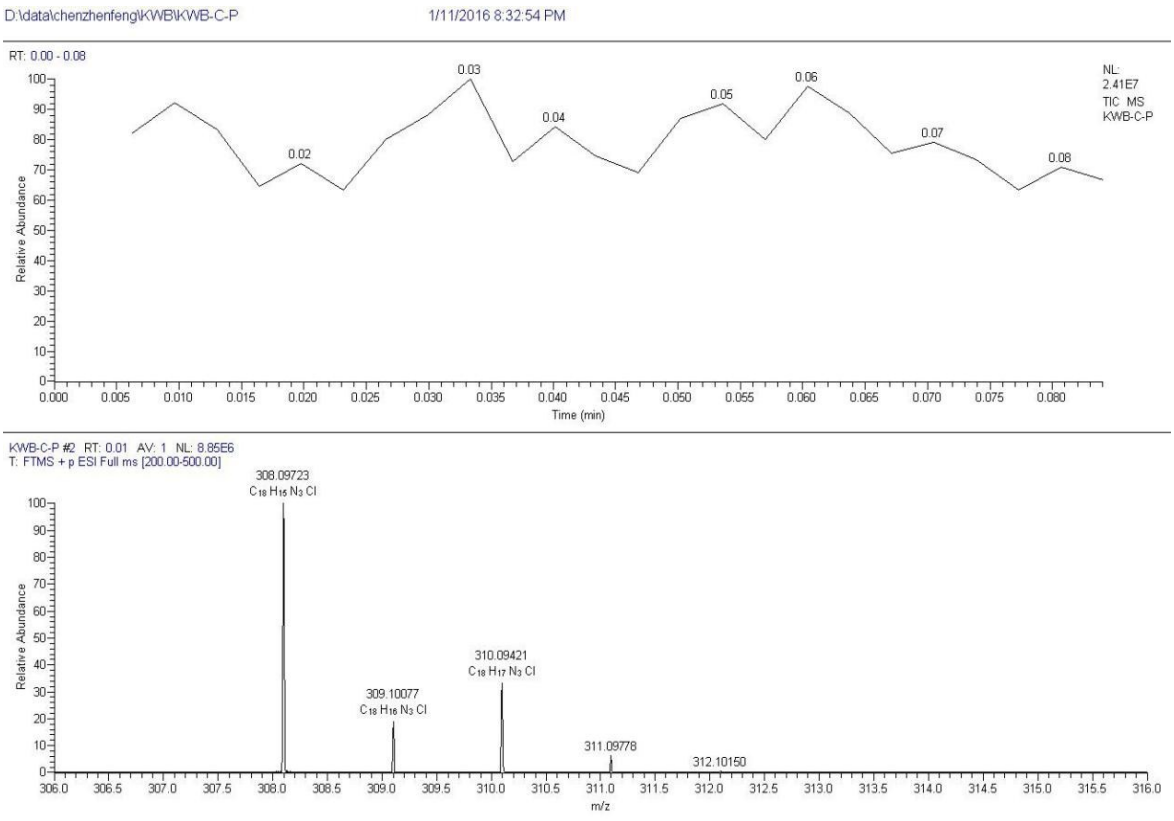

Fig. S2-4. ESI-HRMS of compound 3a$_1$

3a$_2$: Yield, 57.3%; ^{1}H NMR (500 MHz, DMSO-d$_6$) δ 13.08 (s, 1H, NH), 9.01 (s, 1H, HC=C), 8.20 (d, J = 7.6 Hz, 1H, H-Ar), 8.07 (d, J = 8.5 Hz, 1H, H-Ar), 7.95 (d, J = 8.4 Hz, 1H, H-Ar), 7.77 (s, 1H, H-Ar), 7.70 (s, 1H, H-Ar), 7.50 (s, 1H, H-Ar), 7.16 (d, J = 8.5 Hz, 1H, H-Ar); ^{13}C NMR (126 MHz, DMSO-d$_6$) δ 147.48, 147.36, 141.99, 132.66, 129.11, 128.58, 128.19, 126.79, 124.57; ESI-HRMS, calculated *m/z* for $C_{16}H_9ClFN_3$ $[M+H]^+$: 298.0547, found: 298.0543.

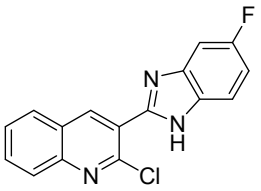

Fig. S2-5. Chemical structure of compound 3a$_2$

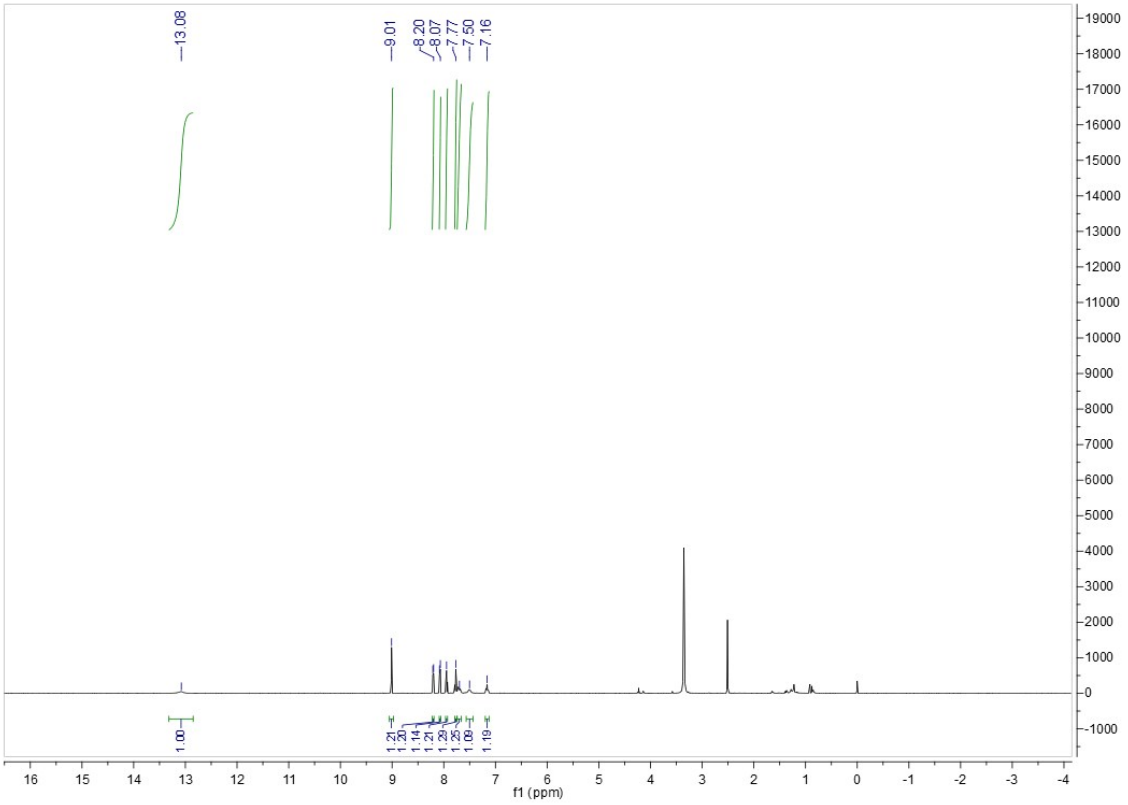

Fig. S2-6. 1H NMR of compound 3a$_2$

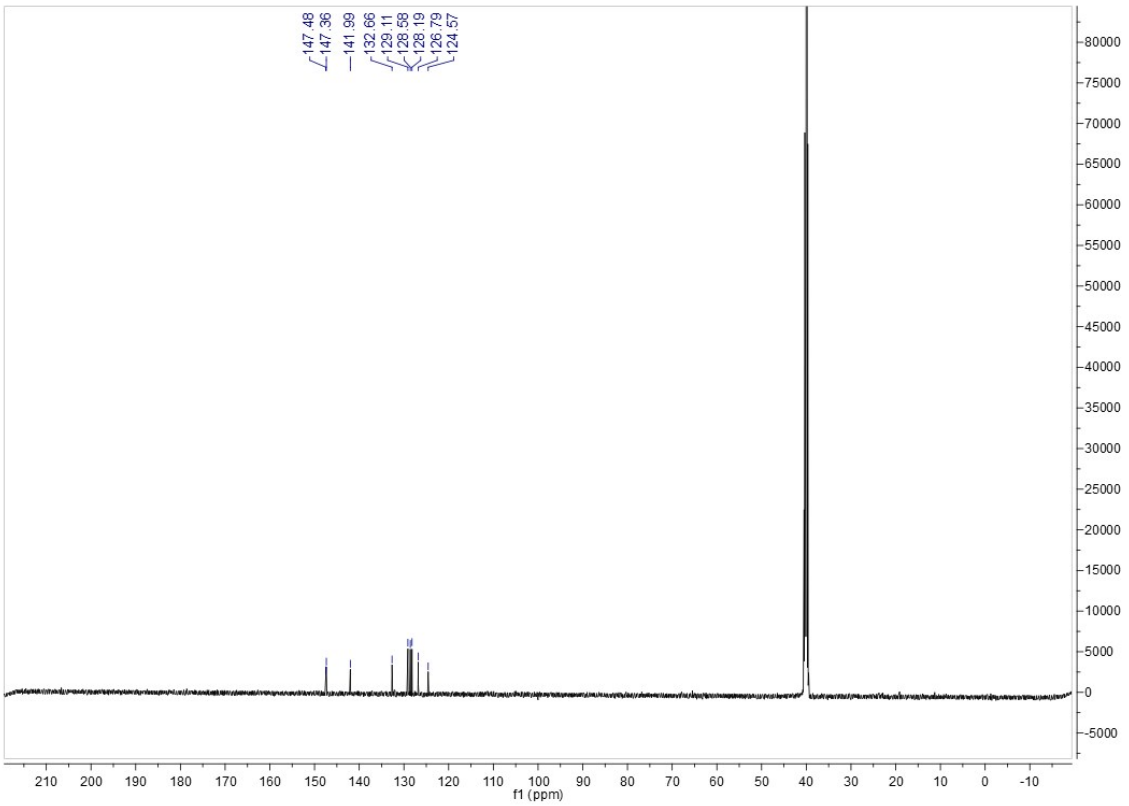

Fig. S2-7. ^{13}C NMR of compound 3a$_2$

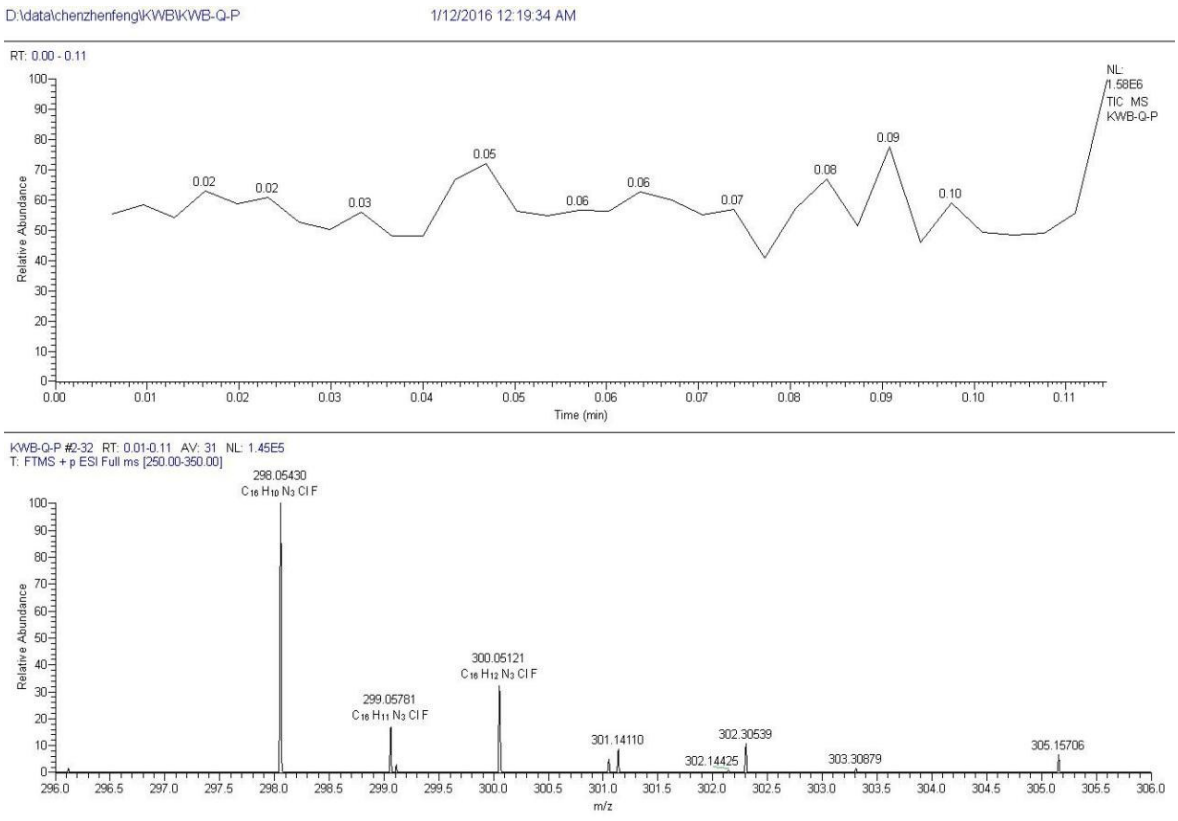

Fig. S2-8. ESI-HRMS of compound 3a$_2$

3a$_3$: Yield, 56.9%; ^{1}H NMR (400 MHz, DMSO-d$_6$) δ 13.17 (s, 1H, NH), 9.03 (s, 1H, HC=C), 8.21 (d, J = 8.0 Hz, 1H, H-Ar), 8.08 (d, J = 8.4 Hz, 1H, H-Ar), 7.95 (s, 1H, H-Ar), 7.77 (s, 2H, H-Ar), 7.70 (s, 1H, H-Ar), 7.32 (s, 1H, H-Ar); ^{13}C NMR (101 MHz, DMSO-d$_6$) δ 147.43, 147.40, 142.16, 132.75, 129.15, 128.61, 128.20, 126.77, 124.41; ESI-HRMS, calculated *m/z* for $C_{16}H_9Cl_2N_3$ [M−H]$^-$: 312.0096, found: 312.0098.

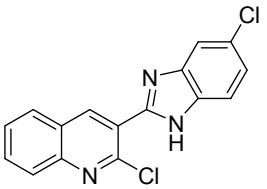

Fig. S2-9. Chemical structure of compound 3a$_3$

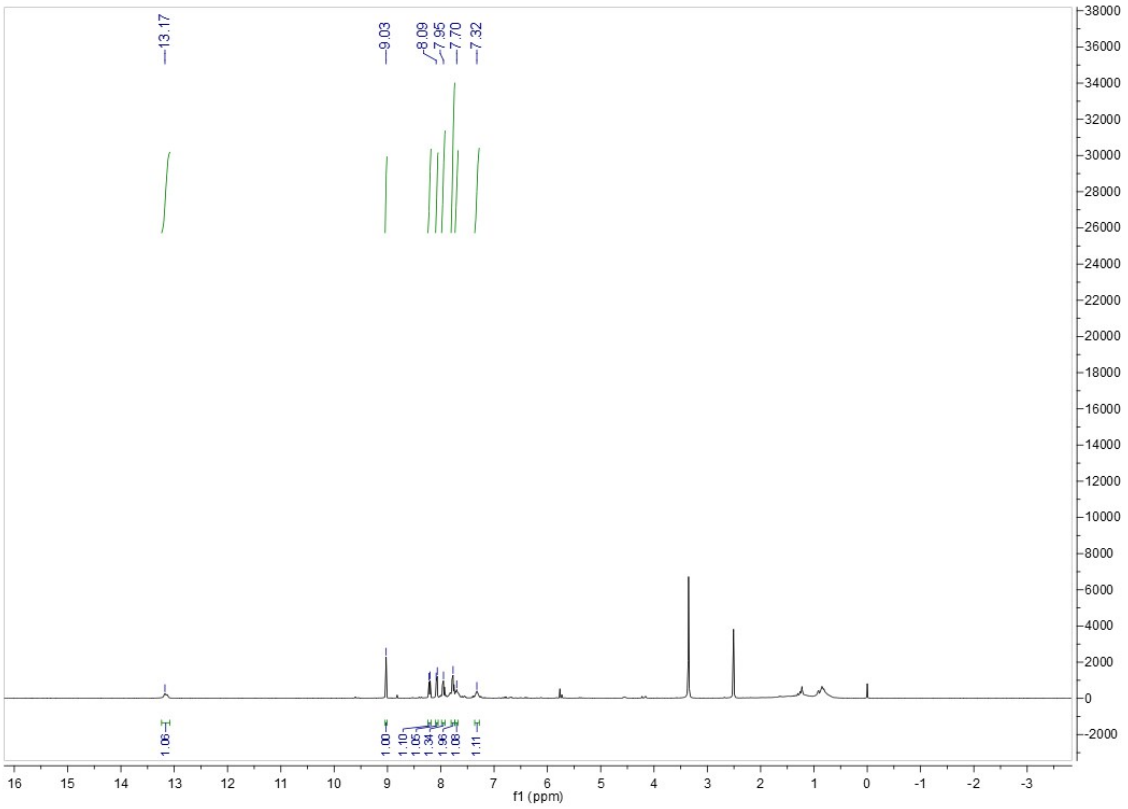

Fig. S2-10. 1H NMR of compound 3a$_3$

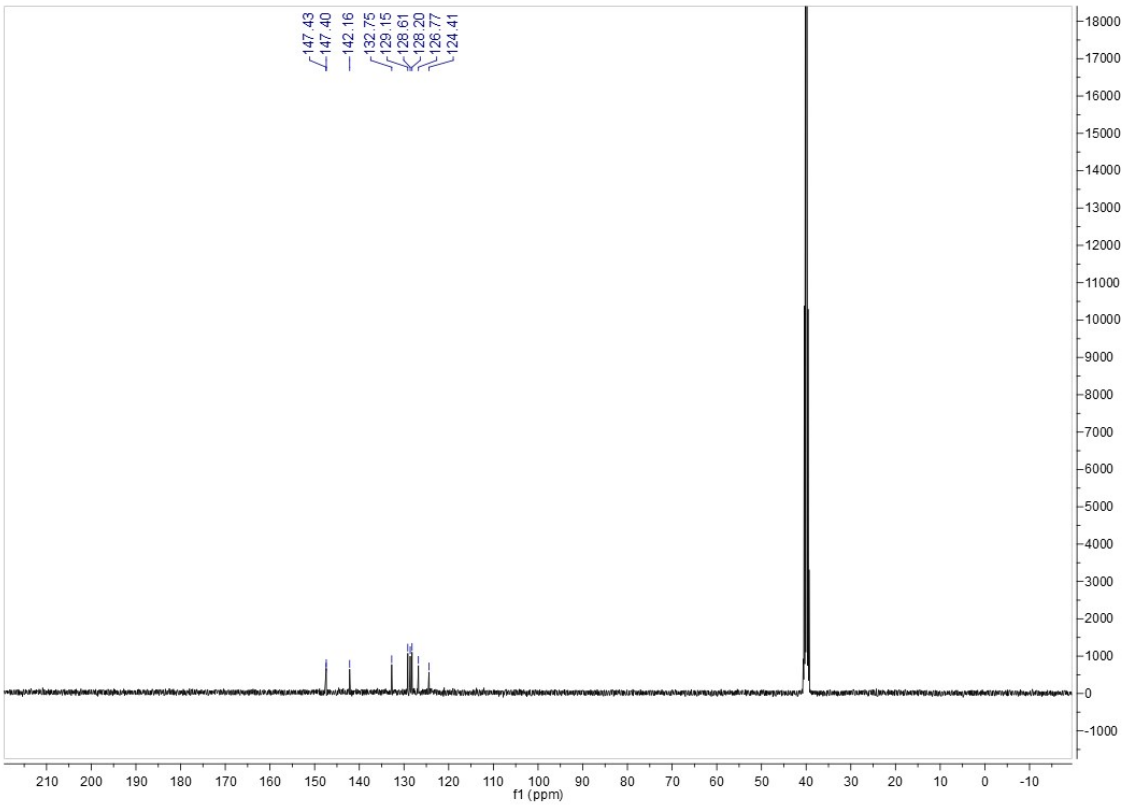

Fig. S2-11. ^{13}C NMR of compound $3a_3$

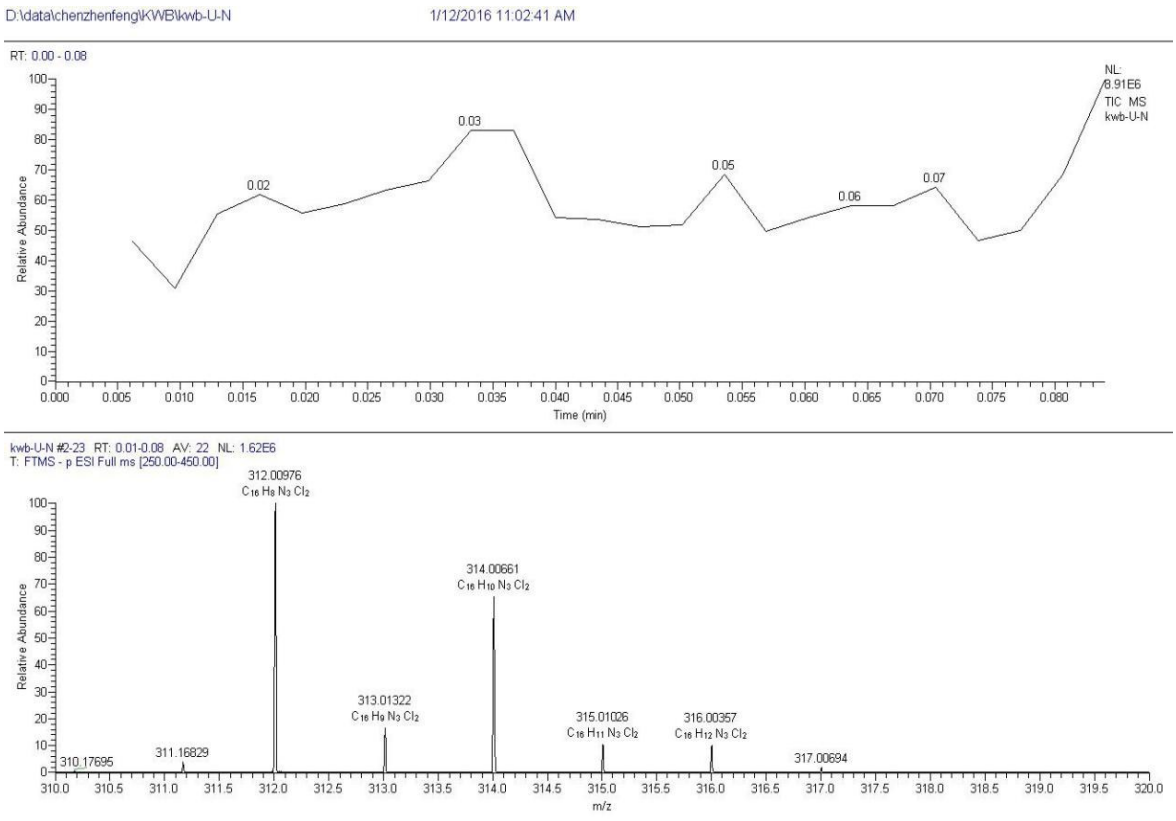

Fig. S2-12. ESI-HRMS of compound $3a_3$

3a$_4$: Yield 55.4%, ^{1}H NMR (500 MHz, DMSO-d$_6$) δ 13.18 (s, 1H), 9.02 (s, 1H), 8.21 (d, J = 7.7 Hz, 1H), 8.07 (d, J = 7.9 Hz, 1H), 7.95 (s, 1H), 7.91 (s, 1H), 7.77 (s, 1H), 7.67 (s, 1H), 7.44 (s, 1H); ^{13}C NMR (126 MHz, DMSO-d$_6$) δ 147.44, 147.42, 142.14, 132.75, 129.14, 128.61, 128.20, 126.76, 124.38. ESI-HRMS *m/z* Calc for $C_{16}H_9BrClN_3$ $[M-H]^-$:355.9590; found: 355.9625.

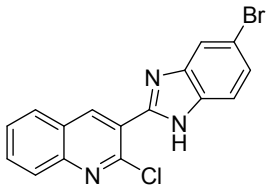

Fig. S2-13. Chemical structure of compound 3a$_4$

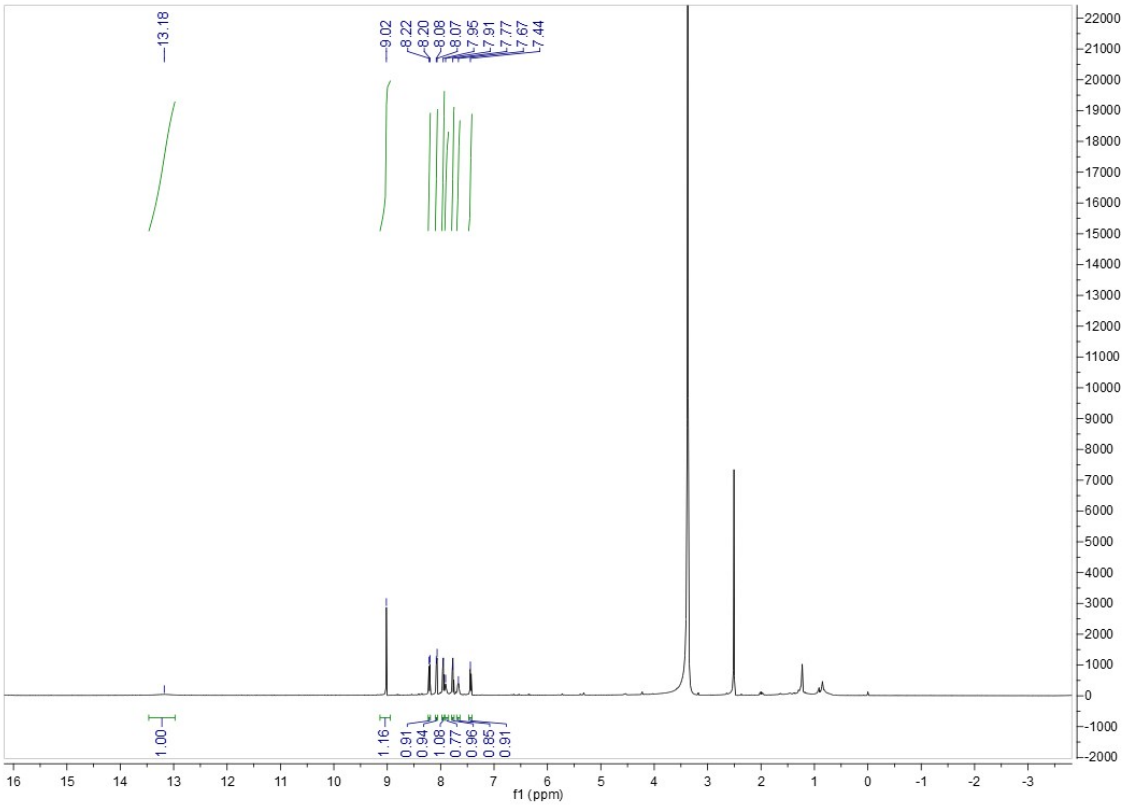

Fig. S2-14. ^{1}H NMR of compound 3a$_4$

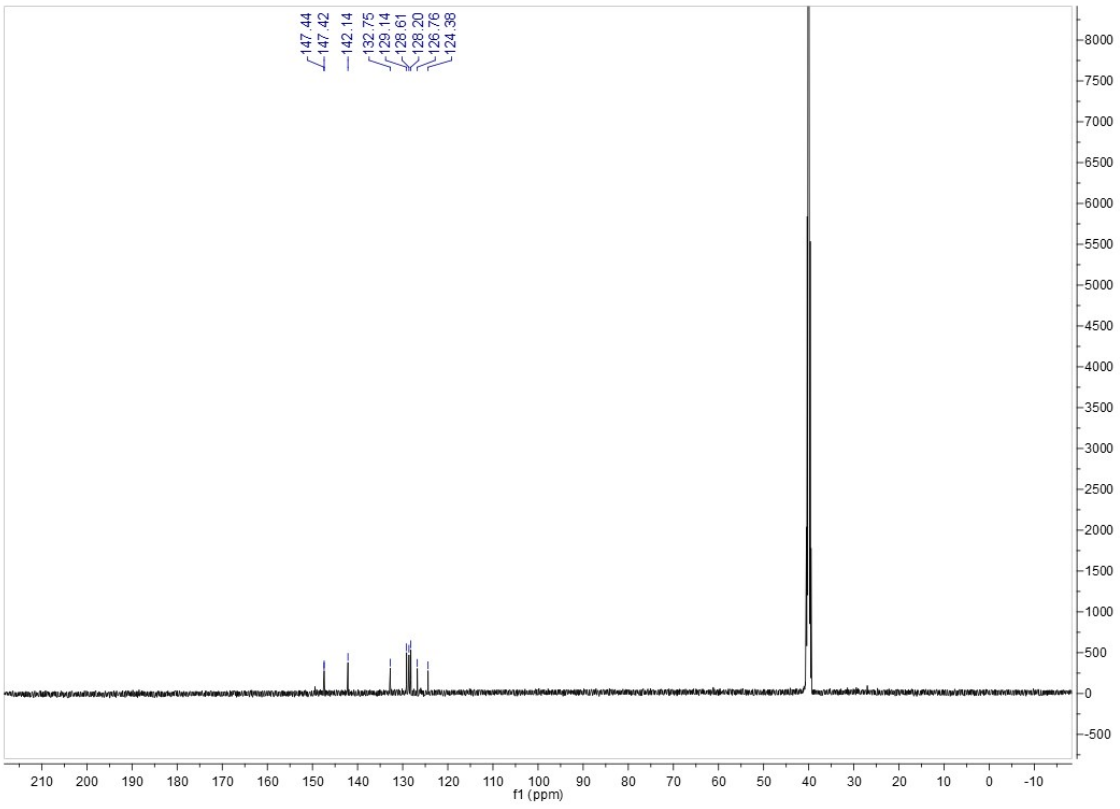

Fig. S2-15. ^{13}C NMR of compound $3a_4$

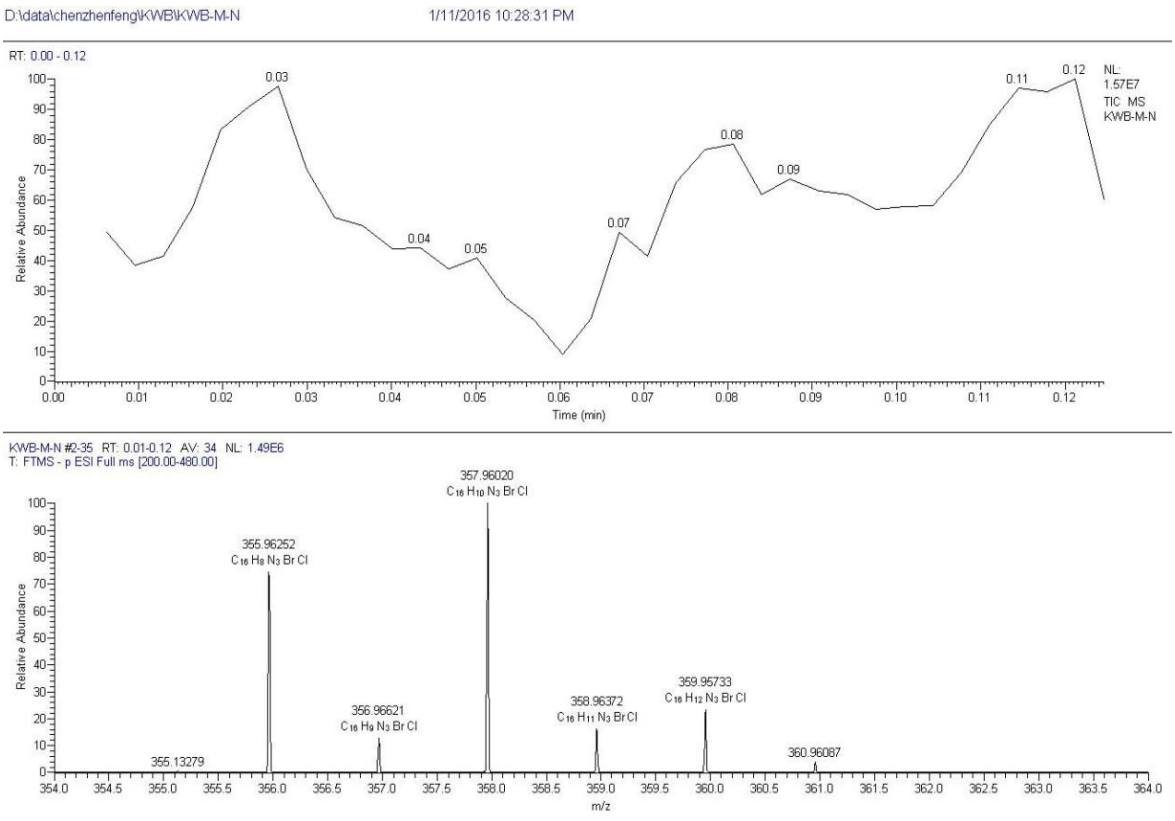

Fig. S2-16. ESI-HRMS of compound $3a_4$

3a$_5$: Yield, 55.1%; ^{1}H NMR (400 MHz, DMSO-d$_6$) δ 13.30 (s, 1H, NH), 9.03 (s, 1H, HC=C), 8.21 (d, J = 7.6 Hz, 1H, H-Ar), 8.08 (d, J = 8.4 Hz, 2H, H-Ar), 7.96 (s, 2H, H-Ar), 7.77 (s, 1H, H-Ar); ^{13}C NMR (101 MHz, DMSO-d$_6$) δ 150.82, 147.47, 147.32, 142.32, 132.89, 129.19, 128.67, 128.21, 126.71, 124.03; ESI-HRMS, calculated *m/z* for $C_{16}H_8Cl_3N_3$ $[M-H]^-$: 345.9706, found: 345.9747.

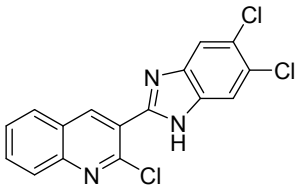

Fig. S2-17. Chemical structure of compound 3a$_5$

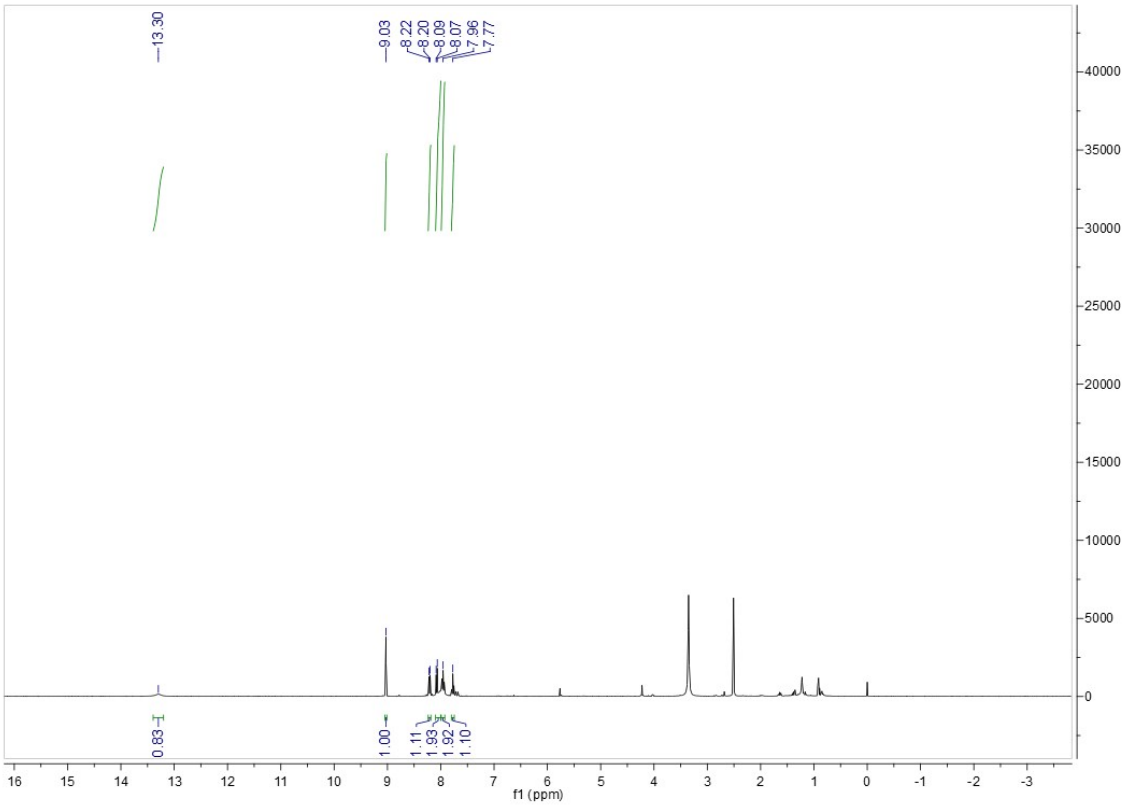

Fig. S2-18. ^{1}H NMR of compound 3a$_5$

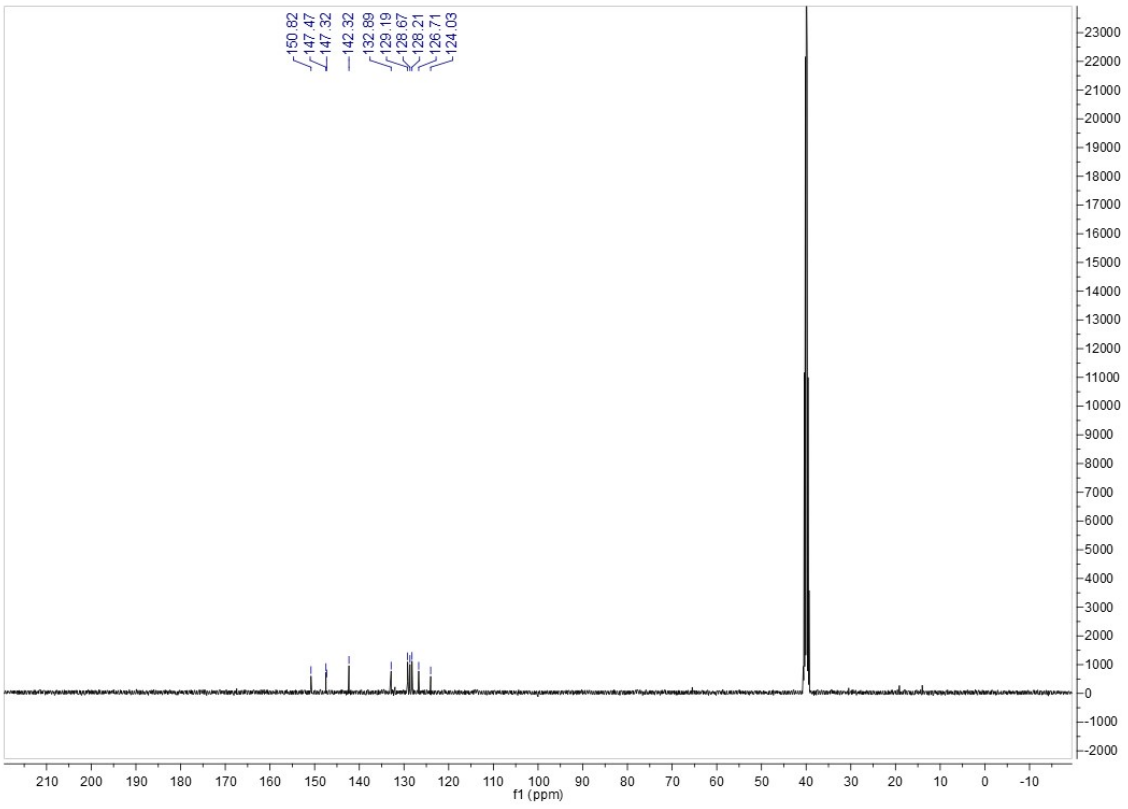

Fig. S2-19. ^{13}C NMR of compound $3a_5$

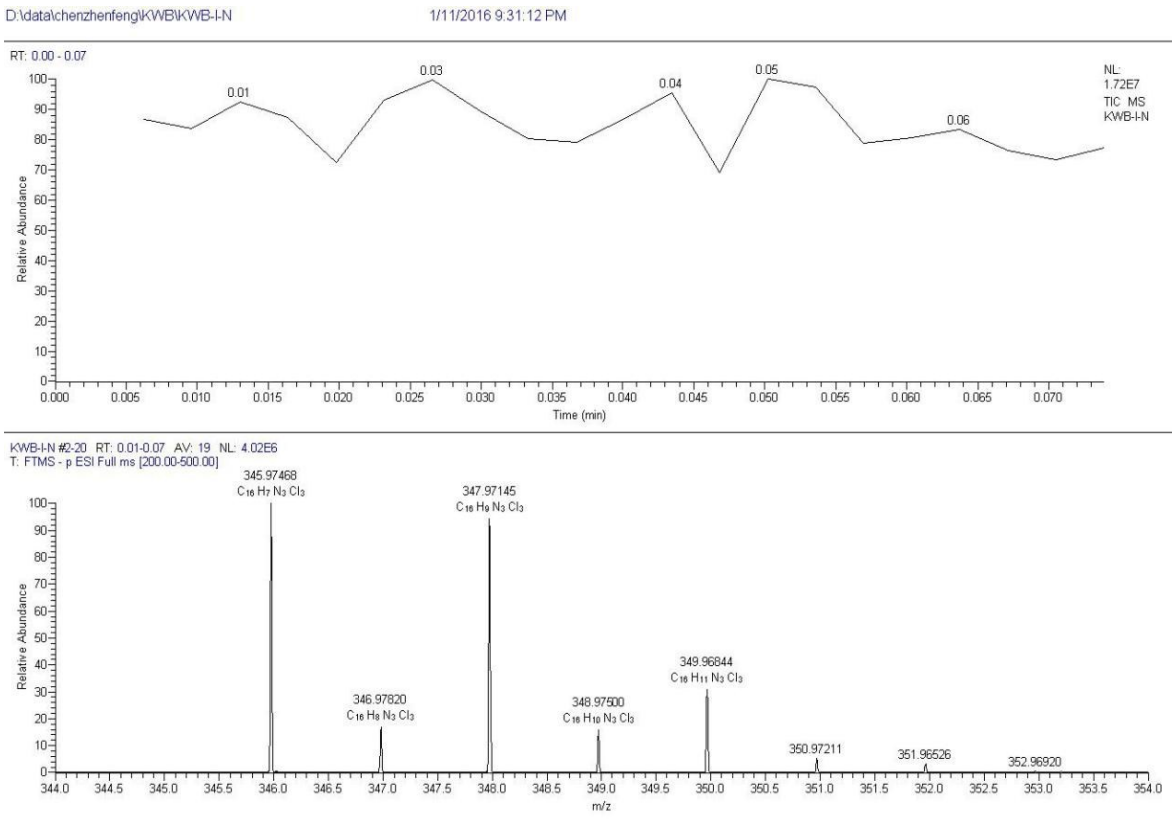

Fig. S2-20. ESI-HRMS of compound $3a_5$

3a$_6$: Yield, 63.2%; ^{1}H NMR (400 MHz, DMSO-d$_6$) δ 12.97 (s, 1H, NH), 9.01 (s, 1H, HC=C), 8.21 (d, J = 7.4 Hz, 1H, H-Ar), 8.08 (d, J = 8.0 Hz, 1H, H-Ar), 7.94 (s, 1H, H-Ar), 7.77 (s, 2H, H-Ar), 7.67 (s, 1H, H-Ar), 7.30 (s, 2H, H-Ar); ^{13}C NMR (101 MHz, DMSO-d$_6$) δ 148.21, 147.63, 147.31, 141.97, 132.58, 129.09, 128.55, 128.19, 126.83, 124.92; ESI-HRMS, calculated *m/z* for $C_{16}H_{10}ClN_3$ $[M-H]^-$: 278.0485, found: 278.0489.

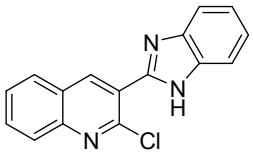

Fig. S2-21. Chemical structure of compound 3a$_6$

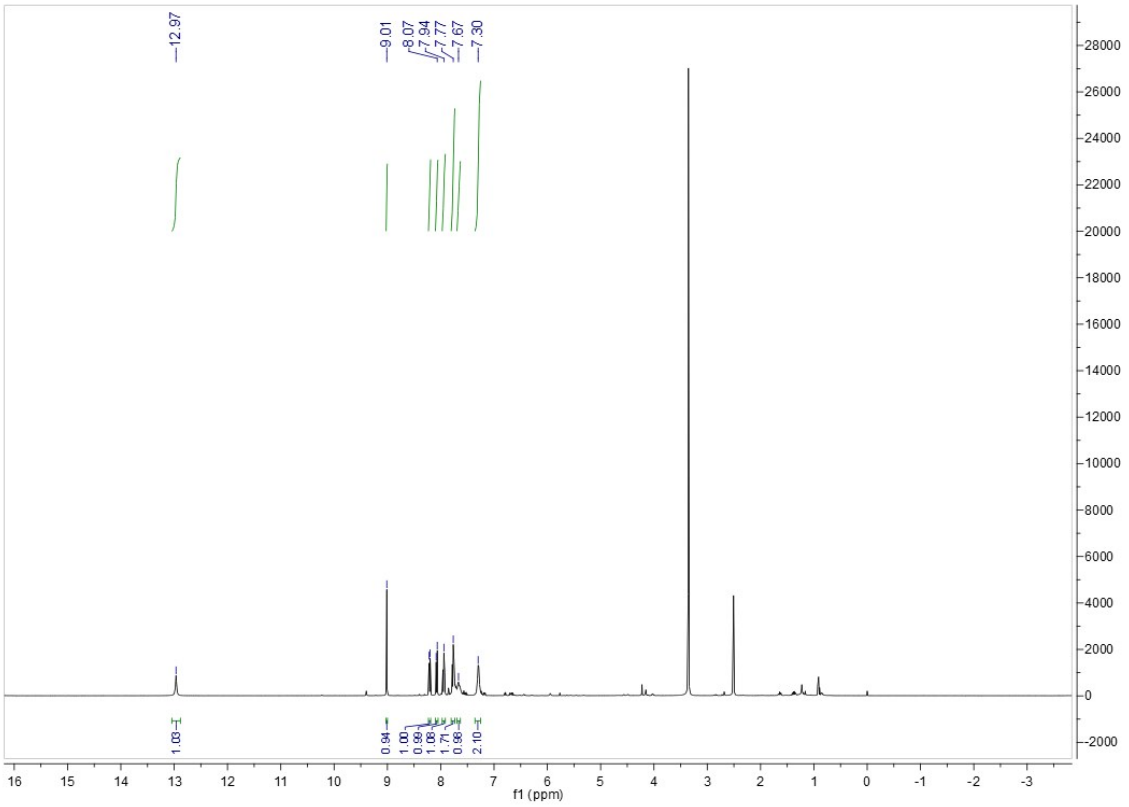

Fig. S2-22. ^{1}H NMR of compound 3a$_6$

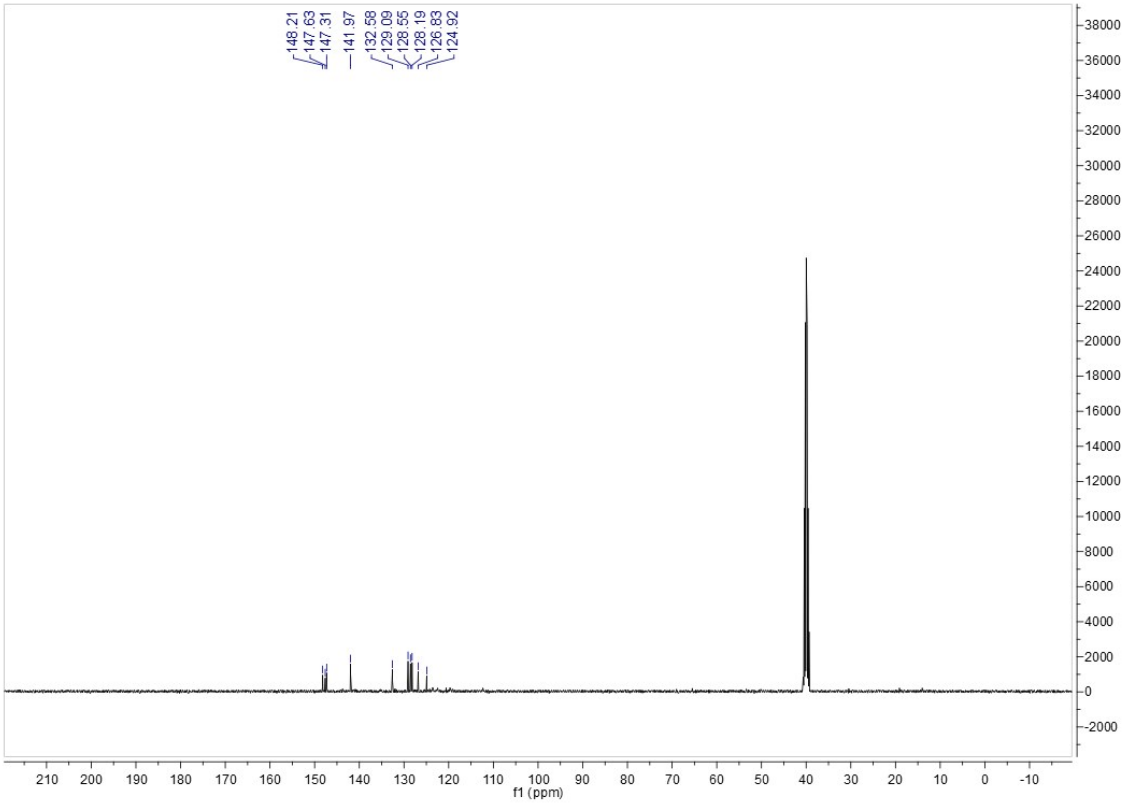

Fig. S2-23. ^{13}C NMR of compound 3a$_6$

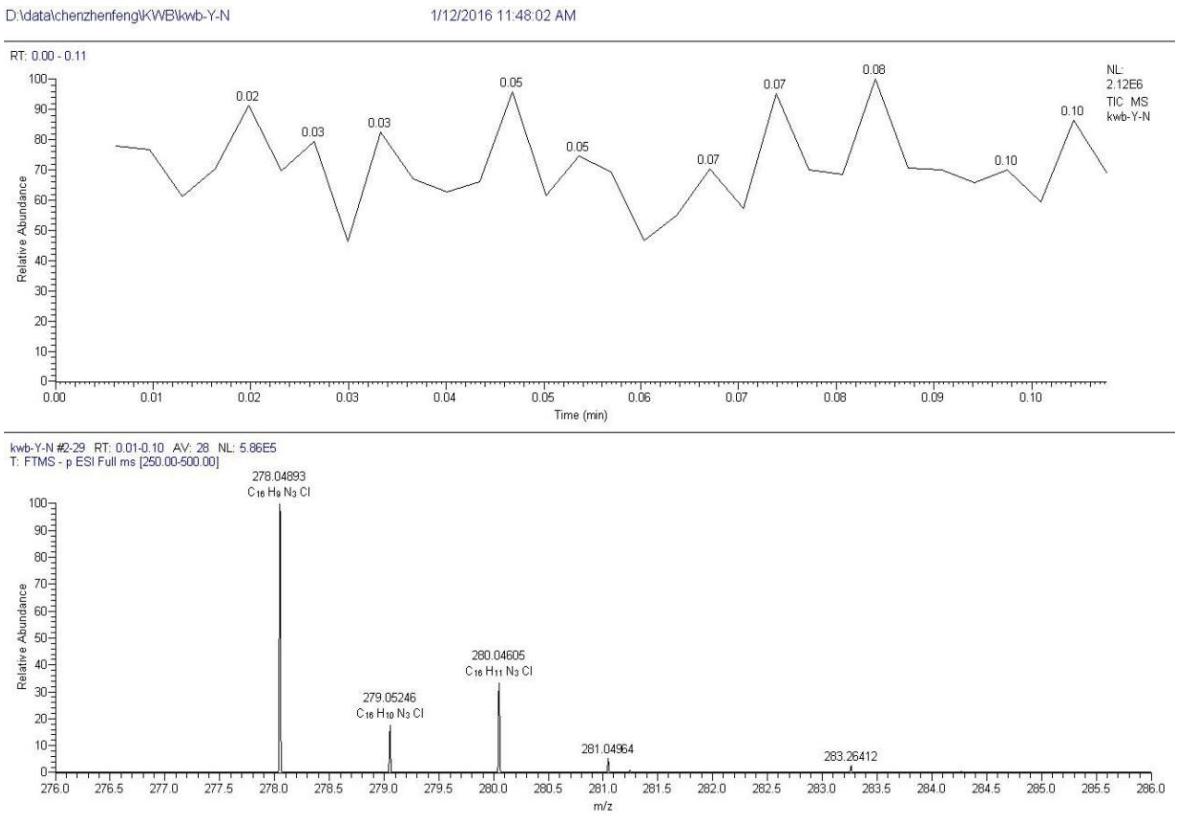

Fig. S2-24. ESI-HRMS of compound 3a$_6$

3b$_1$: Yield, 58.1%; ^{1}H NMR (500 MHz, DMSO-d$_6$) δ 12.66 (s, 1H, NH), 8.84 (s, 1H, HC=C), 7.94 (s, 2H, H-Ar), 7.84 (s, 1H, H-Ar), 7.46 (s, 2H, H-Ar), 2.54 (s, 3H, -CH$_3$), 2.36 (s, 6H, -CH$_3$); ^{13}C NMR (126 MHz, DMSO-d$_6$) δ 147.32, 146.78, 145.84, 140.84, 138.21, 134.49, 127.90, 127.54, 126.88, 125.09, 21.62, 20.50; ESI-HRMS, calculated *m/z* for $C_{19}H_{16}ClN_3$ $[M+H]^+$: 322.1111, found: 322.1129.

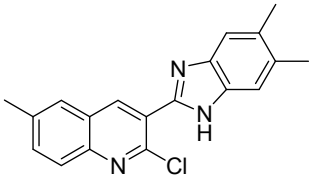

Fig. S2-25. Chemical structure of compound 3b$_1$

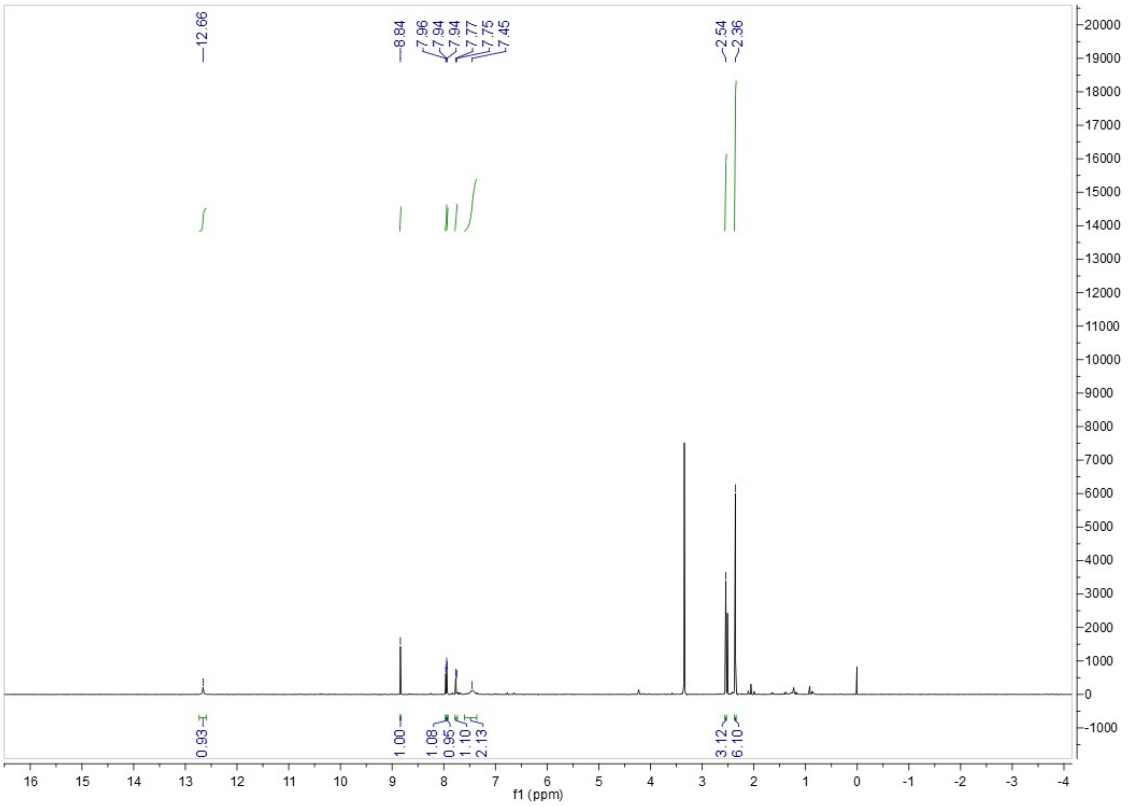

Fig. S2-26. ^{1}H NMR of compound 3b$_1$

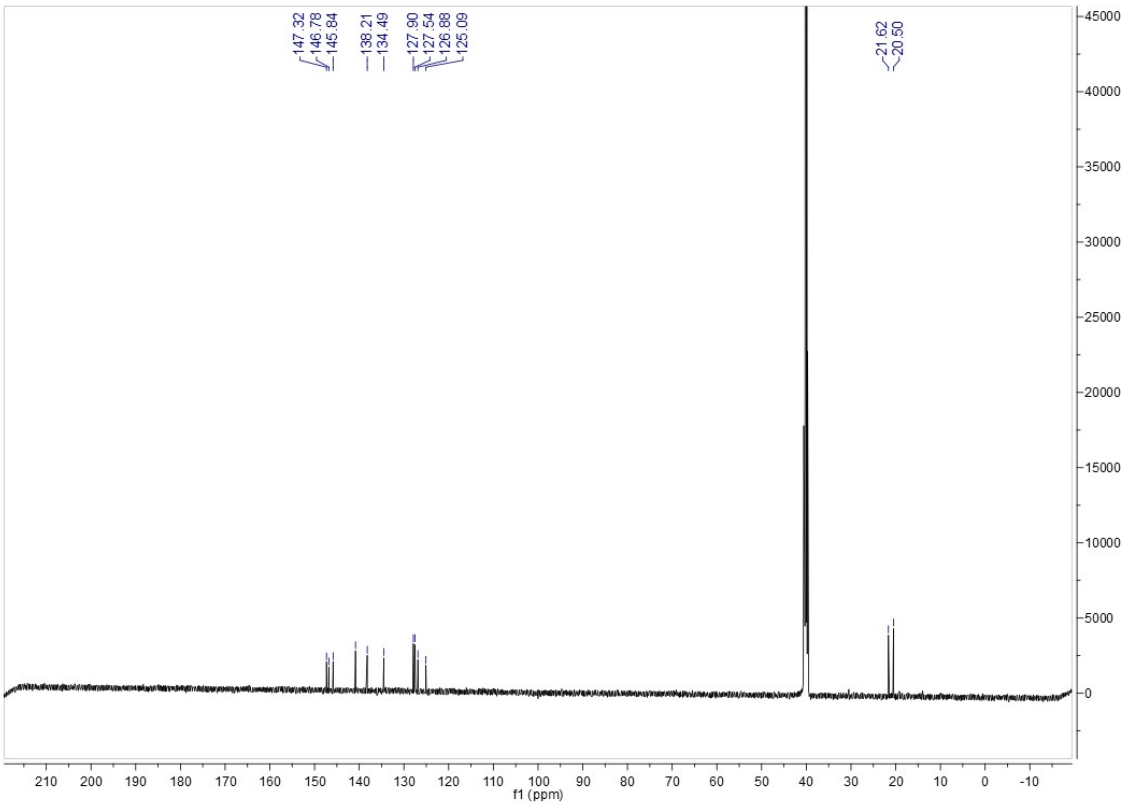

Fig. S2-27. ^{13}C NMR of compound 3b$_1$

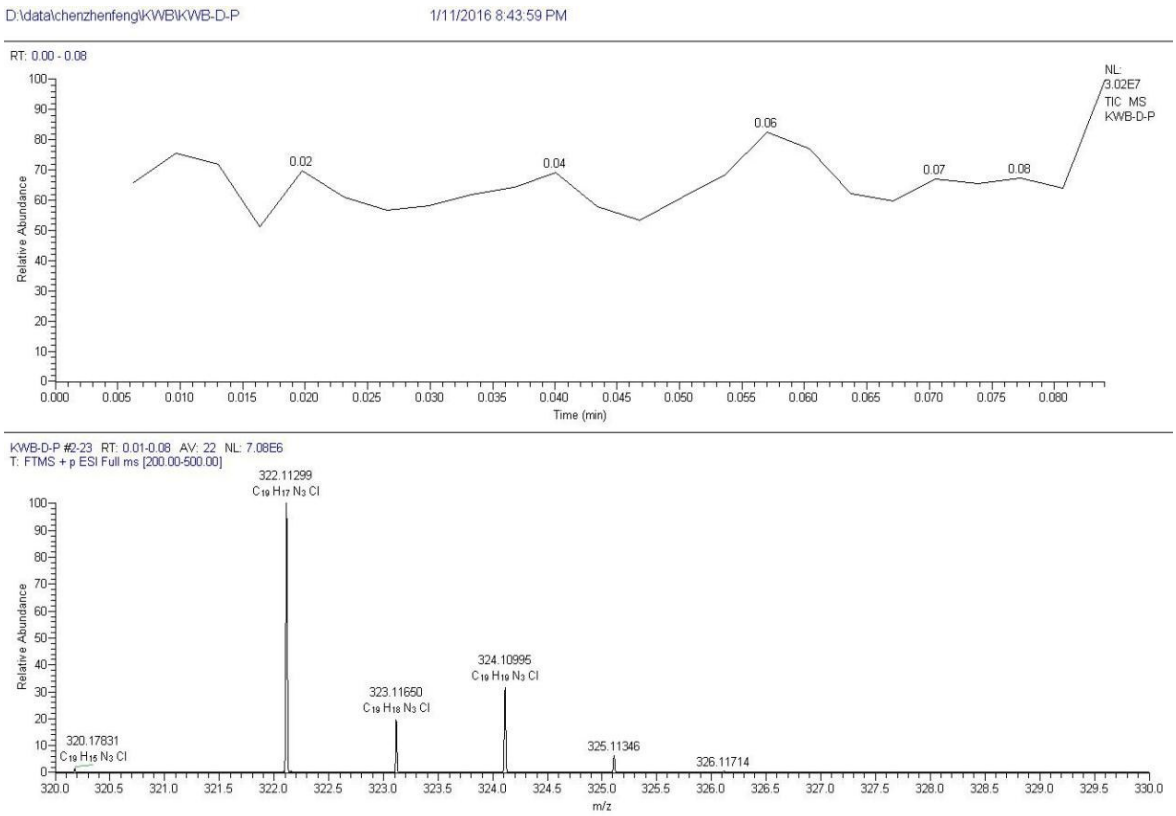

Fig. S2-28. ESI-HRMS of compound 3b$_1$

3b$_2$: Yield, 64.6%; ^{1}H NMR (400 MHz, DMSO-d$_6$) δ 12.14 (s, 1H, NH), 8.87 (s, 1H, HC=C), 7.96 (d, J = 8.6 Hz, 1H, H-Ar), 7.94 (s, 1H, H-Ar), 7.77 (d, J = 8.6 Hz, 1H, H-Ar), 7.70 (s, 1H, H-Ar), 7.51 (s, 1H, H-Ar), 7.16 (s, 1H, H-Ar), 2.54 (s, 3H, -CH$_3$); ^{13}C NMR (101 MHz, DMSO-d$_6$) δ 146.57, 145.98, 141.23, 138.35, 134.76, 127.92, 127.61, 126.79, 124.52, 21.62; ESI-HRMS, calculated *m/z* for $C_{17}H_{11}ClFN_3$ $[M+H]^+$: 312.0704, found: 312.0702.

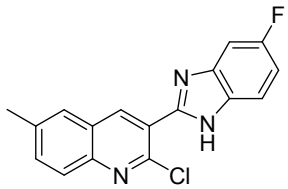

Fig. S2-29. Chemical structure of compound 3b$_2$

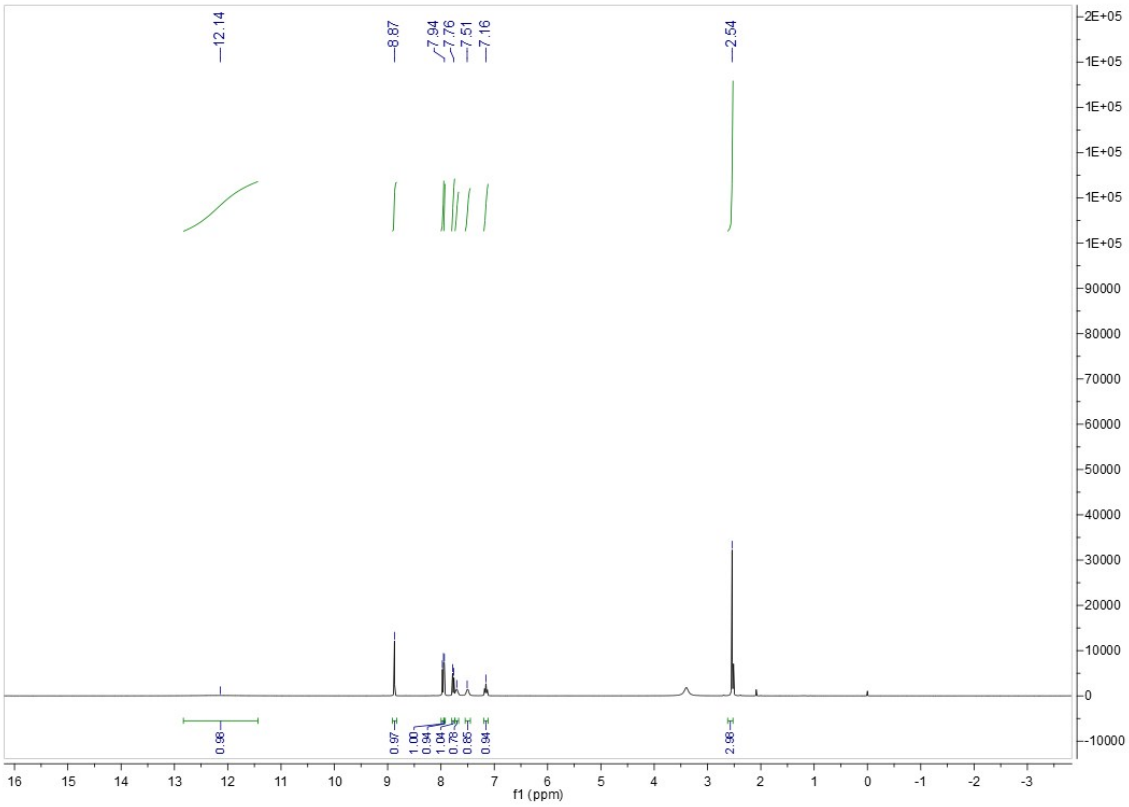

Fig. S2-30. ^{1}H NMR of compound 3b$_2$

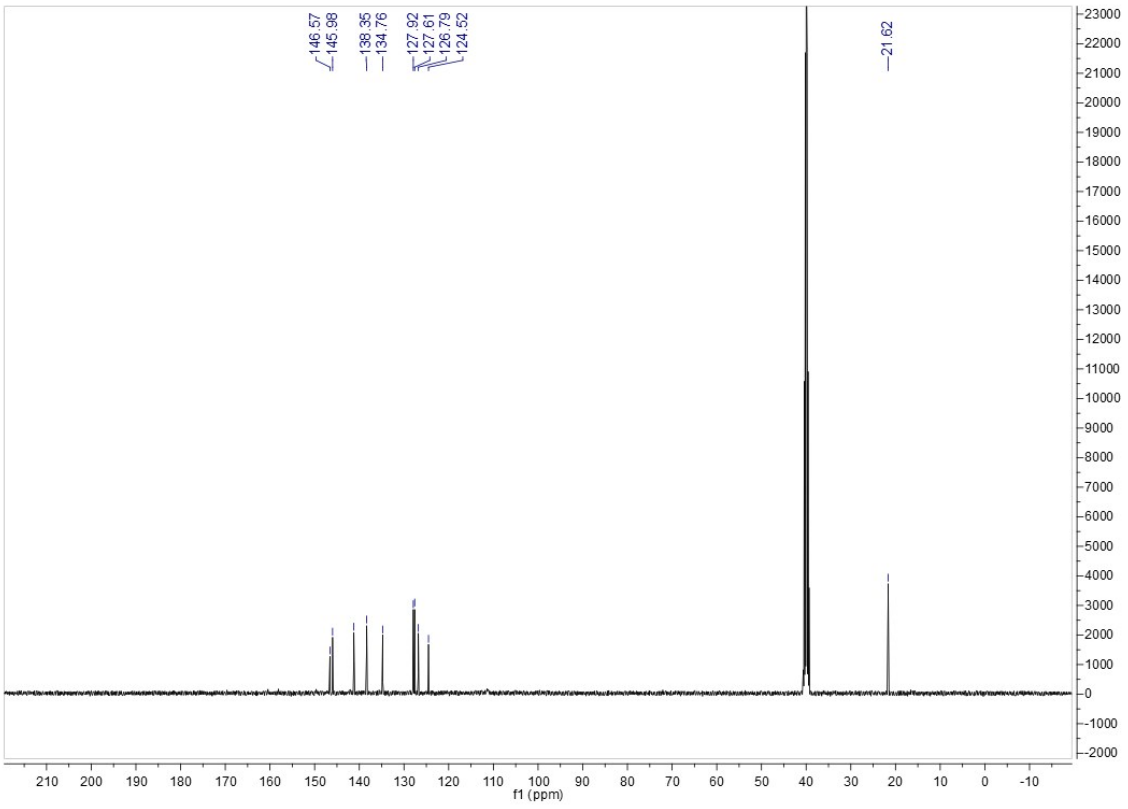

Fig. S2-31. ^{13}C NMR of compound $3b_2$

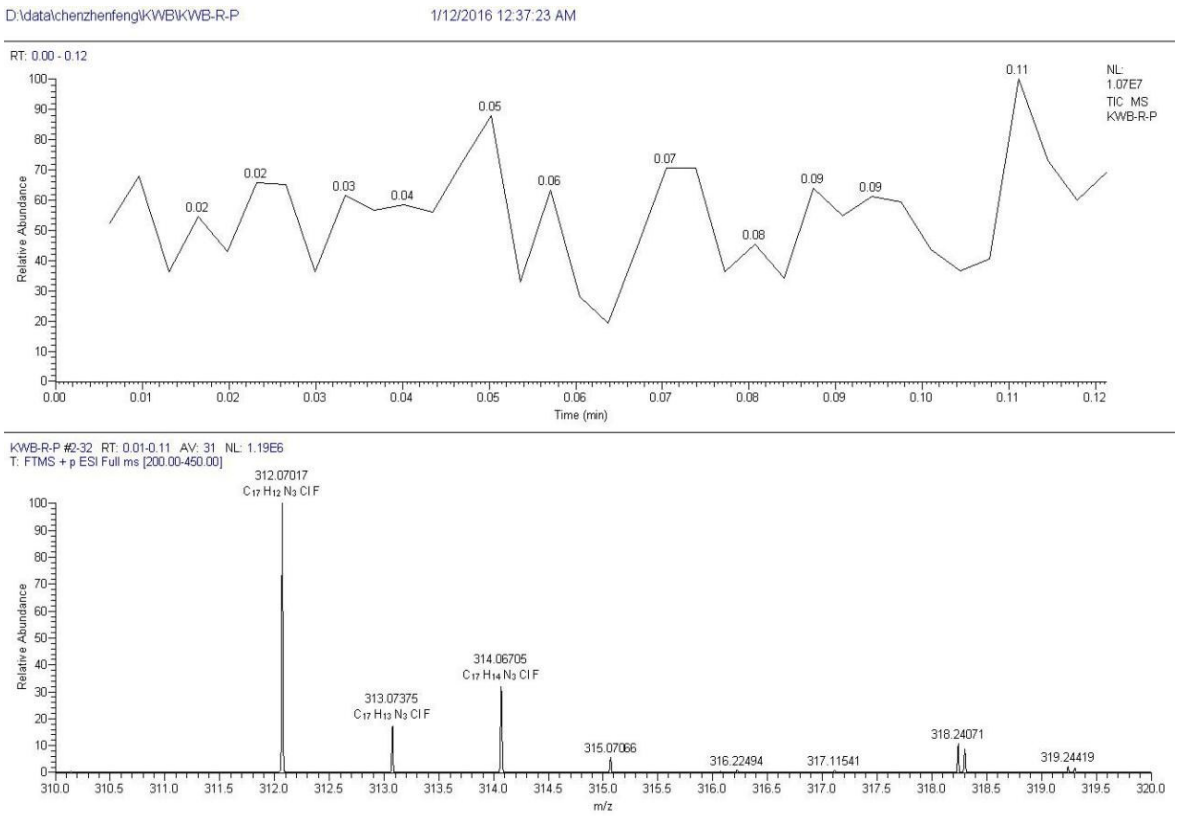

Fig. S2-32. ESI-HRMS of compound $3b_2$

3b$_3$: Yield, 55.9%; ^{1}H NMR (400 MHz, DMSO-d$_6$) δ 13.13 (s, 1H, NH), 8.88 (s, 1H, HC=C), 7.97 (d, J = 8.7 Hz, 1H, H-Ar), 7.95 (s, 1H, H-Ar), 7.78 (d, J = 8.6 Hz, 2H, H-Ar), 7.70 (s, 1H, H-Ar), 7.32 (d, J = 8.6 Hz, 1H, H-Ar), 2.54 (s, 3H, -CH$_3$); ^{13}C NMR (101 MHz, DMSO-d$_6$) δ 146.53, 146.04, 141.38, 138.40, 134.86, 127.94, 127.64, 126.77, 124.36, 21.64; ESI-HRMS, calculated *m/z* for $C_{17}H_{11}Cl_2N_3$ $[M-H]^-$: 326.0252, found: 326.0255.

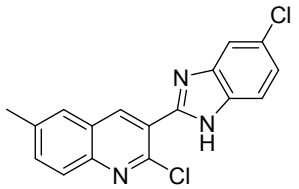

Fig. S2-33. Chemical structure of compound 3b$_3$

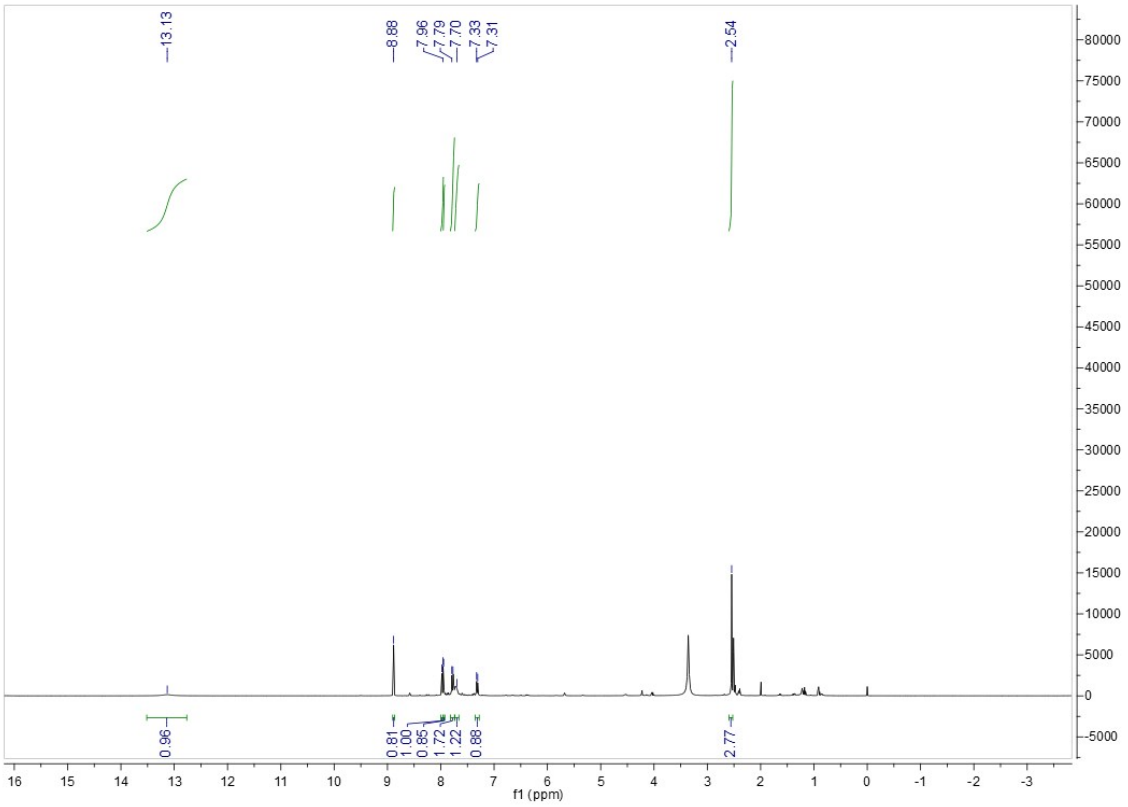

Fig. S2-34. ^{1}H NMR of compound 3b$_3$

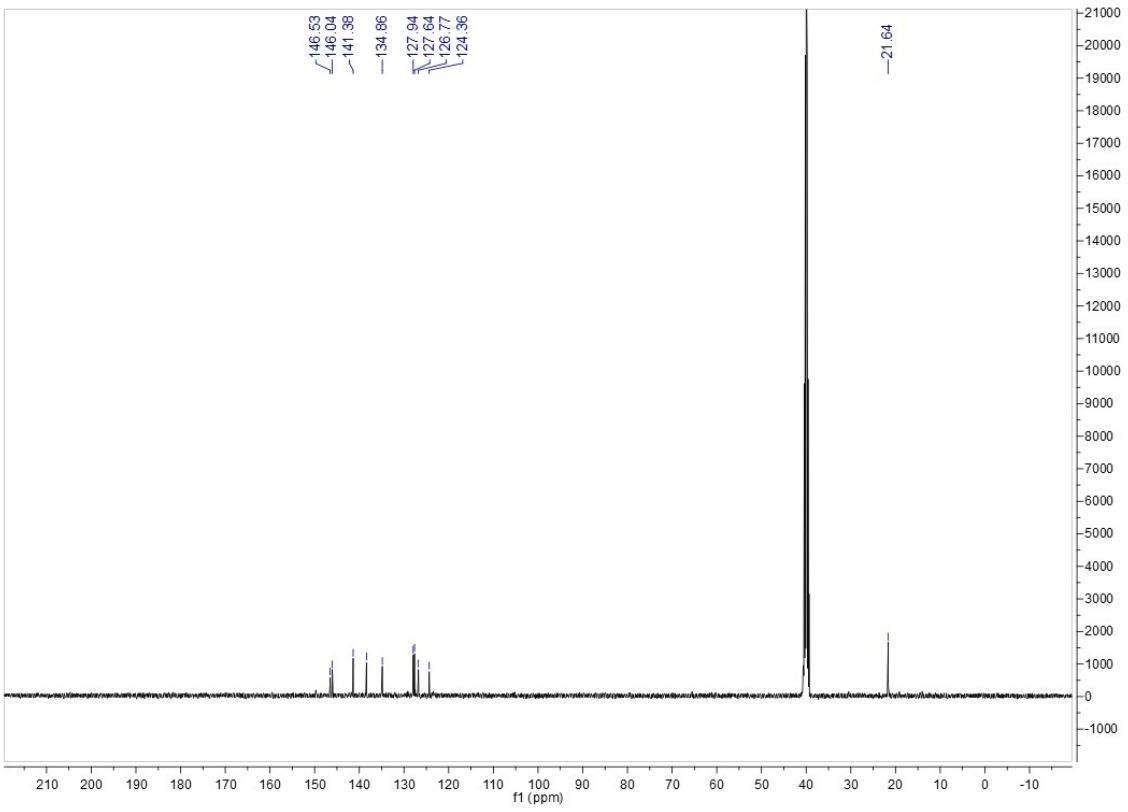

Fig. S2-35. ^{13}C NMR of compound $3b_3$

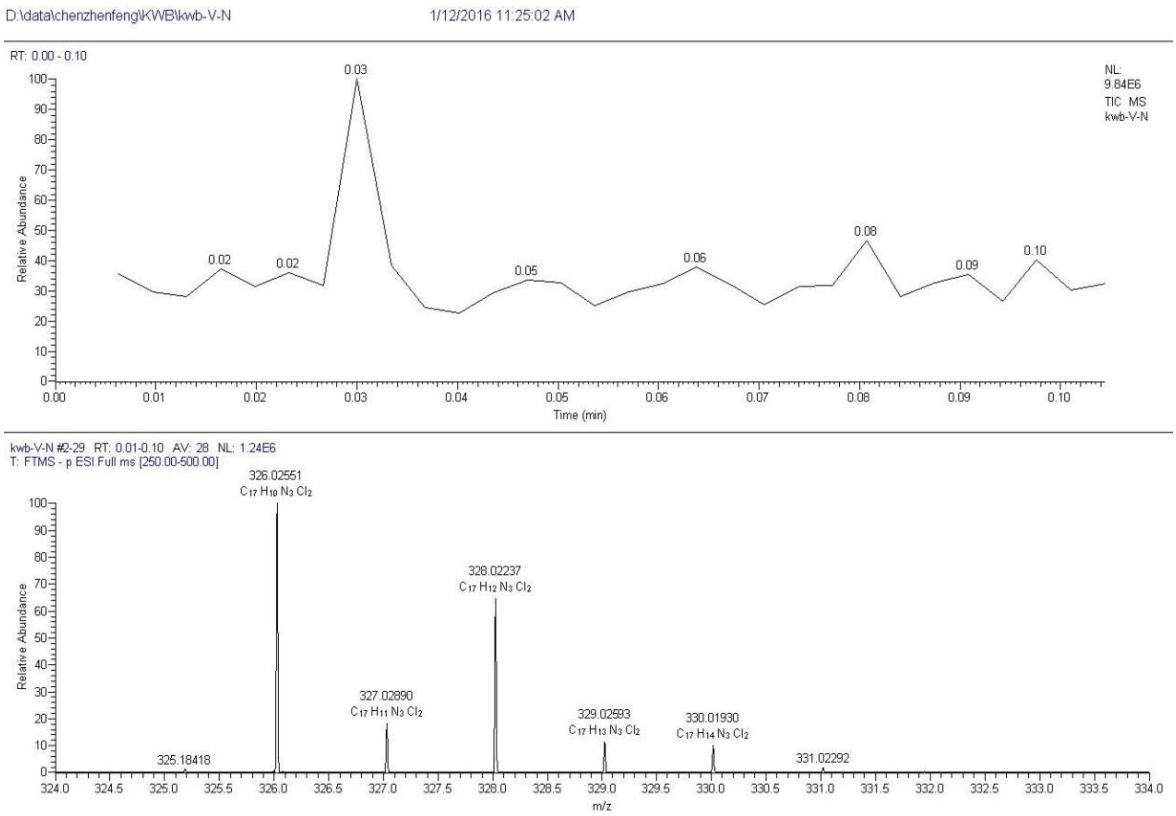

Fig. S2-36. ESI-HRMS of compound $3b_3$

3b$_4$: Yield, 61.0%; ^{1}H NMR (400 MHz, DMSO-d$_6$) δ 13.16 (s, 1H, NH), 8.88 (s, 1H, HC=C), 7.97 (d, J = 8.8 Hz, 1H, H-Ar), 7.95 (s, 1H, H-Ar), 7.78 (d, J = 8.6 Hz, 1H, H-Ar), 7.73 (s, 1H, H-Ar), 7.68 (s, 1H, H-Ar), 7.43 (d, J = 8.3 Hz, 1H, H-Ar), 2.54 (s, 3H, -CH$_3$); ^{13}C NMR (101 MHz, DMSO-d$_6$) δ 146.53, 146.04, 141.40, 138.41, 134.87, 127.94, 127.65, 126.77, 124.34, 21.64; ESI-HRMS, calculated *m/z* for $C_{17}H_{11}BrClN_3$ [M−H]$^-$: 369.9747, found: 369.9774.

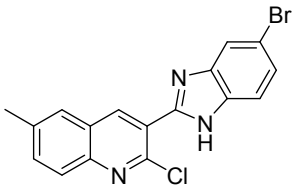

Fig. S2-37. Chemical structure of compound 3b$_4$

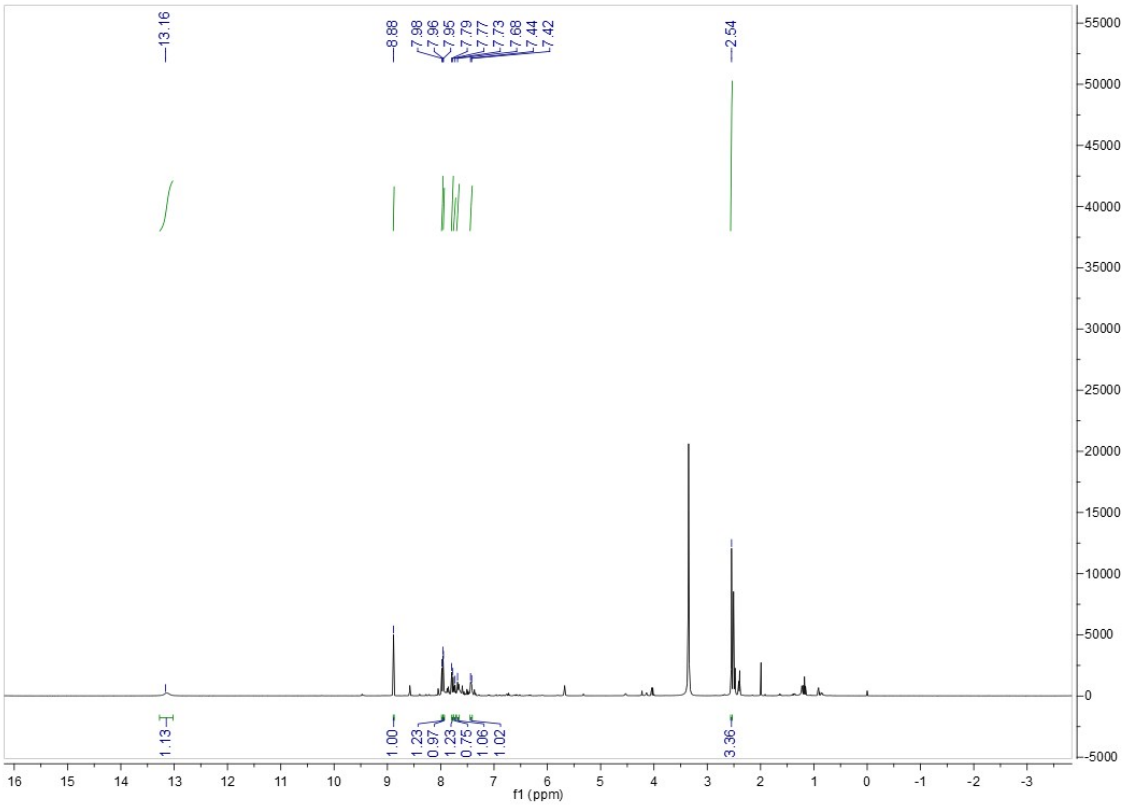

Fig. S2-38. ^{1}H NMR of compound 3b$_4$

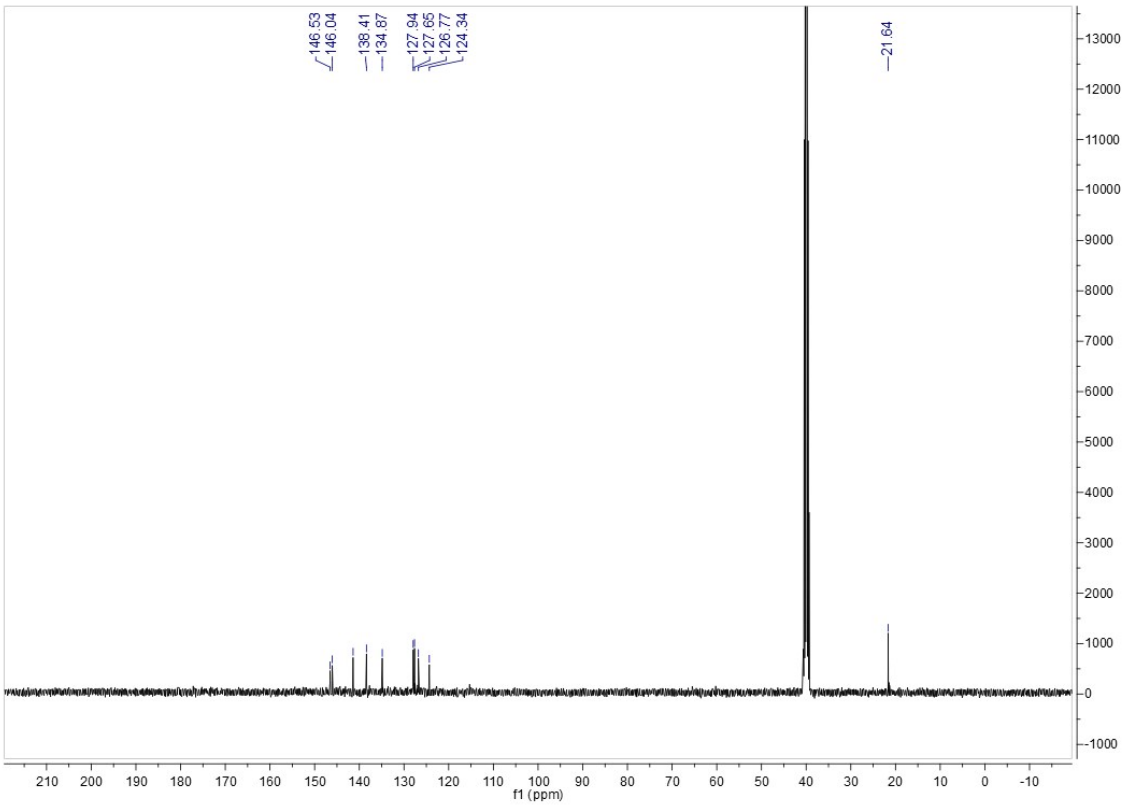

Fig. S2-39. ^{13}C NMR of compound $3b_4$

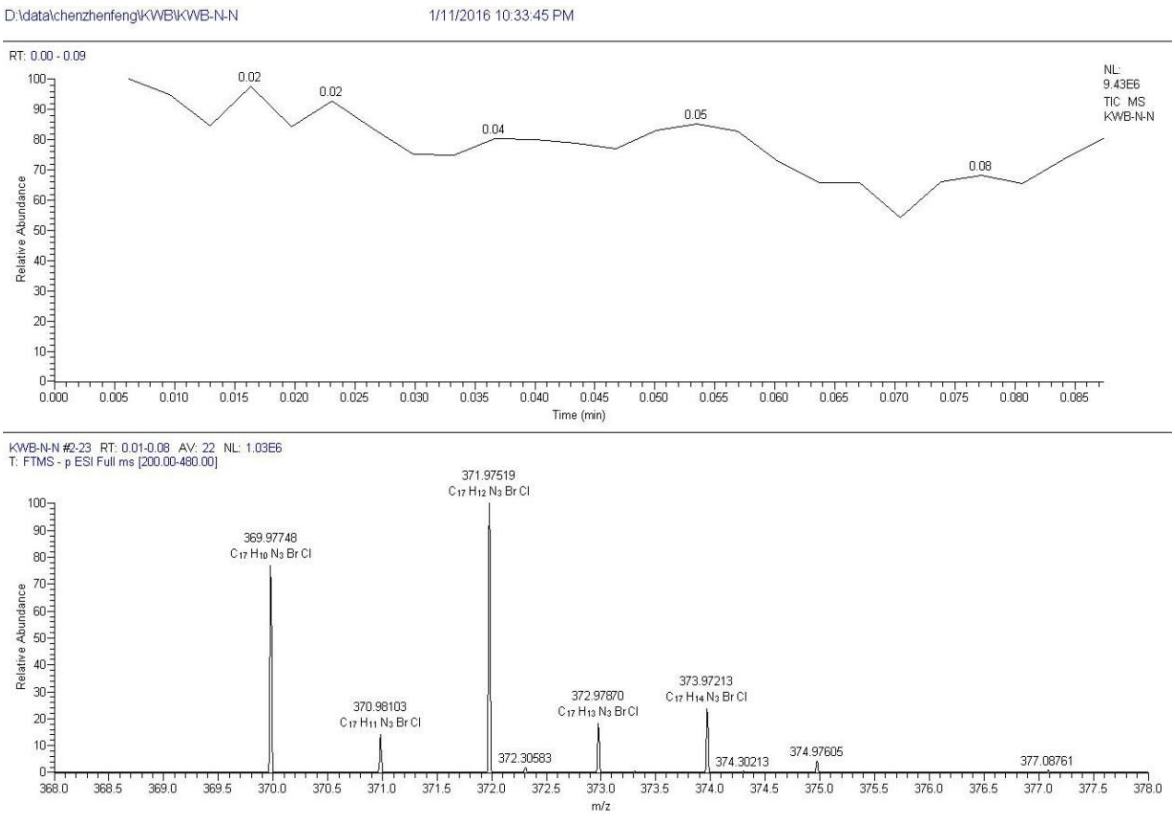

Fig. S2-40. ESI-HRMS of compound $3b_4$

$3b_5$: Yield, 59.9%; ^{1}H NMR (500 MHz, DMSO-d_6) δ 13.26 (s, 1H, NH), 8.88 (s, 1H, HC=C), 7.96 (d, J = 8.6 Hz, 2H, H-Ar), 7.94 (s, 2H, H-Ar), 7.78 (s, 1H, H-Ar), 2.54 (s, 3H, -CH_3); ^{13}C NMR (126 MHz, DMSO-d_6) δ 150.92, 146.41, 146.14, 141.46, 138.44, 134.94, 127.94, 127.66, 126.71, 123.99, 21.61; ESI-HRMS, calculated *m/z* for $C_{17}H_{11}BrClN_3$ $[M-H]^-$: 359.9862, found: 359.9903.

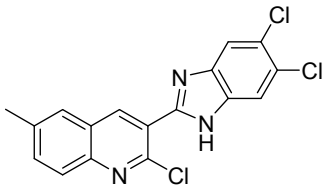

Fig. S2-41. Chemical structure of compound $3b_5$

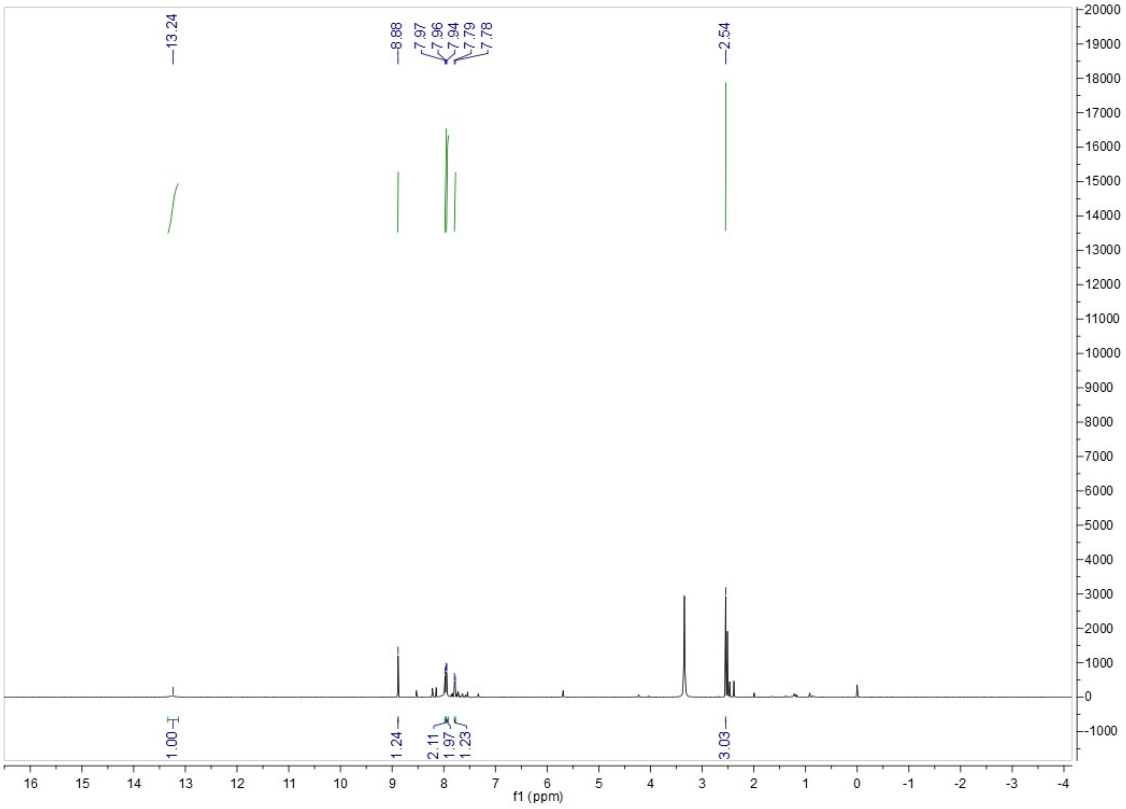

Fig. S2-42. ^{1}H NMR of compound $3b_5$

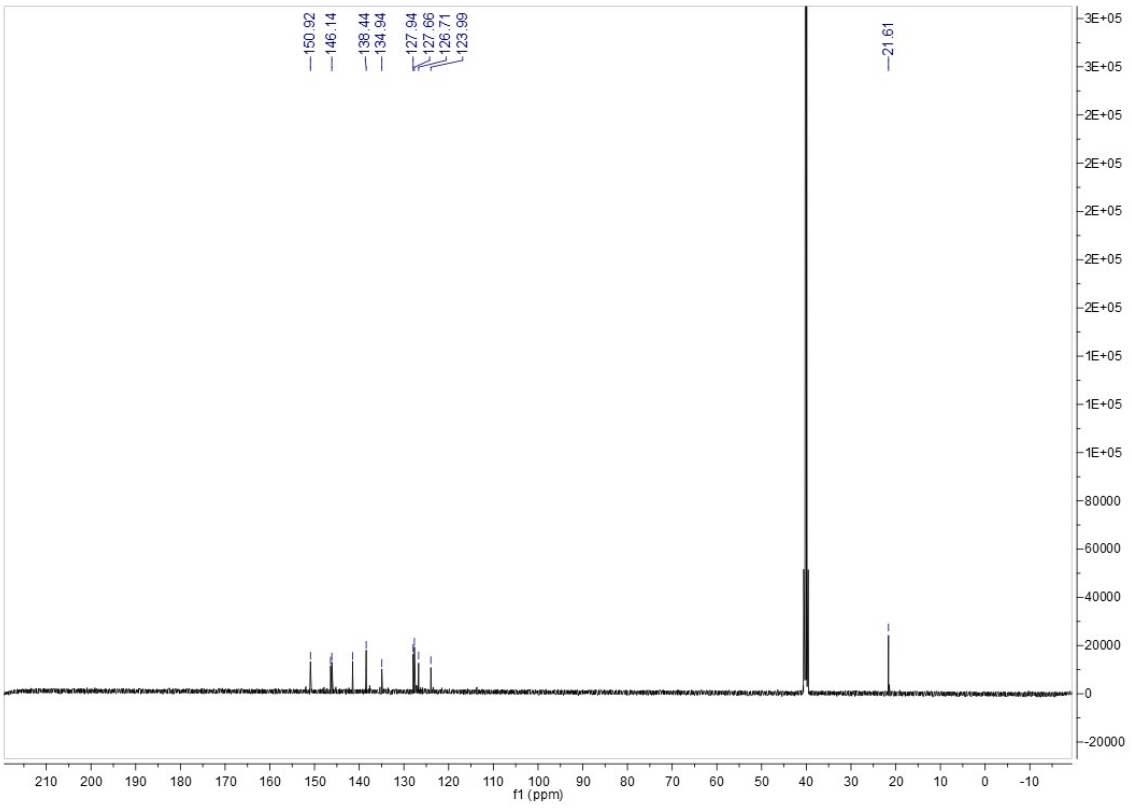

Fig. S2-43. ^{13}C NMR of compound $3b_5$

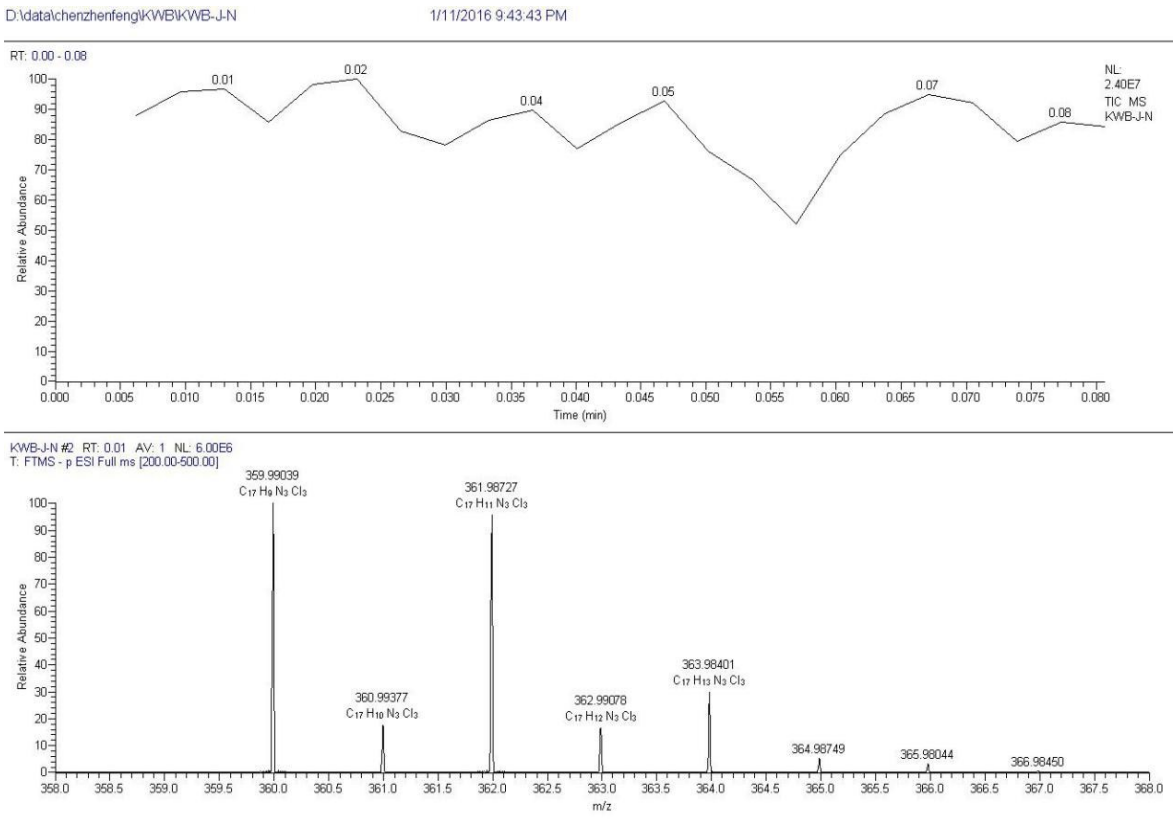

Fig. S2-44. ESI-HRMS of compound $3b_5$

3b$_6$: Yield, 61.7%; ^{1}H NMR (400 MHz, DMSO-d$_6$) δ 12.96 (s, 1H, NH), 8.87 (s, 1H, HC=C), 7.97 (d, J = 8.7 Hz, 1H, H-Ar), 7.95 (s, 1H, H-Ar), 7.77 (d, J = 8.6 Hz, 1H, H-Ar), 7.69 (s, 2H, H-Ar), 7.29 (d, J = 6.0 Hz, 2H, H-Ar), 2.54 (s, 3H, -CH$_3$); ^{13}C NMR (101 MHz, DMSO-d$_6$) δ 148.32, 146.73, 145.95, 141.19, 138.32, 134.69, 127.93, 127.60, 126.83, 124.87, 21.64; ESI-HRMS, calculated *m/z* for $C_{17}H_{12}ClN_3$ $[M+H]^+$: 294.0798, found: 294.0790.

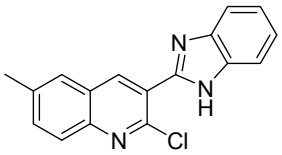

Fig. S2-45. Chemical structure of compound 3b$_6$

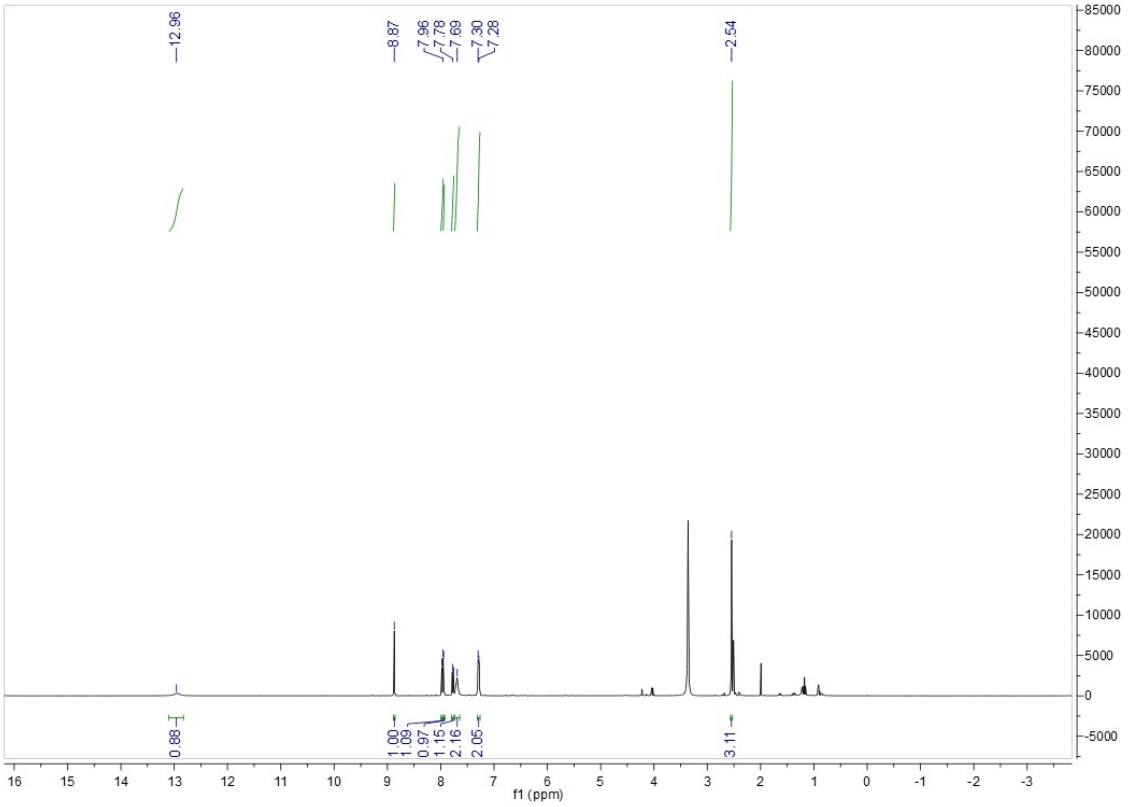

Fig. S2-46. ^{1}H NMR of compound 3b$_6$

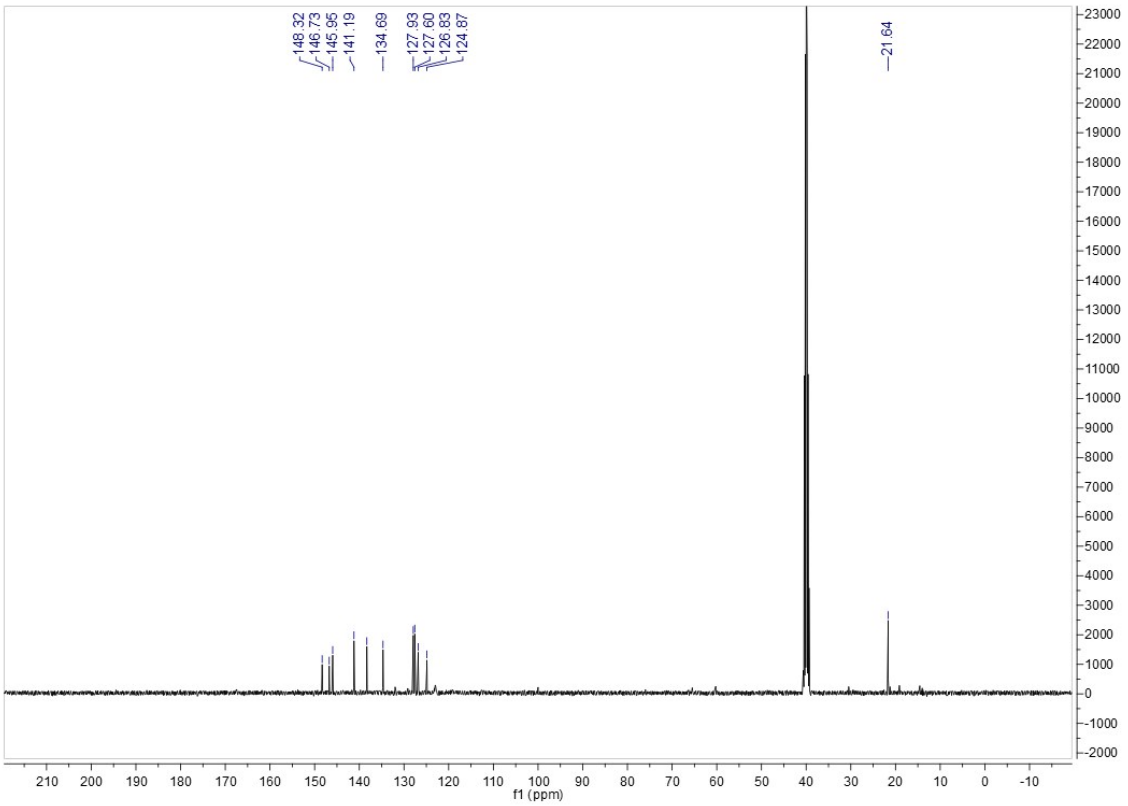

Fig. S2-47. ^{13}C NMR of compound 3b$_6$

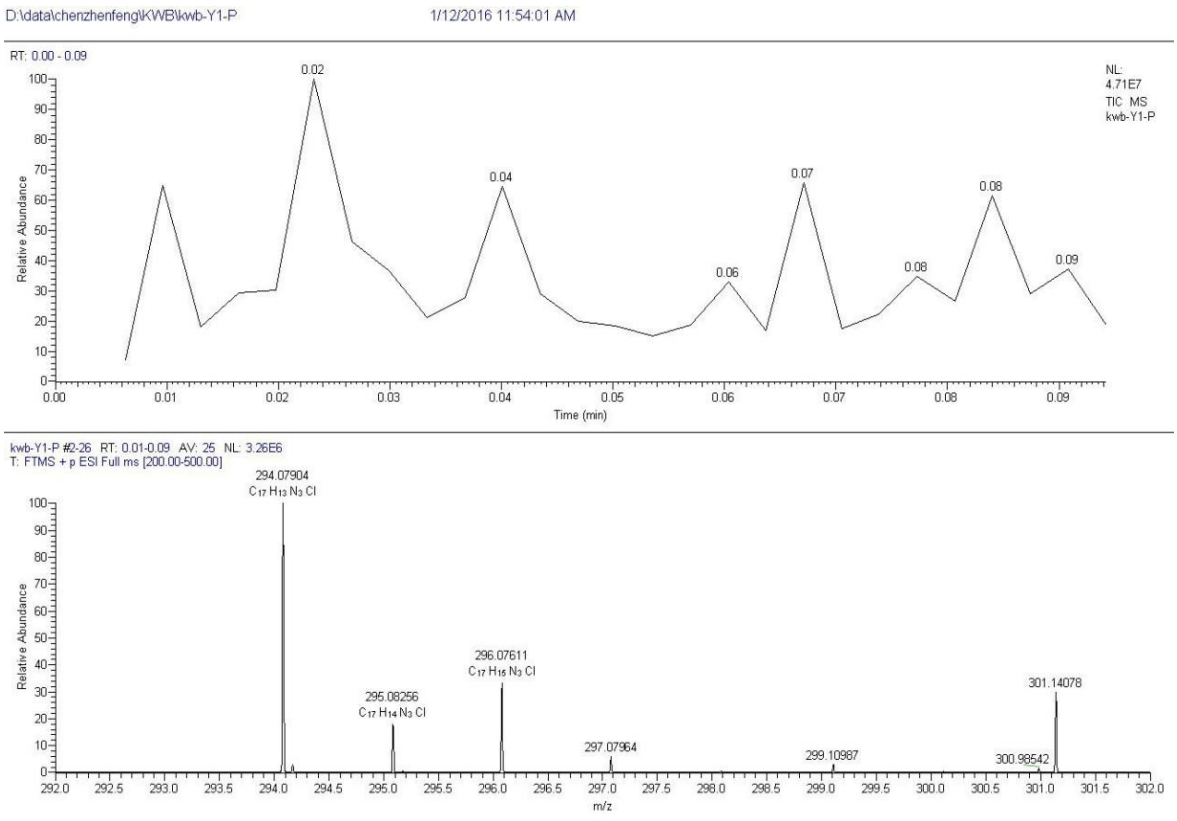

Fig. S2-48. ESI-HRMS of compound 3b$_6$

3c$_1$: Yield, 59.0%; ^{1}H NMR (500 MHz, DMSO-d$_6$) δ 12.78 (s, 1H, NH), 8.84 (s, 1H, HC=C), 7.96 (d, J = 9.2 Hz, 1H, H-Ar), 7.60 (s, 1H, H-Ar), 7.55 (d, J = 9.1 Hz, 1H, H-Ar), 7.46 (s, 2H, H-Ar), 3.93 (s, 3H, -OCH$_3$), 2.36 (s, 6H, -CH$_3$); ^{13}C NMR (126 MHz, DMSO-d$_6$) δ 158.70, 147.27, 144.89, 143.27, 140.29, 131.65, 129.64, 128.16, 125.06, 124.67, 106.81, 56.24, 20.49. ESI-HRMS, calculated *m/z* for $C_{19}H_{16}ClN_3O$ $[M+H]^+$: 338.1060, found: 338.1076.

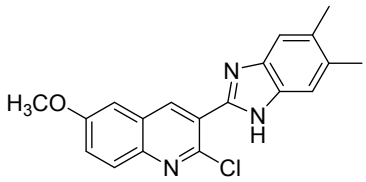

Fig. S2-49. Chemical structure of compound 3c$_1$

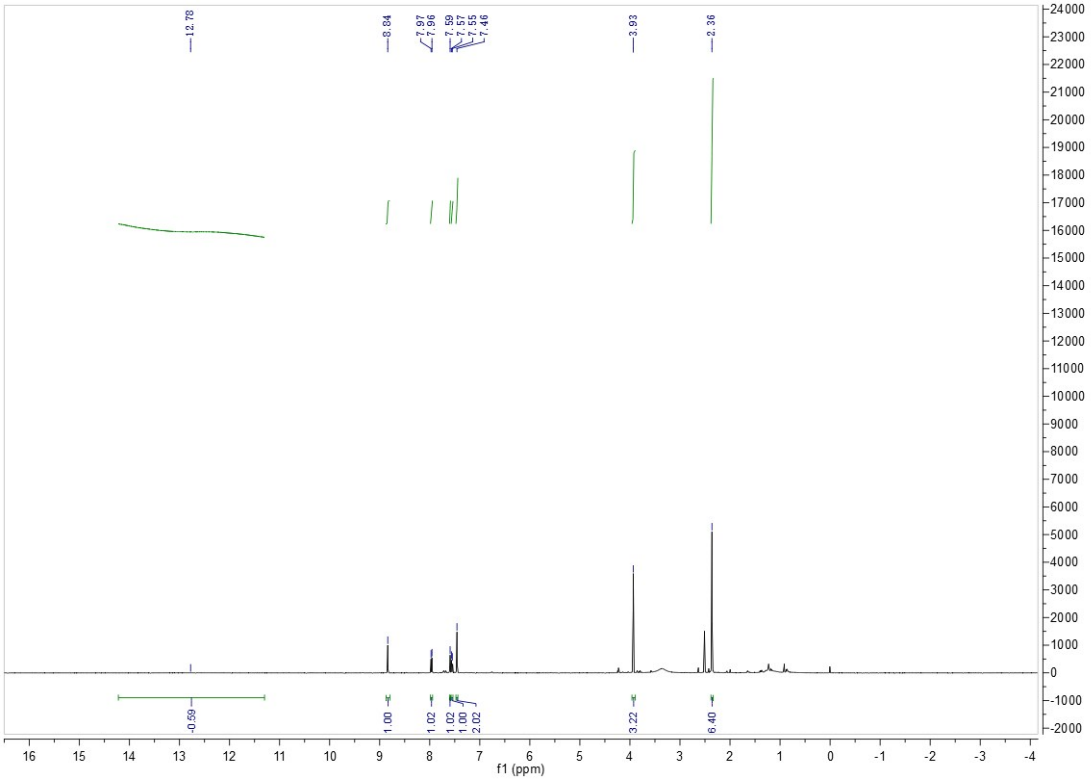

Fig. S2-50. ^{1}H NMR of compound 3c$_1$

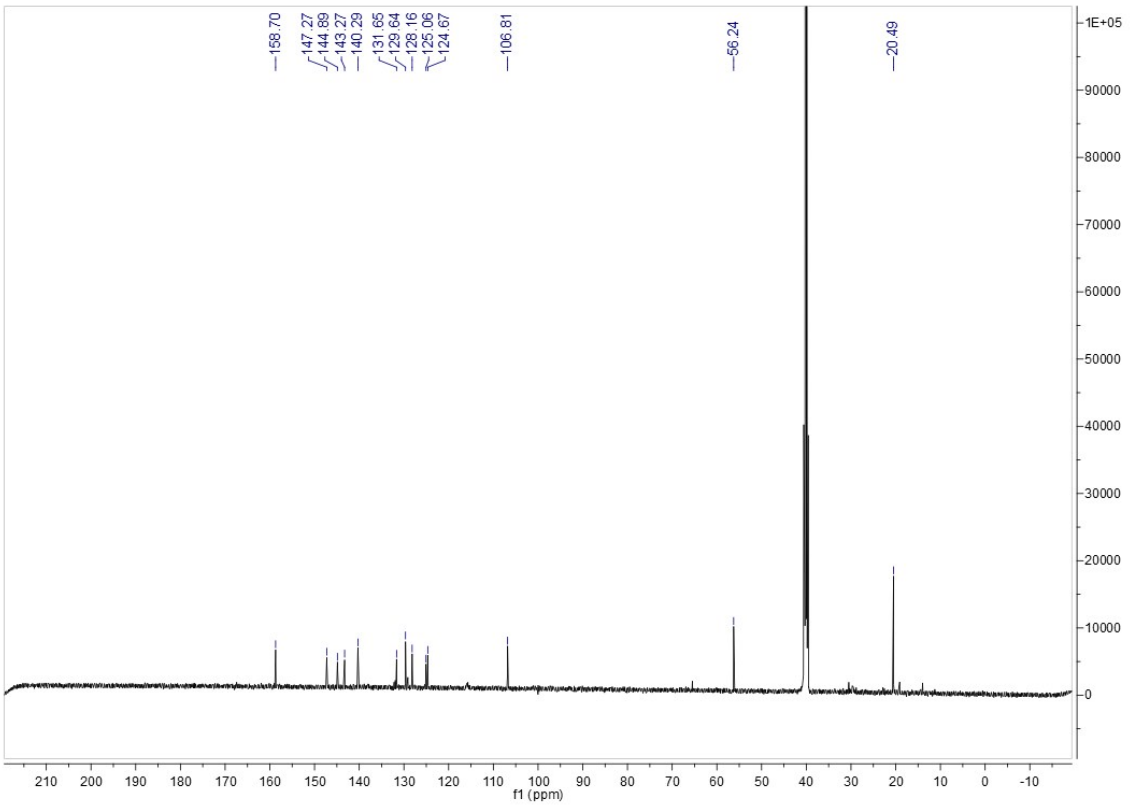

Fig. S2-51. ^{13}C NMR of compound 3c$_1$

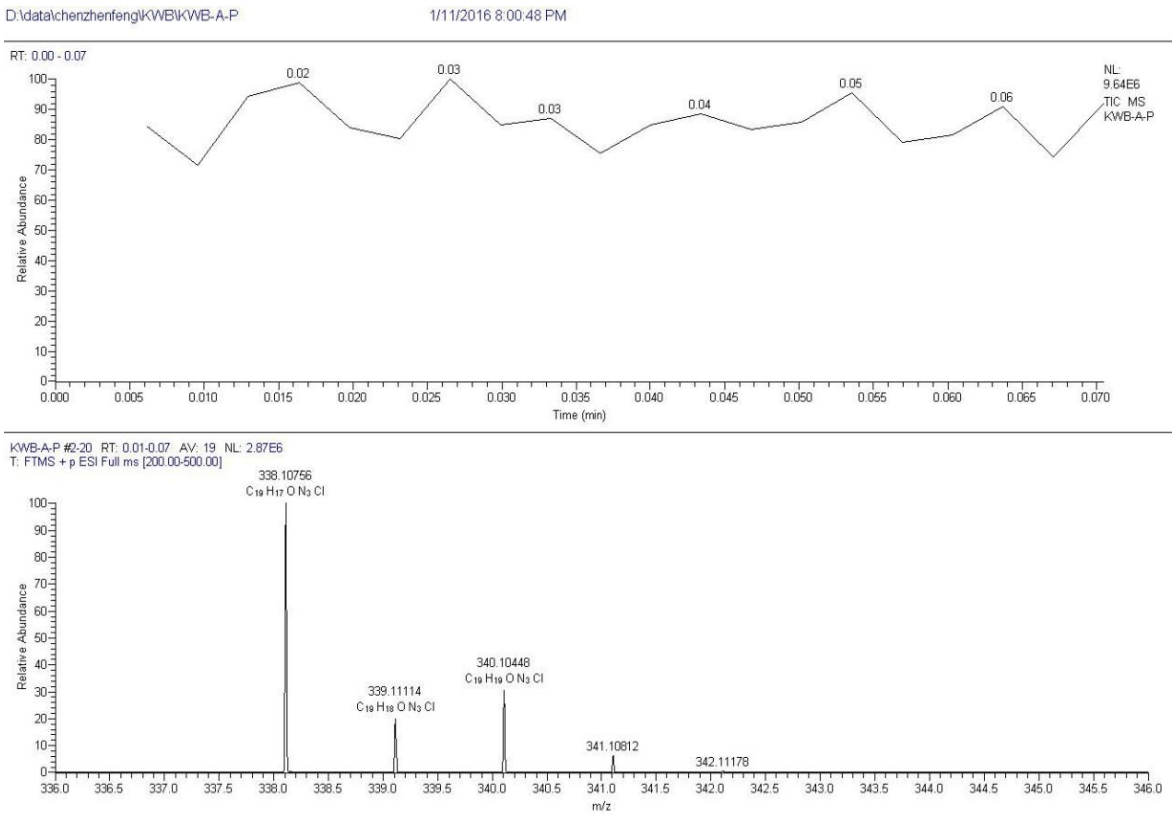

Fig. S2-52. ESI-HRMS of compound 3c$_1$

3c$_2$: Yield, 56.4%; ^{1}H NMR (500 MHz, DMSO-d$_6$) δ 13.05 (s, 1H, NH), 8.87 (s, 1H, HC=C), 7.97 (d, J = 9.1 Hz, 1H, H-Ar), 7.76 (s, 1H, H-Ar), 7.59 (s, 1H, H-Ar), 7.57 (d, J = 9.1 Hz, 1H, H-Ar), 7.44 (s, 1H, H-Ar), 7.15 (s, 1H, H-Ar), 3.93 (s, 3H, -OCH$_3$); ^{13}C NMR (126 MHz, DMSO-d$_6$) δ 158.70, 143.38, 129.65, 128.11, 124.92, 124.66, 106.76, 56.23; ESI-HRMS, calculated *m/z* for $C_{17}H_{11}ClFN_3O$ $[M+H]^+$: 328.0653, found: 328.0640.

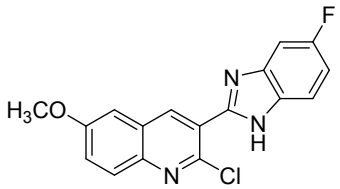

Fig. S2-53. Chemical structure of compound 3c$_2$

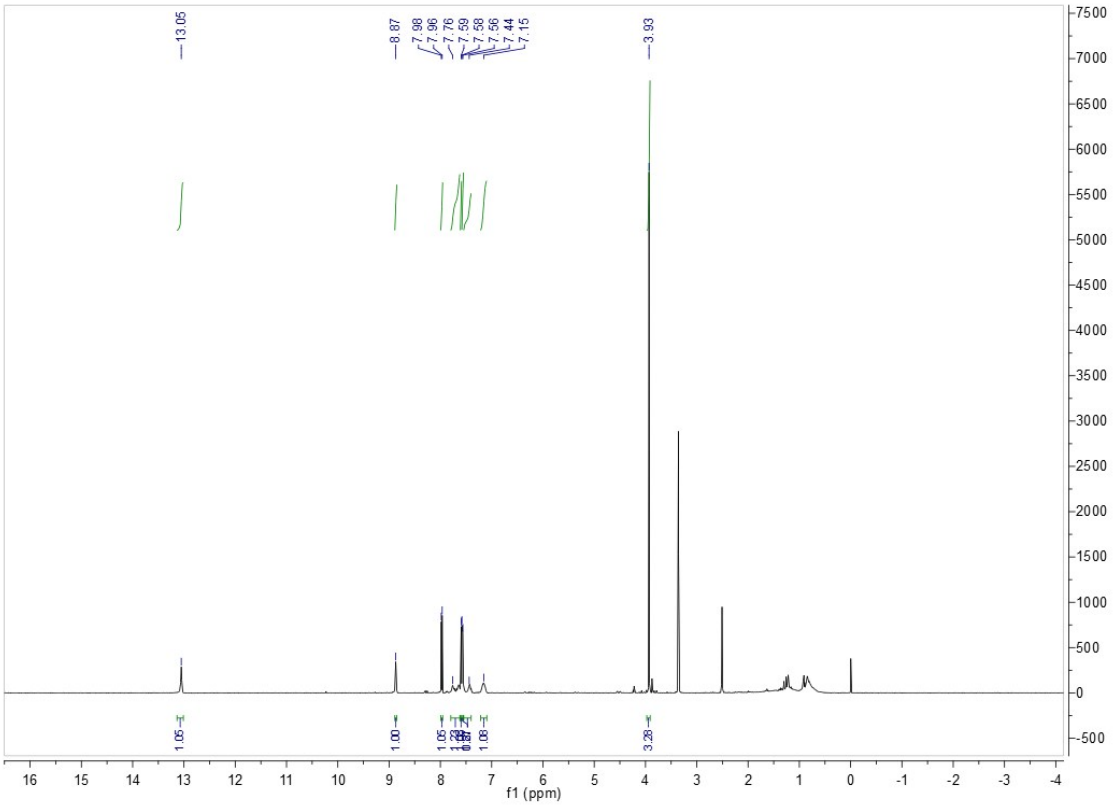

Fig. S2-54. ^{1}H NMR of compound 3c$_2$

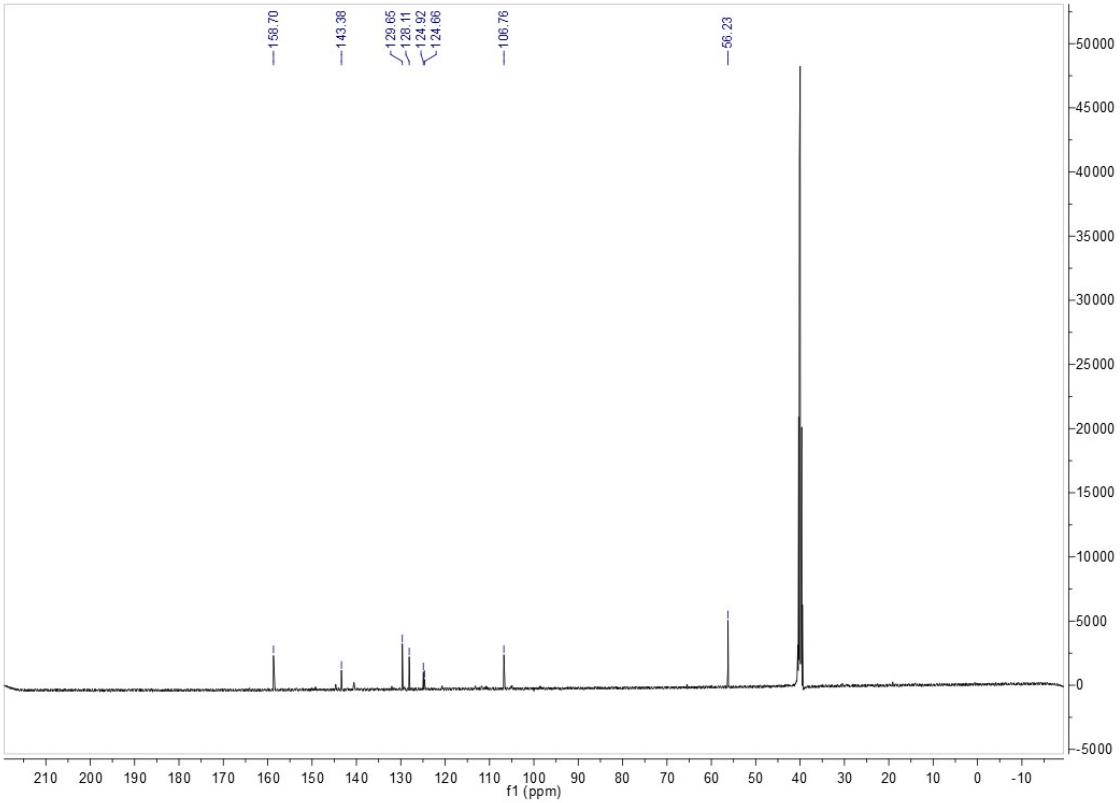

Fig. S2-55. ^{13}C NMR of compound $3c_2$

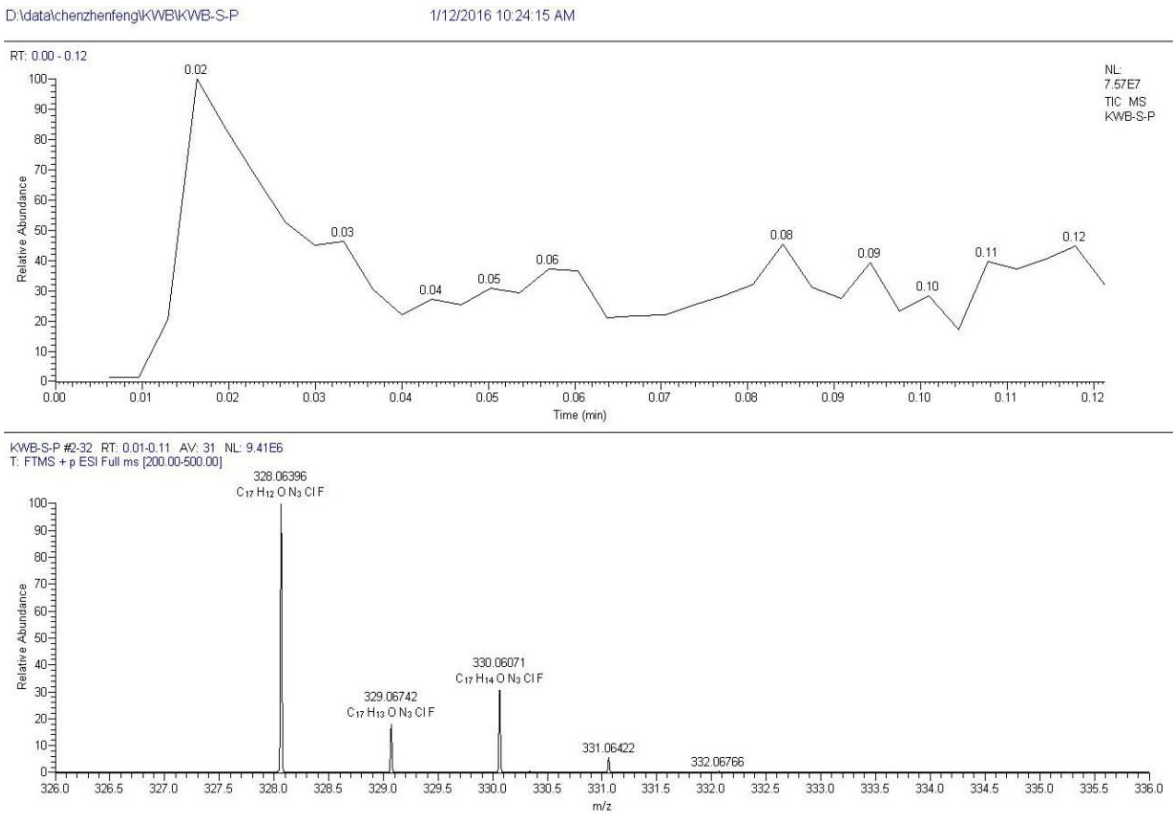

Fig. S2-56. ESI-HRMS of compound $3c_2$

3c$_3$: Yield 55.1%, ^{1}H NMR (400 MHz, DMSO-d$_6$) δ 13.12 (s, 1H, NH), 8.88 (s, 1H, HC=C), 7.98 (d, J = 9.0 Hz, 1H, H-Ar), 7.76 (s, 1H, H-Ar), 7.70 (s, 1H, H-Ar), 7.60 (s, 1H, H-Ar), 7.58 (d, J = 9.0 Hz, 1H, H-Ar), 7.32 (d, J = 8.6 Hz, 1H, H-Ar), 3.93 (s, 3H, -OCH$_3$);^{13}C NMR (101 MHz, DMSO-d$_6$) δ 158.74, 149.73, 144.65, 143.45, 140.73, 129.68, 128.10, 125.02, 124.51, 106.81, 56.26. ESI-HRMS *m/z* Calc for $C_{17}H_{11}Cl_2N_3O$ $[M-H]^-$:342.0201; found: 342.0205.

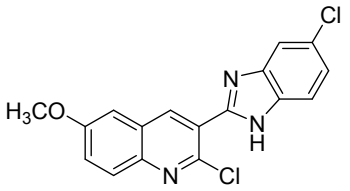

Fig. S2-57. Chemical structure of compound 3c$_3$

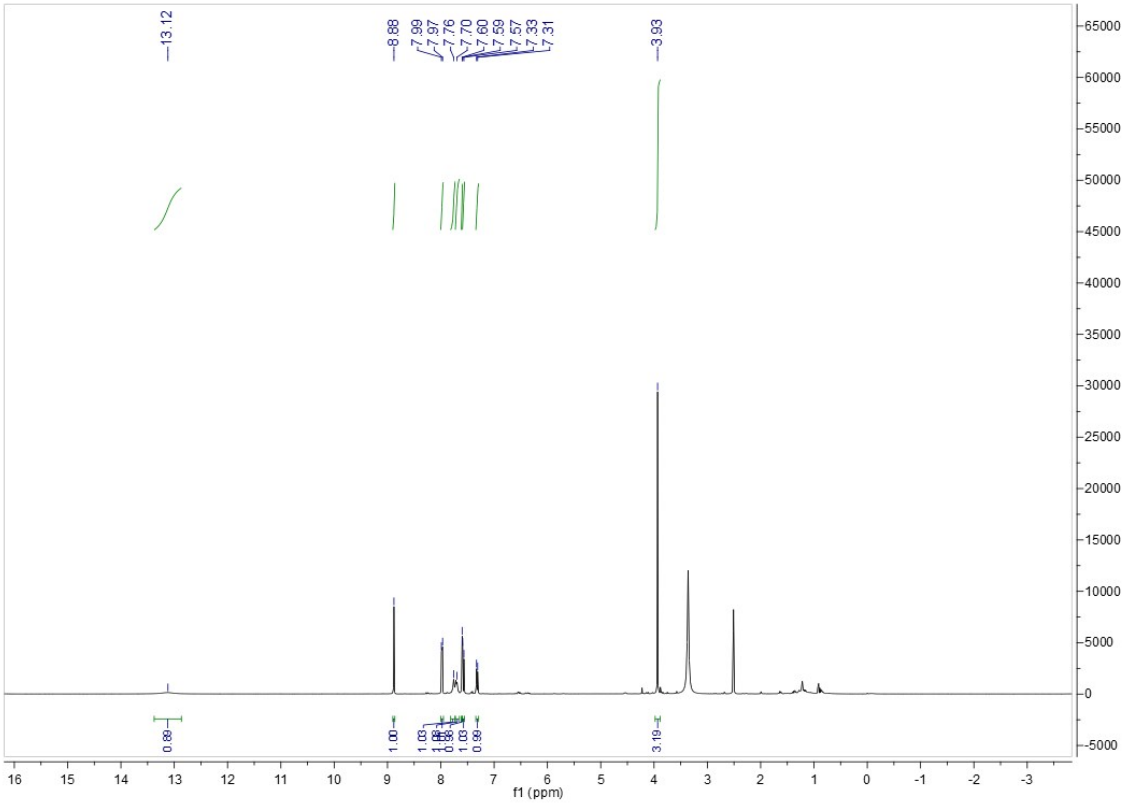

Fig. S2-58. ^{1}H NMR of compound 3c$_3$

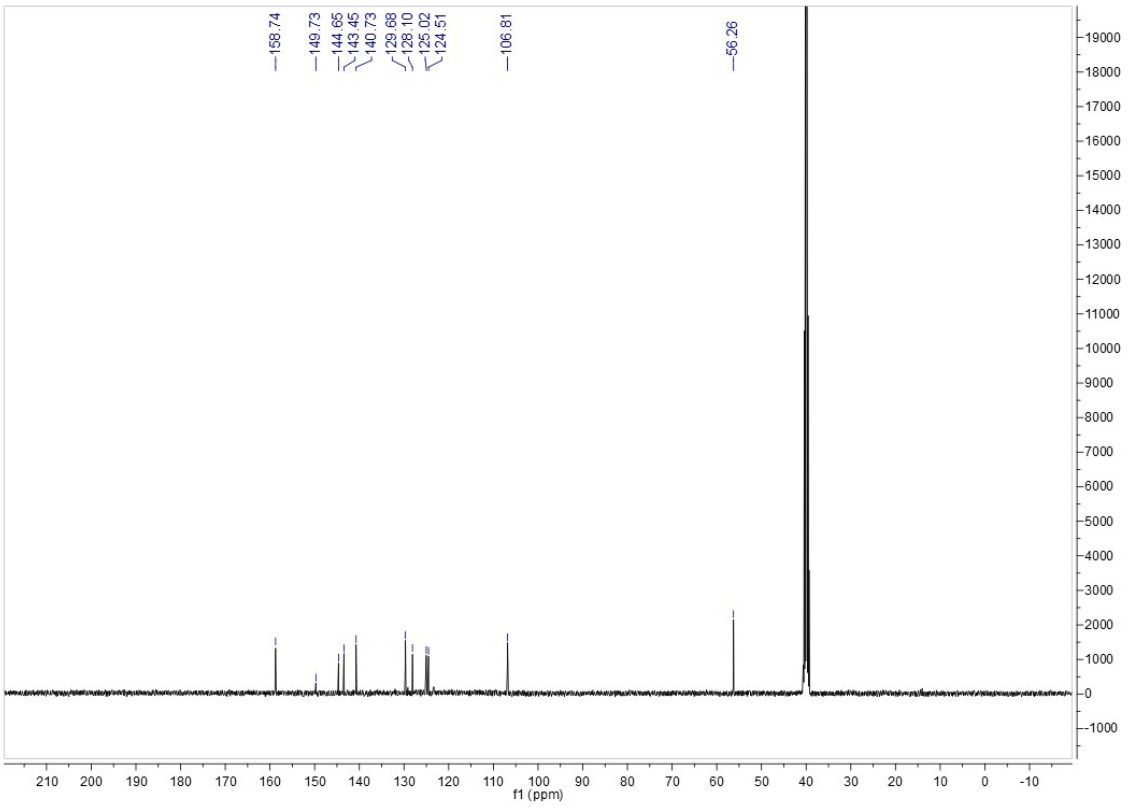

Fig. S2-59. ^{13}C NMR of compound $3c_3$

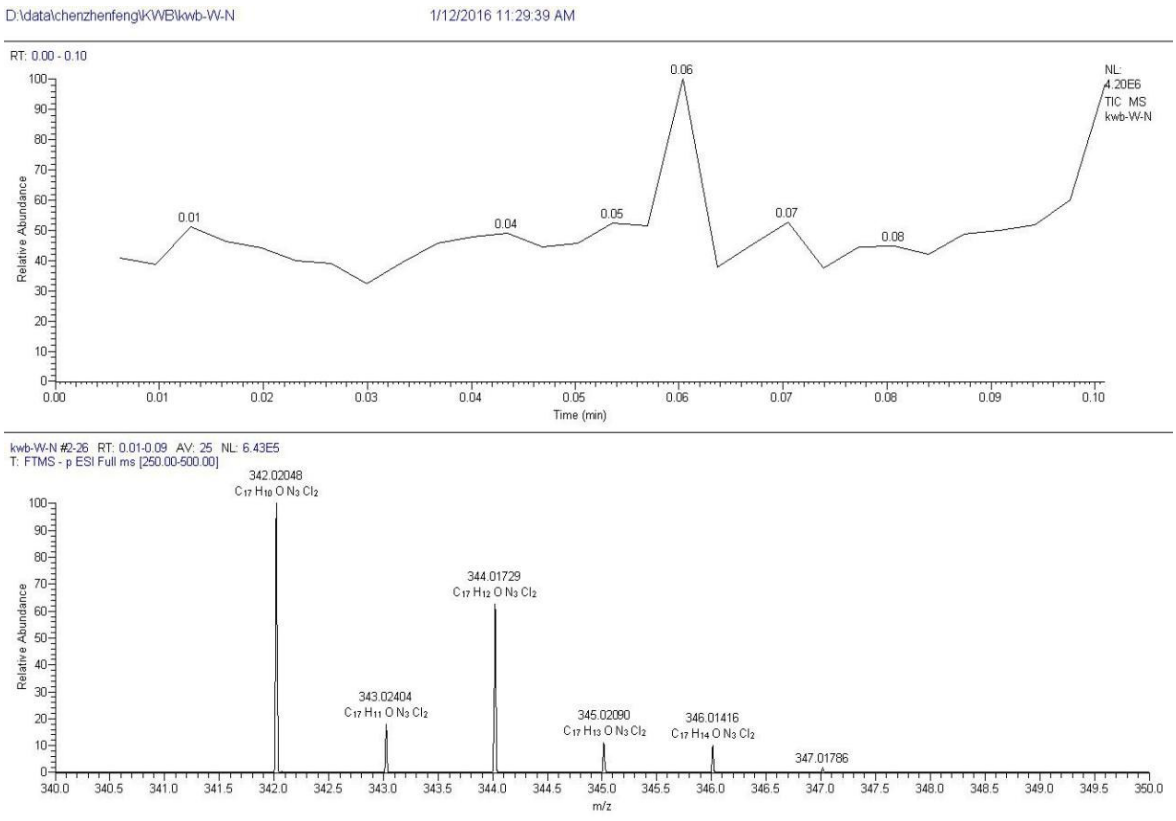

Fig. S2-60. ESI-HRMS of compound $3c_3$

3c$_4$: Yield, 57.1%; ^{1}H NMR (400 MHz, DMSO-d$_6$) δ 13.14 (s, 1H, NH), 8.88 (s, 1H, HC=C), 7.98 (d, J = 9.1 Hz, 1H, H-Ar), 7.90 (s, 1H, H-Ar), 7.68 (s, 1H, H-Ar), 7.60 (s, 1H, H-Ar), 7.58 (d, J = 9.1 Hz, 1H, H-Ar), 7.43 (d, J = 8.4 Hz, 1H, H-Ar), 3.93 (s, 3H, -OCH$_3$); ^{13}C NMR (101 MHz, DMSO-d$_6$) δ 158.73, 144.64, 143.45, 140.75, 129.68, 128.10, 125.04, 124.47, 106.80, 56.26; ESI-HRMS, calculated *m/z* for $C_{17}H_{11}Cl_2N_3O$ [M−H]$^-$: 385.9696, found: 385.9715.

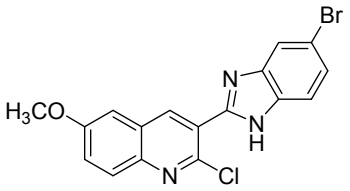

Fig. S2-61. Chemical structure of compound 3c$_4$

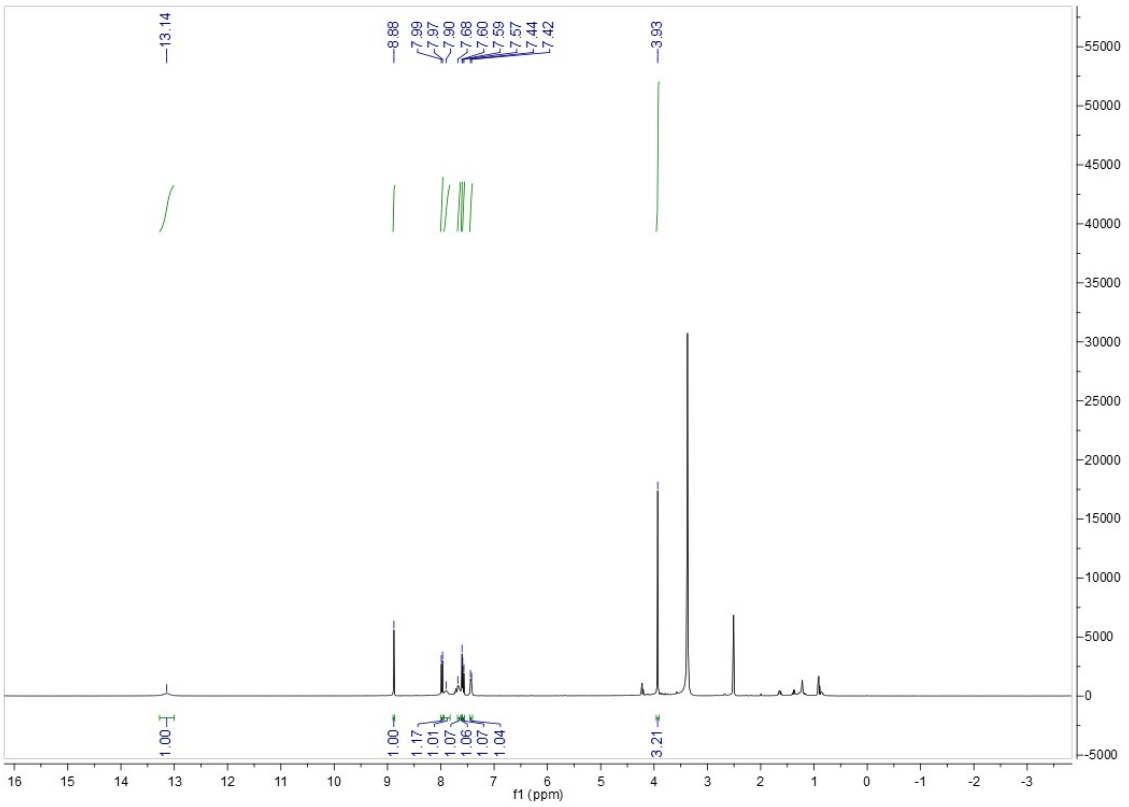

Fig. S2-62. ^{1}H NMR of compound 3c$_4$

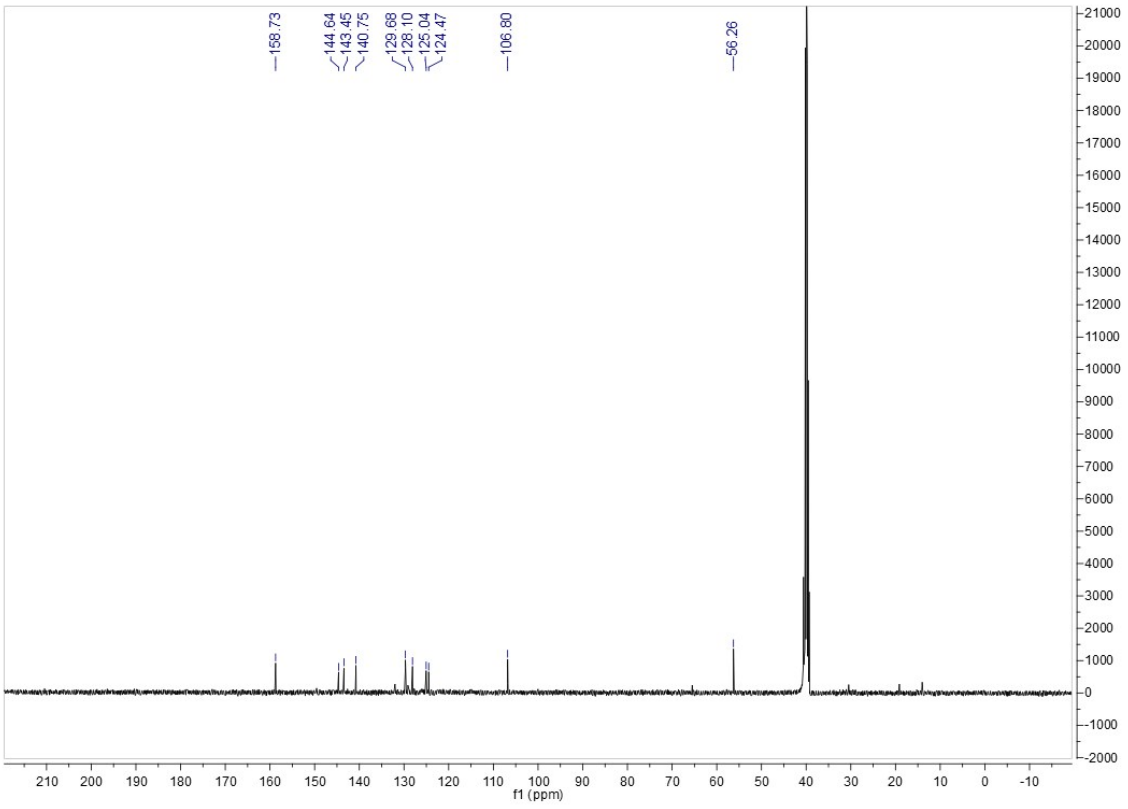

Fig. S2-63. ^{13}C NMR of compound $3c_4$

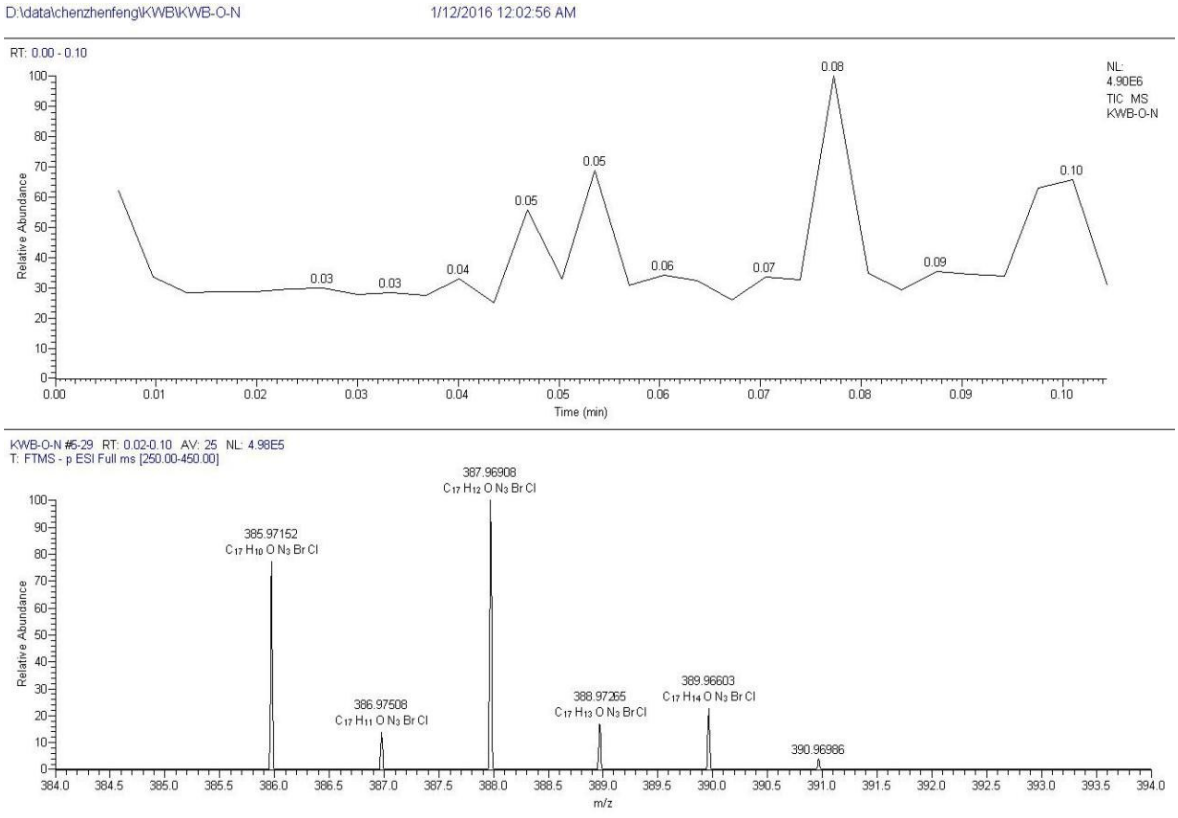

Fig. S2-64. ESI-HRMS of compound $3c_4$

3c$_5$: Yield, 57.5%; ^{1}H NMR (400 MHz, DMSO-d$_6$) δ 13.26 (s, 1H, NH), 8.88 (s, 1H, HC=C), 7.97 (s, 3H, H-Ar), 7.60 (s, 2H, H-Ar), 3.93 (s, 3H, -OCH$_3$); ^{13}C NMR (101 MHz, DMSO-d$_6$) δ 158.77, 150.93, 144.53, 143.52, 140.87, 129.69, 128.05, 125.15, 124.12, 106.85, 56.27; ESI-HRMS, calculated *m/z* for $C_{17}H_{11}Cl_2N_3O$ $[M-H]^-$: 375.9811, found: 378.9859.

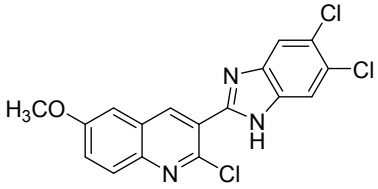

Fig. S2-65. Chemical structure of compound 3c$_5$

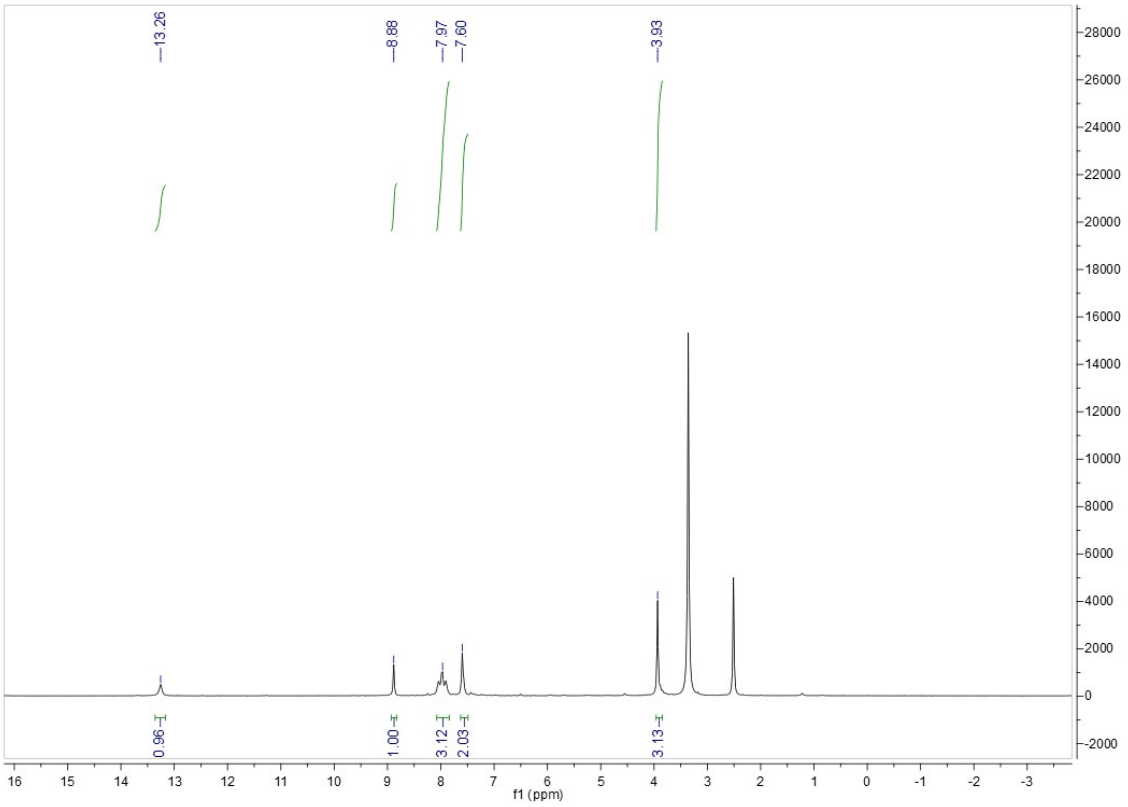

Fig. S2-66. ^{1}H NMR of compound 3c$_5$

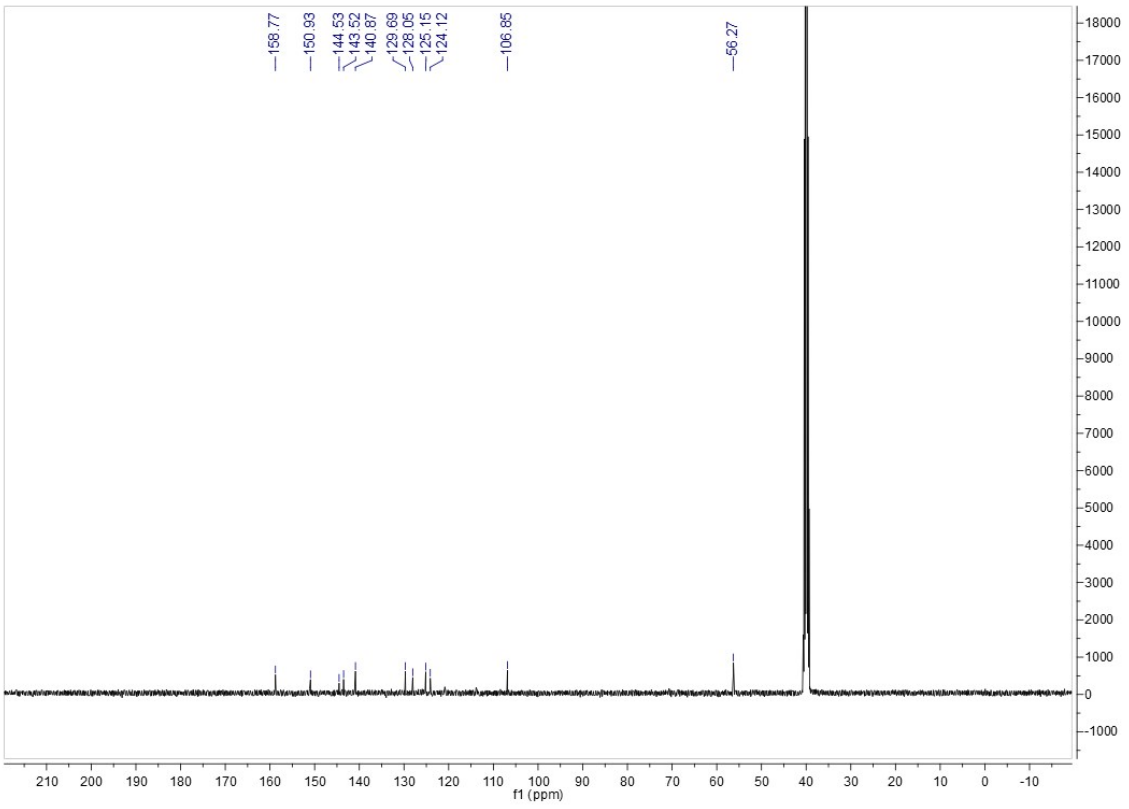

Fig. S2-67. ^{13}C NMR of compound $3c_5$

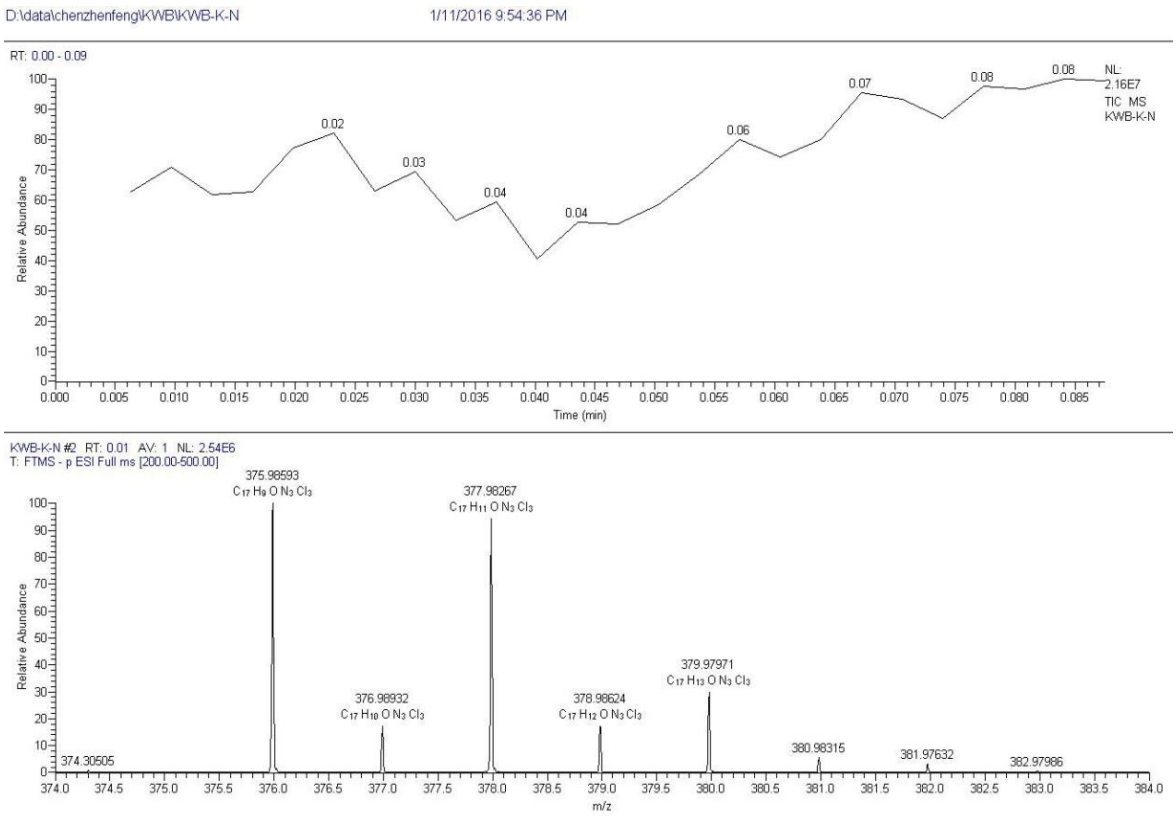

Fig. S2-68. ESI-HRMS of compound $3c_5$

3c$_6$: Yield, 65.1%; ^{1}H NMR (400 MHz, DMSO-d$_6$) δ 12.68 (s, 1H, NH), 9.10 (s, 1H, HC=C), 7.75 (s, 1H, H-Ar), 7.66 (s, 1H, H-Ar), 7.52 (s, 1H, H-Ar), 7.39 (d, J = 9.0 Hz, 1H, H-Ar), 7.29 (s, 1H, H-Ar), 7.22 (s, 1H, H-Ar), 7.20 (s, 1H, H-Ar), 3.84 (s, 3H, -OCH$_3$); ^{13}C NMR (101 MHz, DMSO-d$_6$) δ 160.79, 155.14, 148.34, 143.27, 139.05, 134.88, 133.84, 122.73, 122.36, 121.76, 120.64, 120.25, 118.77, 117.06, 113.27, 110.27, 56.00; ESI-HRMS, calculated *m/z* for $C_{17}H_{12}ClN_3O$ $[M+H]^+$: 310.0747, found: 310.0741.

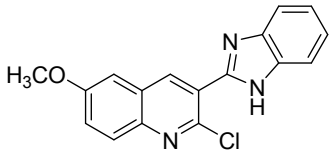

Fig. S2-69. Chemical structure of compound 3c$_6$

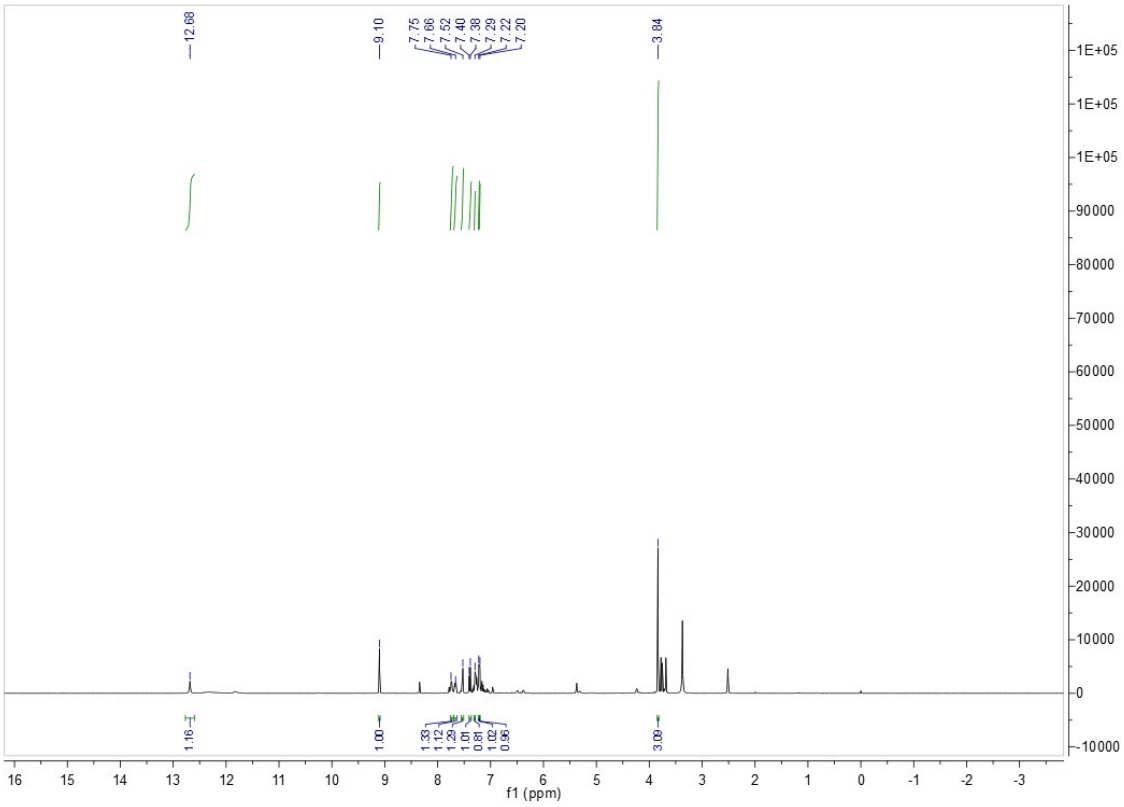

Fig. S2-70. ^{1}H NMR of compound 3c$_6$

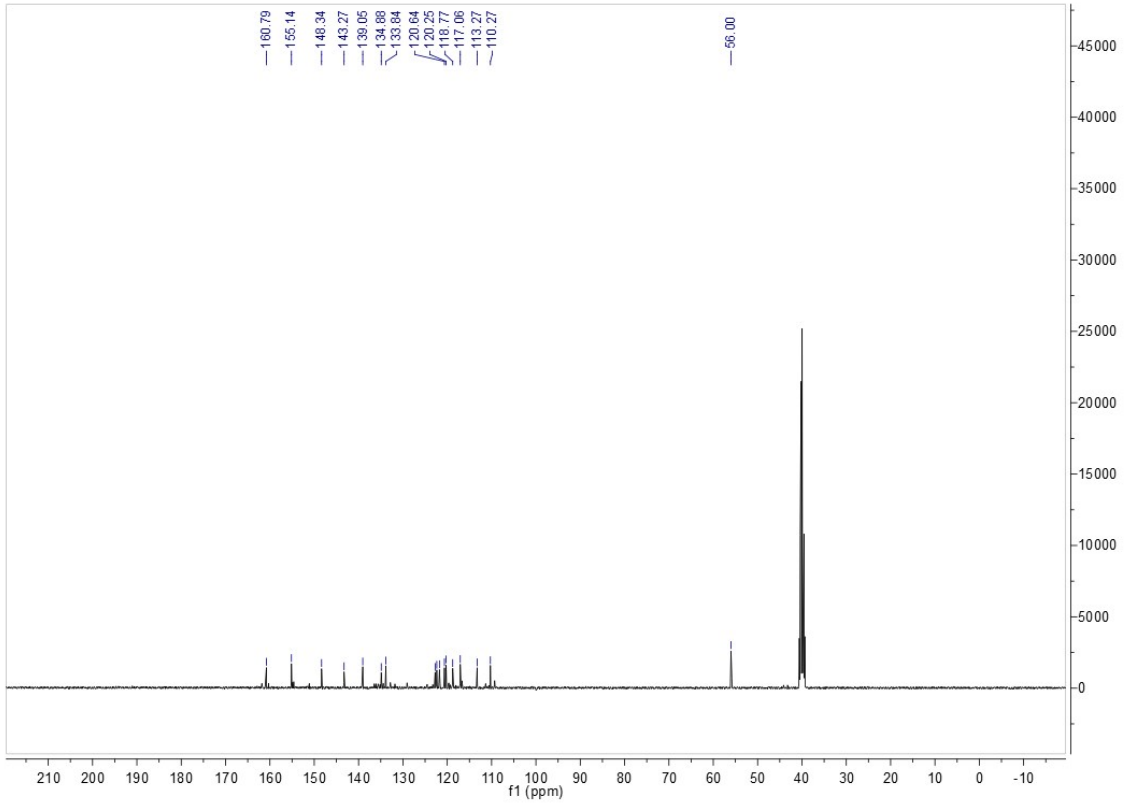

Fig. S2-71. ^{13}C NMR of compound 3c$_6$

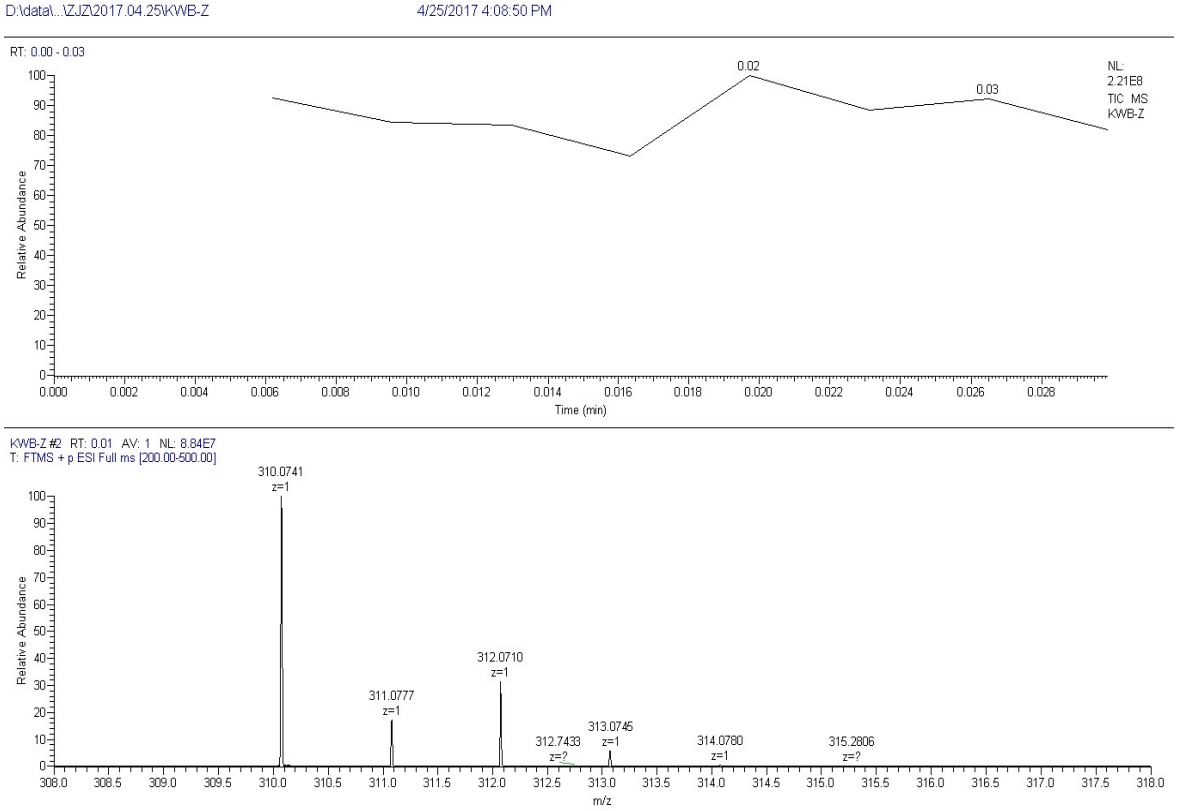

Fig. S2-72. ESI-HRMS of compound 3c$_6$

3d$_1$: Yield, 64.5%; ^{1}H NMR (400 MHz, DMSO-d$_6$) δ 12.59 (s, 1H, NH), 8.75 (s, 1H, HC=C), 7.54 (s, 1H, H-Ar), 7.42 (s, 3H, H-Ar), 6.29 (s, 2H, O-CH$_2$-O), 2.34 (s, 6H, -CH$_3$); ^{13}C NMR (101 MHz, DMSO-d$_6$) δ 152.93, 149.06, 147.43, 145.92, 145.06, 140.02, 124.16, 122.81, 104.52, 103.46, 103.22, 20.54; ESI-HRMS, calculated *m/z* for $C_{19}H_{14}ClN_3O_2$ $[M+H]^+$: 352.0853, found: 352.0880.

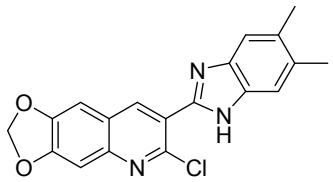

Fig. S2-73. Chemical structure of compound 3d$_1$

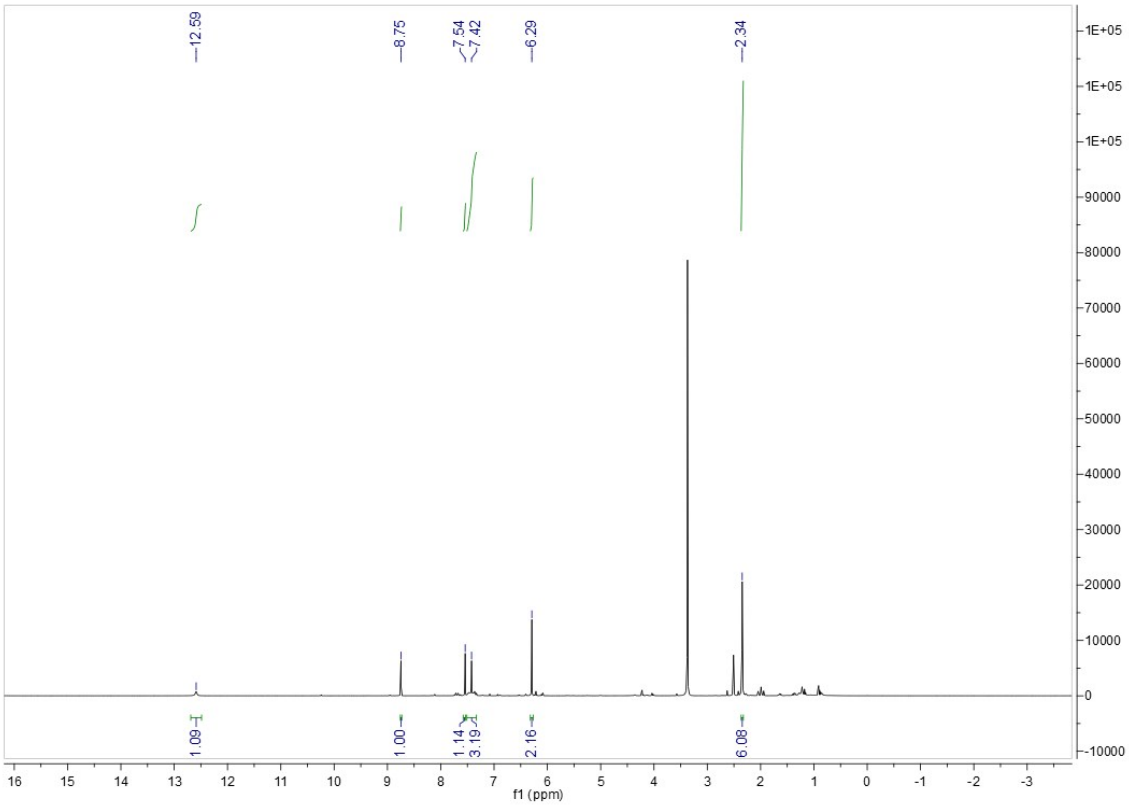

Fig. S2-74. ^{1}H NMR of compound 3d$_1$

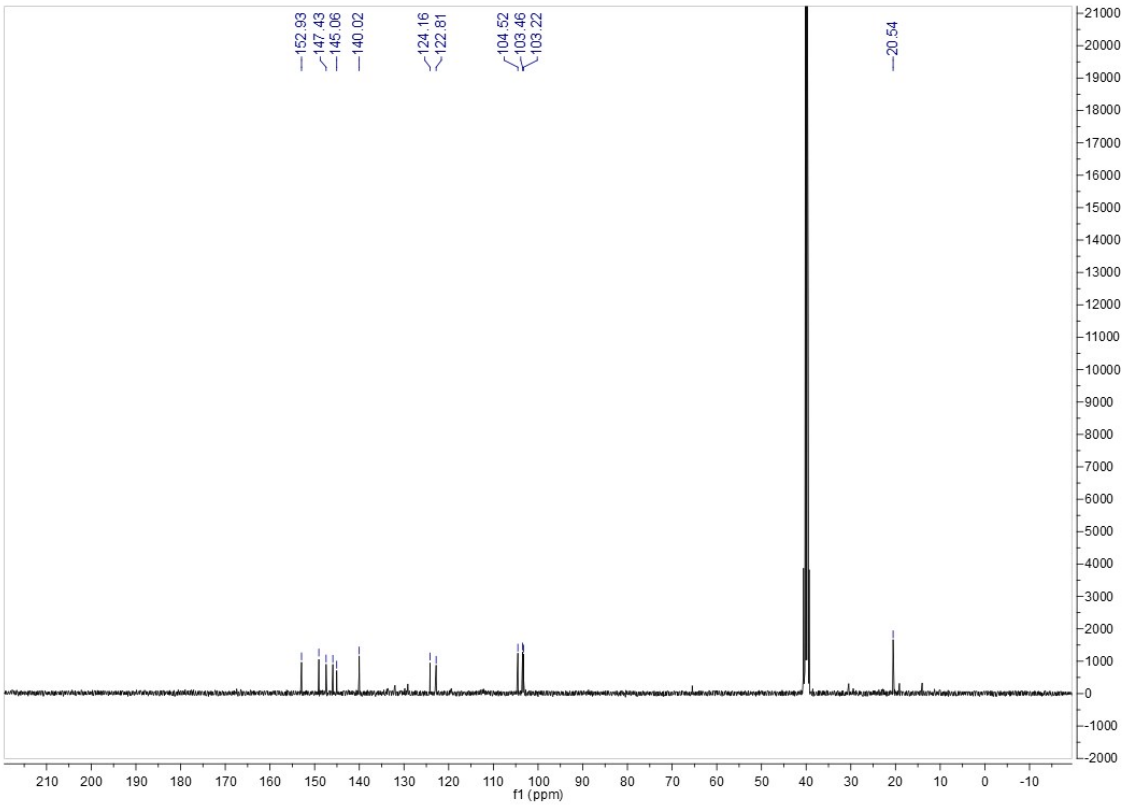

Fig. S2-75. ^{13}C NMR of compound 3d$_1$

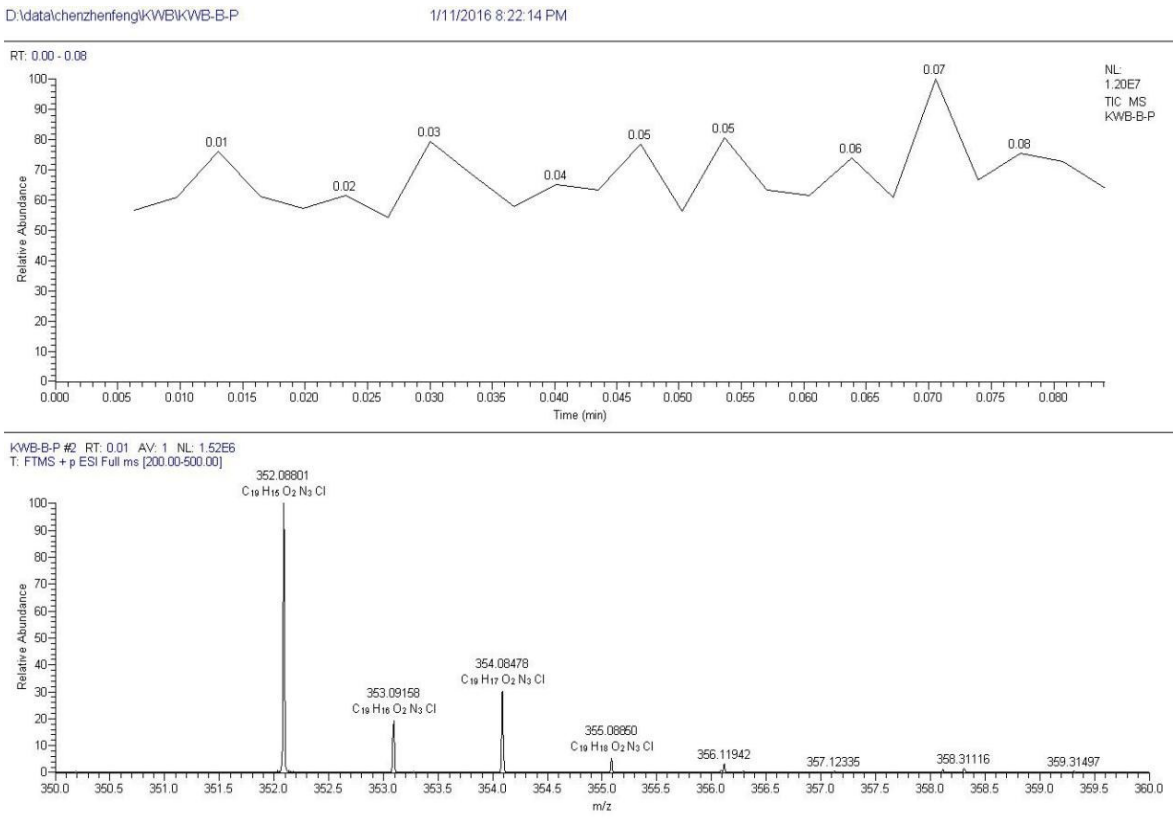

Fig. S2-76. ESI-HRMS of compound 3d$_1$

$3d_2$: Yield, 58.9%; ^{1}H NMR (500 MHz, DMSO-d_6) δ 12.96 (s, 1H, NH), 8.77 (s, 1H, HC=C), 7.68 (s, 1H, H-Ar), 7.54 (s, 1H, H-Ar), 7.47 (s, 1H, H-Ar), 7.43 (s, 1H, H-Ar), 7.14 (s, 1H, H-Ar), 6.30 (s, 2H, O-CH_2-O); ^{13}C NMR (126 MHz, DMSO-d_6) δ 153.14, 149.15, 146.17, 144.91, 140.25, 124.12, 122.24, 104.55, 103.52, 103.28, 100.00; ESI-HRMS, calculated *m/z* for $C_{17}H_9ClFN_3O_2$ $[M+H]^+$: 342.0446, found: 342.0429.

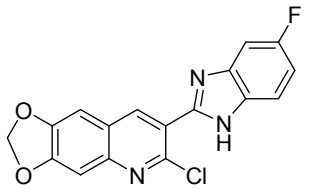

Fig. S2-77. Chemical structure of compound $3d_2$

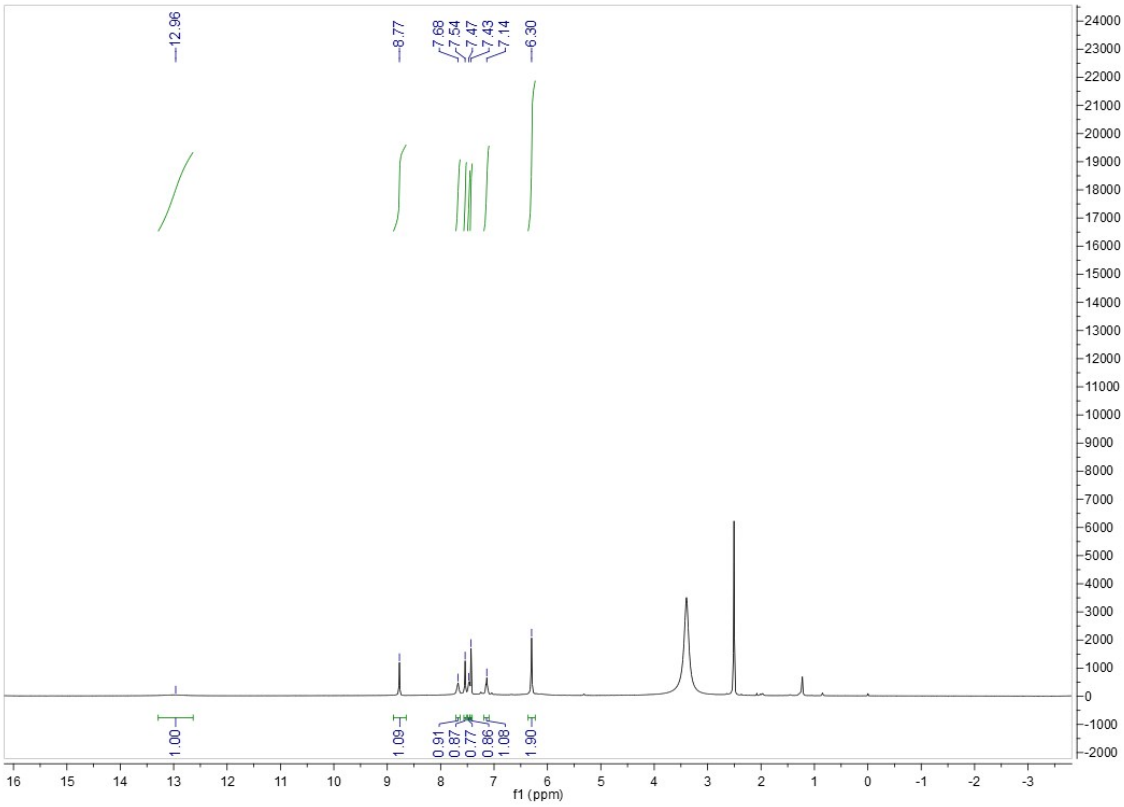

Fig. S2-78. ^{1}H NMR of compound $3d_2$

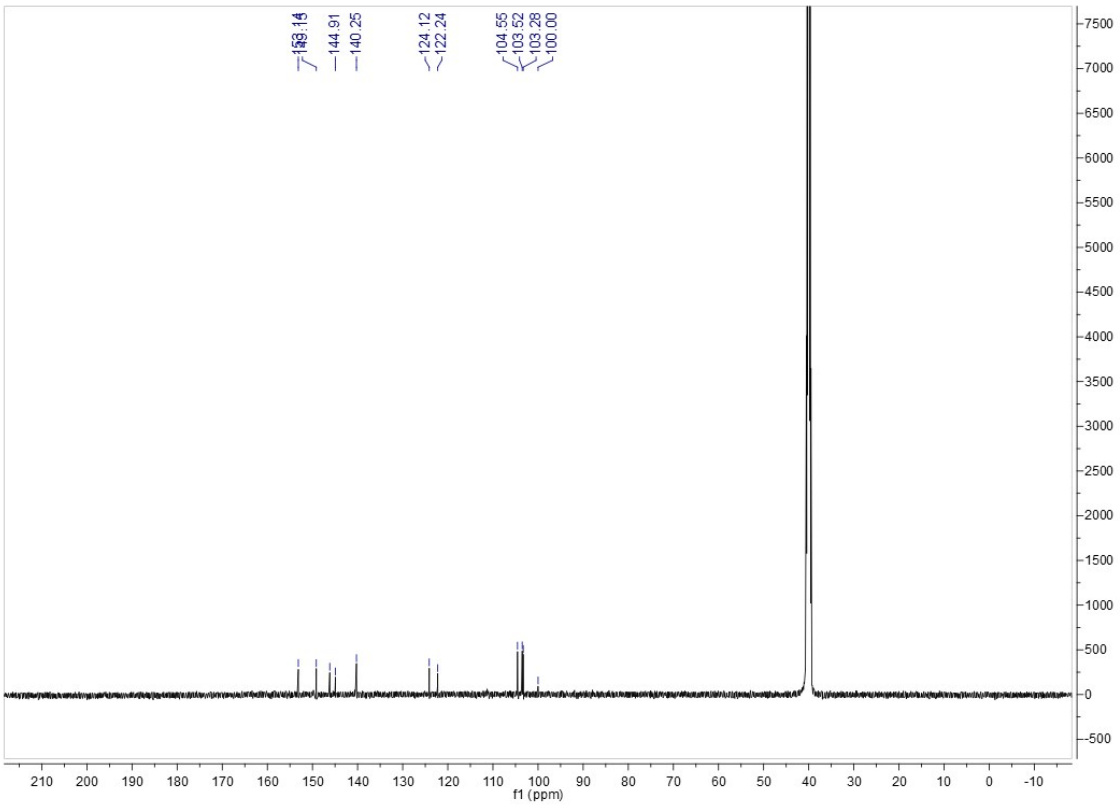

Fig. S2-79. ^{13}C NMR of compound $3d_2$

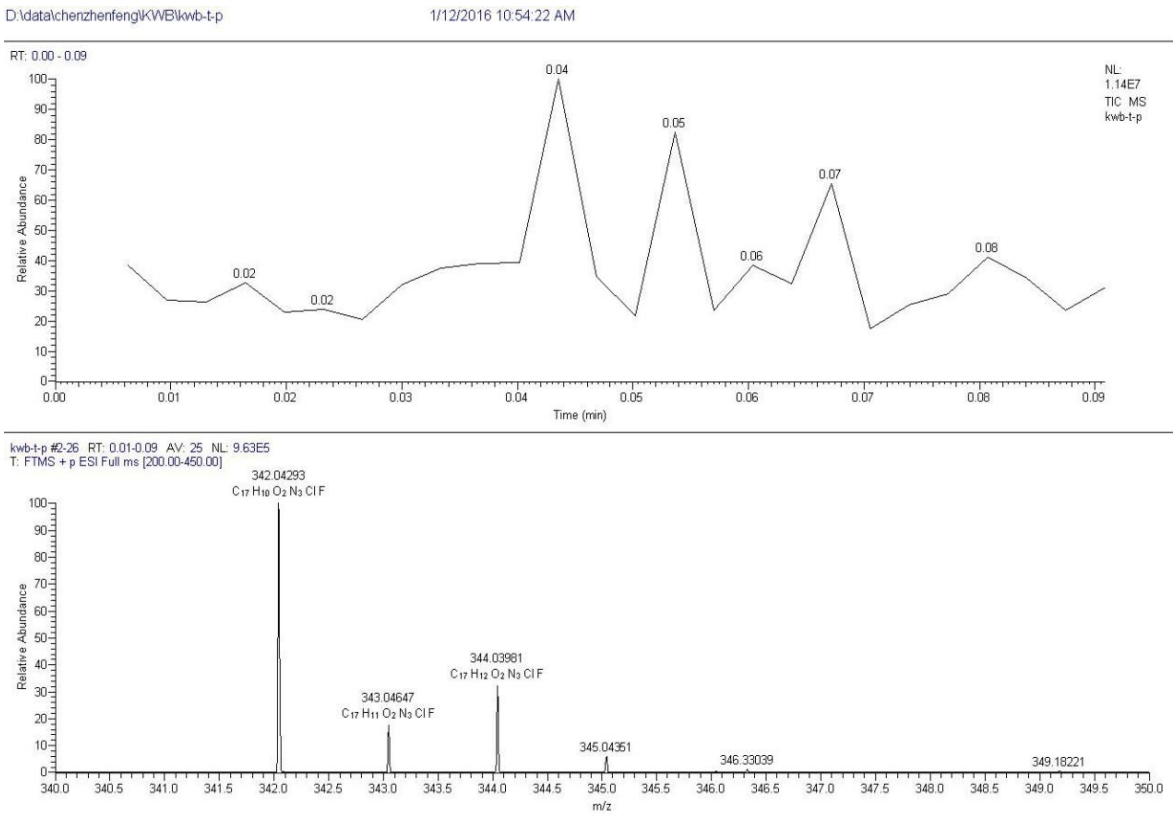

Fig. S2-80. ESI-HRMS of compound $3d_2$

3d$_3$: Yield, 59.1%; ^{1}H NMR (400 MHz, DMSO-d$_6$) δ 13.05 (s, 1H, NH), 8.79 (s, 1H, HC=C), 7.78 (s, 1H, H-Ar), 7.65 (s, 1H, H-Ar), 7.56 (s, 1H, H-Ar), 7.44 (s, 1H, H-Ar), 7.30 (d, J = 8.1 Hz, 1H, H-Ar), 6.30 (s, 2H, O-CH$_2$-O); ^{13}C NMR (101 MHz, DMSO-d$_6$) δ 153.22, 149.19, 146.25, 144.87, 140.40, 124.12, 122.08, 104.57, 103.54, 103.32; ESI-HRMS, calculated *m/z* for $C_{17}H_9Cl_2N_3O_2$ $[M-H]^-$: 355.9994, found: 355.9999.

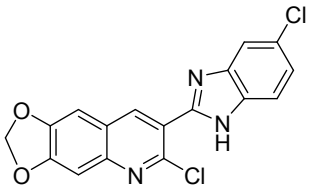

Fig. S2-81. Chemical structure of compound 3d$_3$

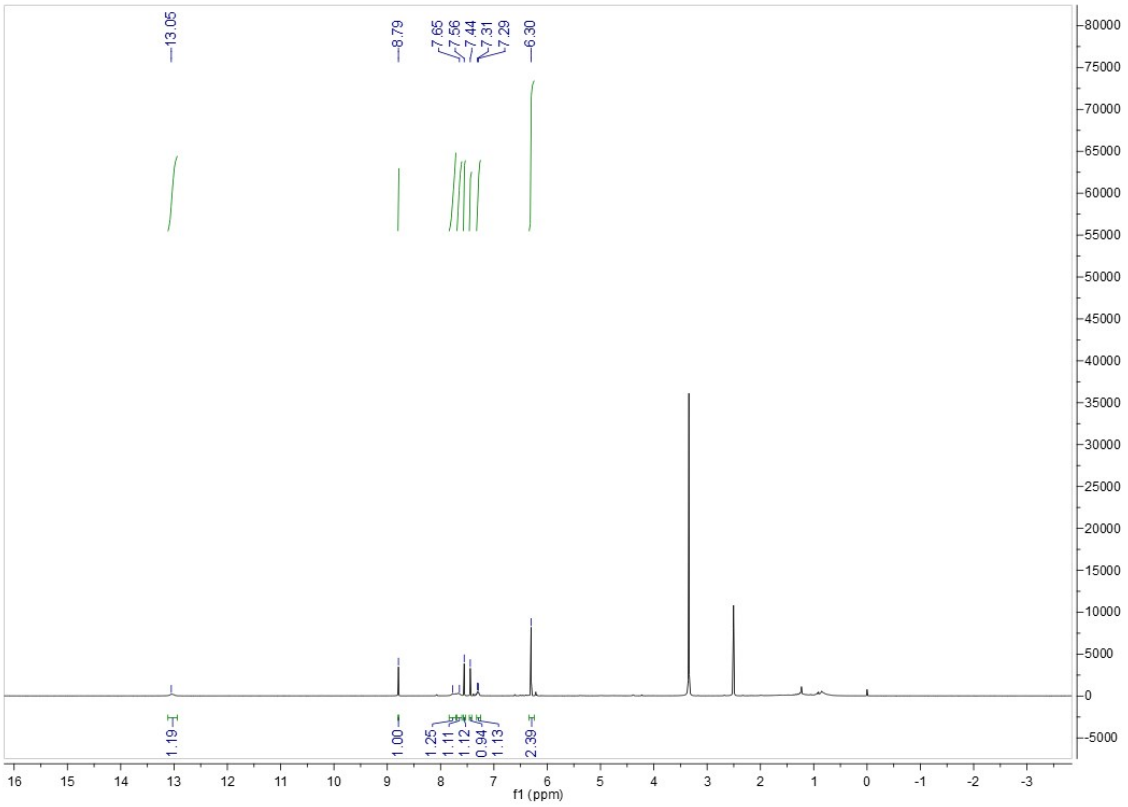

Fig. S2-82. ^{1}H NMR of compound 3d$_3$

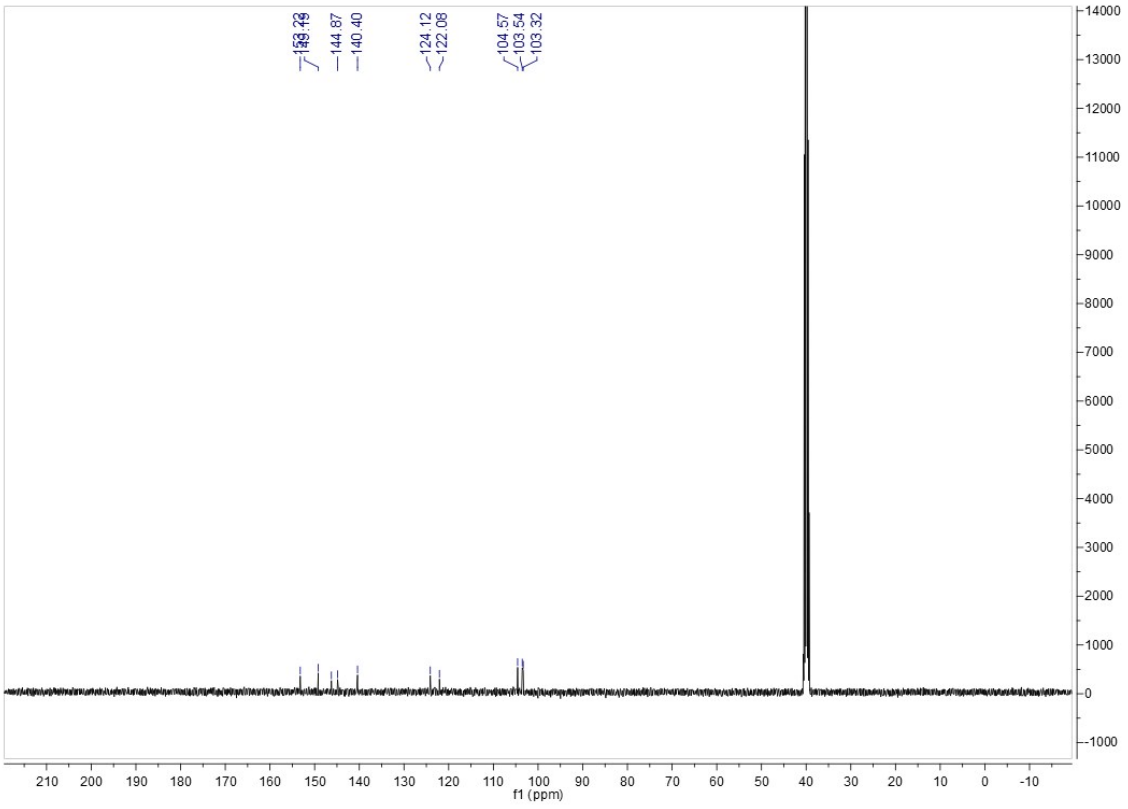

Fig. S2-83. ^{13}C NMR of compound $3d_3$

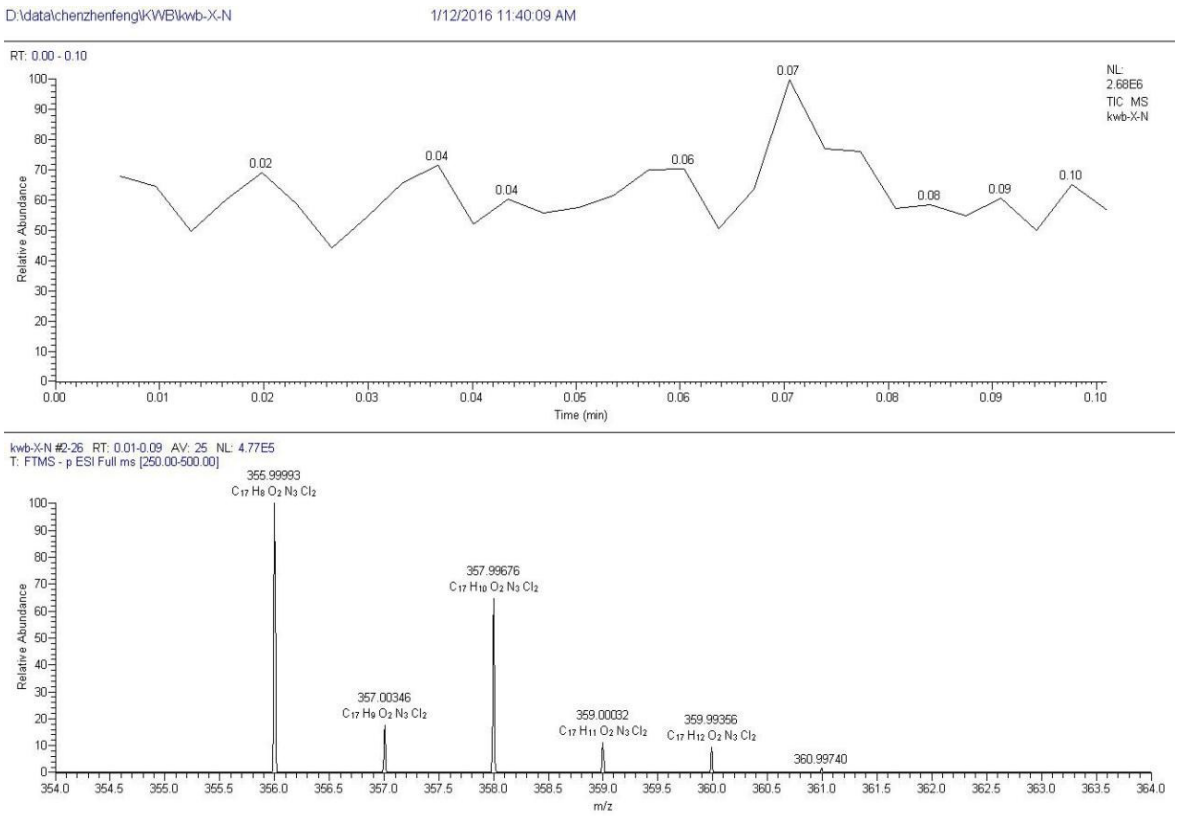

Fig. S2-84. ESI-HRMS of compound $3d_3$

3d$_4$: Yield, 68.6%; ^{1}H NMR (400 MHz, DMSO-d$_6$) δ 13.04 (s, 1H, NH), 8.79 (s, 1H, HC=C), 7.87 (s, 1H, H-Ar), 7.64 (s, 1H, H-Ar), 7.55 (s, 1H, H-Ar), 7.44 (s, 1H, H-Ar), 7.41 (d, J = 8.6 Hz, 1H, H-Ar), 6.30 (s, 2H, O-CH$_2$-O); ^{13}C NMR (101 MHz, DMSO-d$_6$) δ 153.22, 149.18, 146.25, 144.86, 140.40, 124.11, 122.04, 104.57, 103.54, 103.31; ESI-HRMS, calculated *m/z* for $C_{17}H_9BrClN_3O_2$ $[M-H]^-$: 399.9489, found: 399.9508.

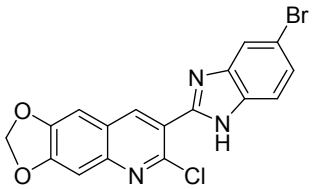

Fig. S2-85. Chemical structure of compound 3d$_4$

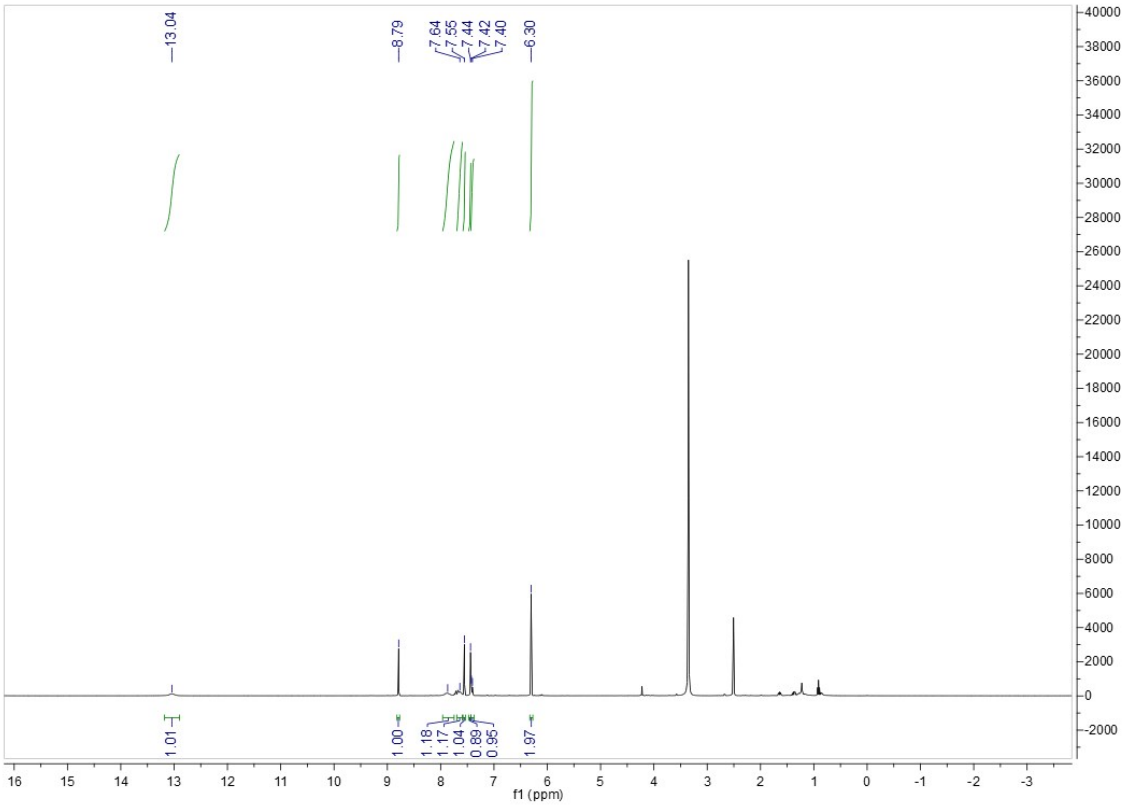

Fig. S2-86. ^{1}H NMR of compound 3d$_4$

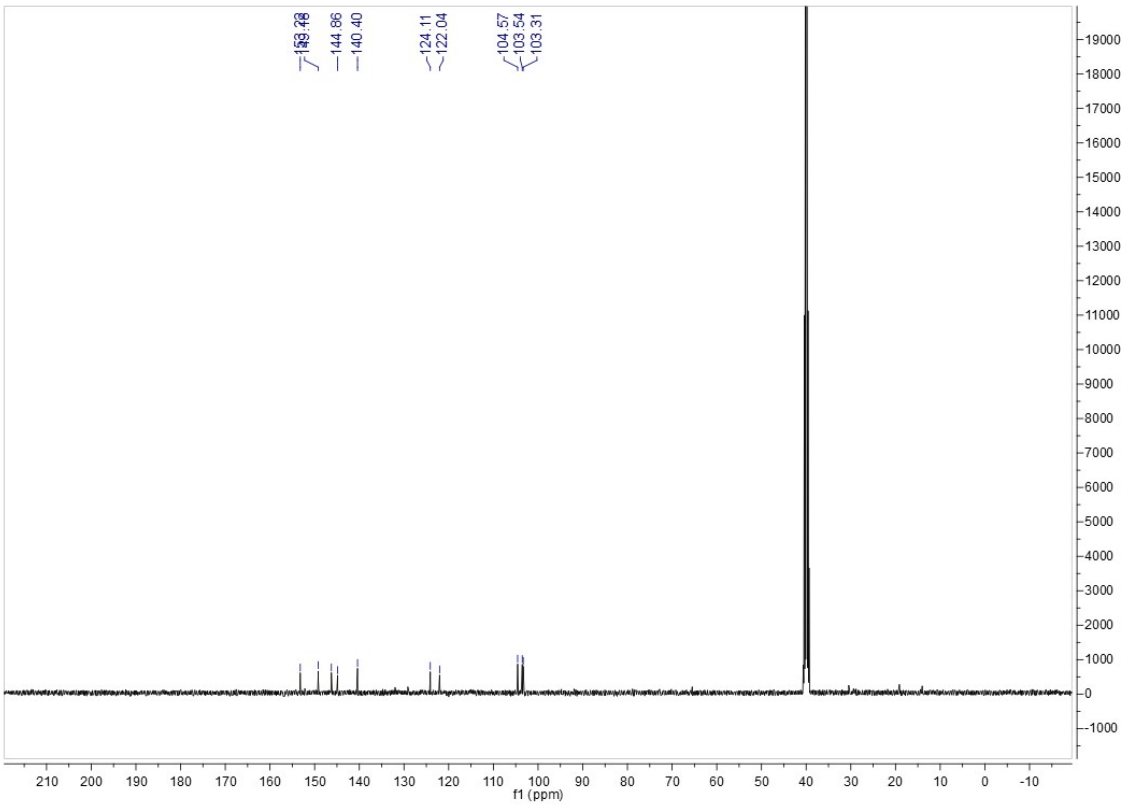

Fig. S2-87. ^{13}C NMR of compound $3d_4$

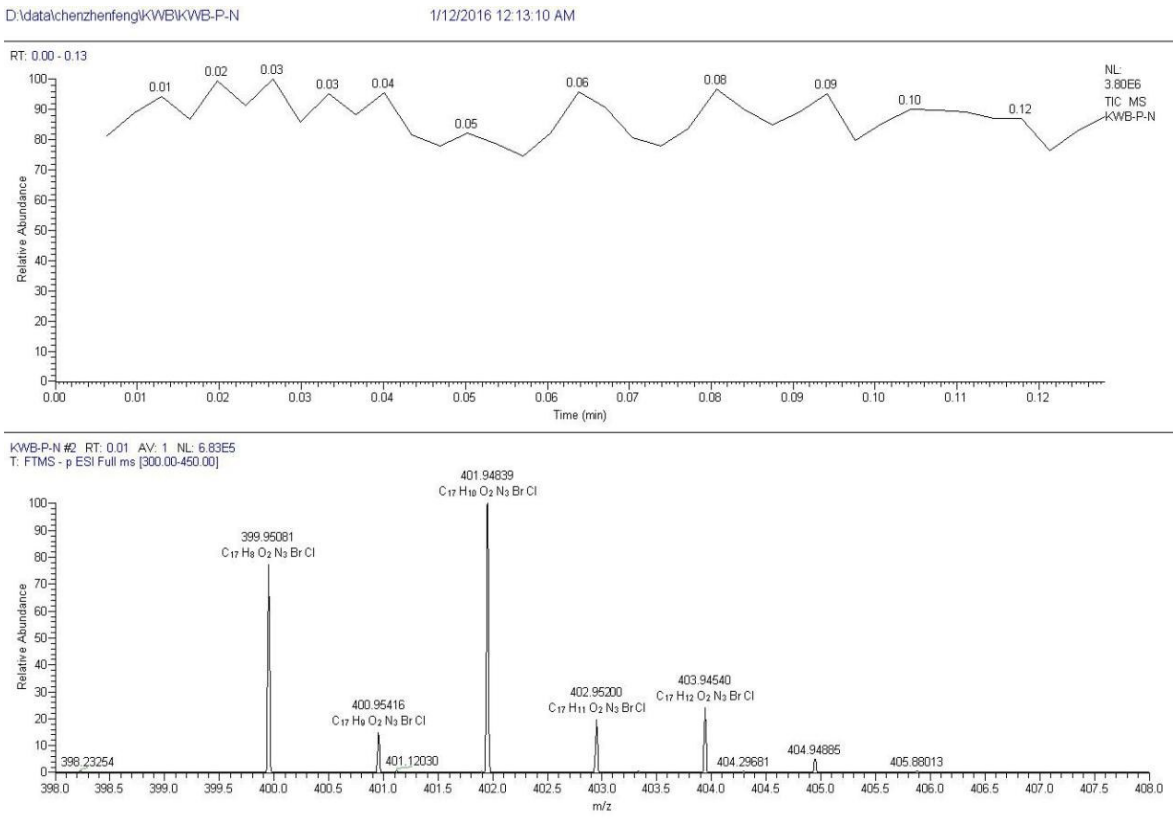

Fig. S2-88. ESI-HRMS of compound $3d_4$

3d$_5$: Yield, 60.5%; ^{1}H NMR (500 MHz, DMSO-d$_6$) δ 13.15 (s, 1H, NH), 8.79 (s, 1H, HC=C), 7.96 (s, 2H, H-Ar), 7.56 (s, 1H, H-Ar), 7.44 (s, 1H, H-Ar), 6.30 (s, 2H, O-CH$_2$-O); ^{13}C NMR (126 MHz, DMSO-d$_6$) δ 153.32, 151.05, 149.23, 146.38, 144.79, 140.46, 131.96, 129.12, 124.07, 121.69, 104.58, 103.57, 103.33; ESI-HRMS, calculated *m/z* for $C_{17}H_8Cl_3N_3O_2$ $[M-H]^-$: 389.9604, found: 389.9649.

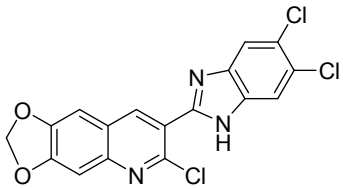

Fig. S2-89. Chemical structure of compound 3d$_5$

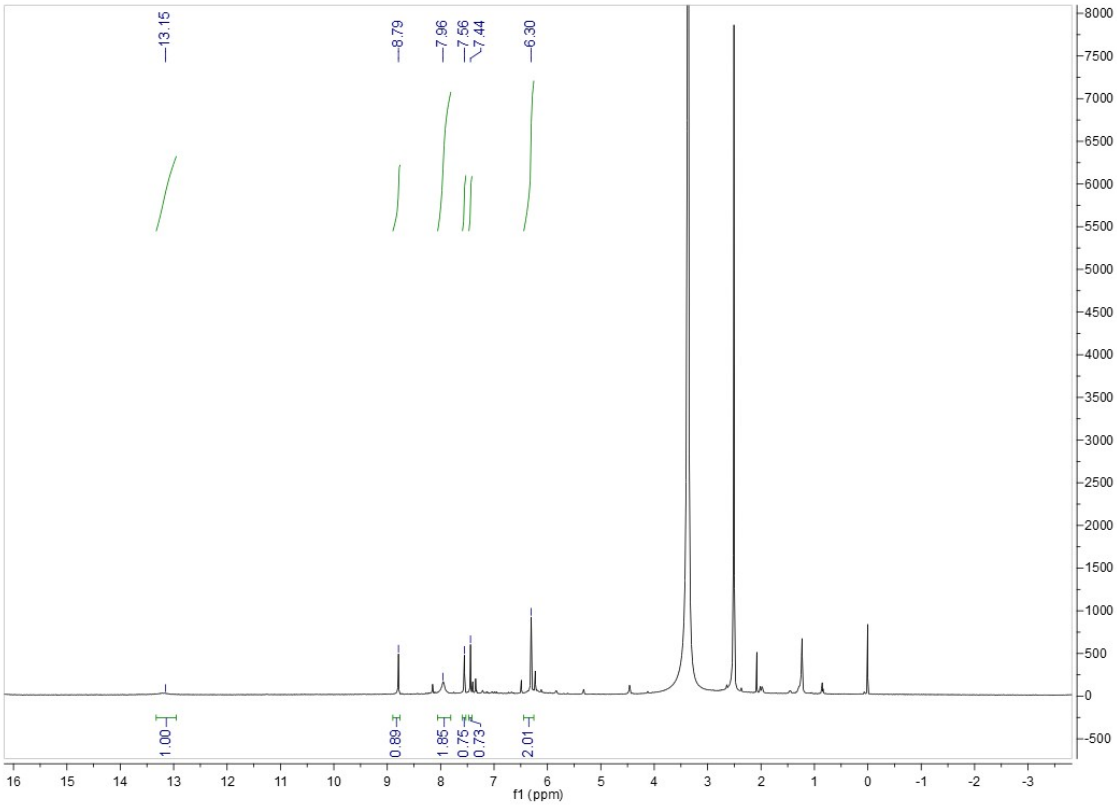

Fig. S2-90. ^{1}H NMR of compound 3d$_5$

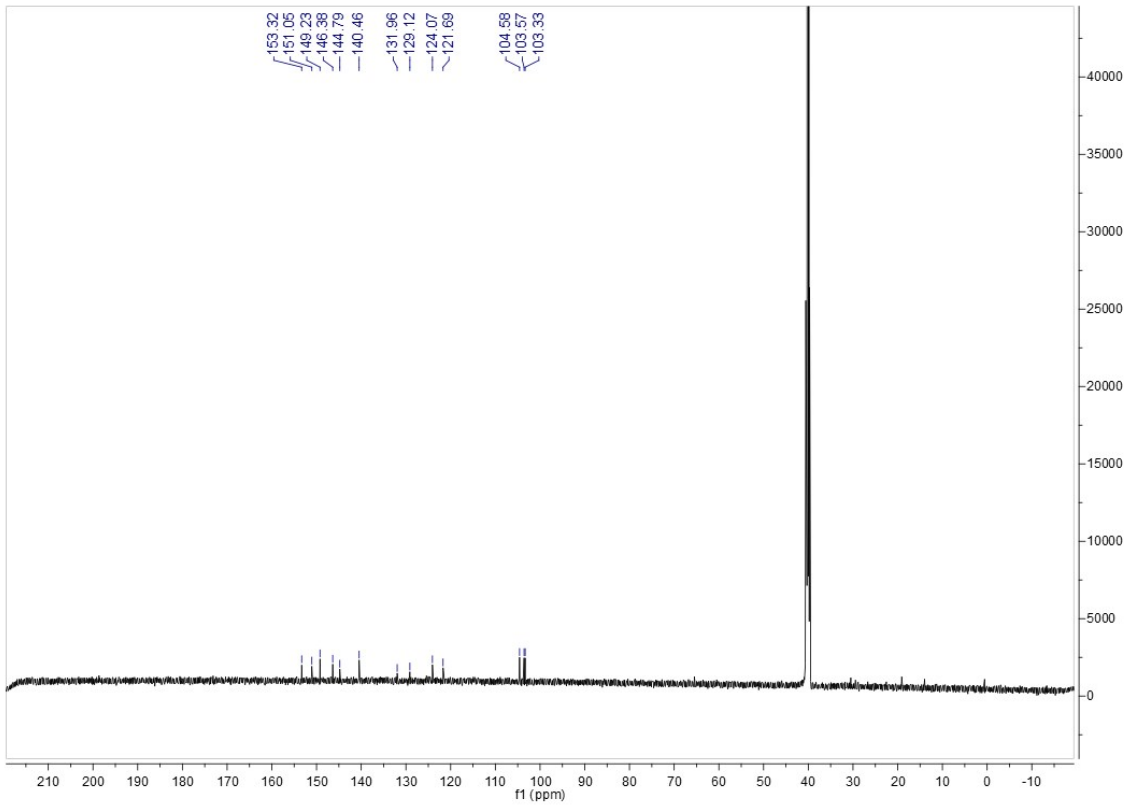

Fig. S2-91. ^{13}C NMR of compound 3d$_5$

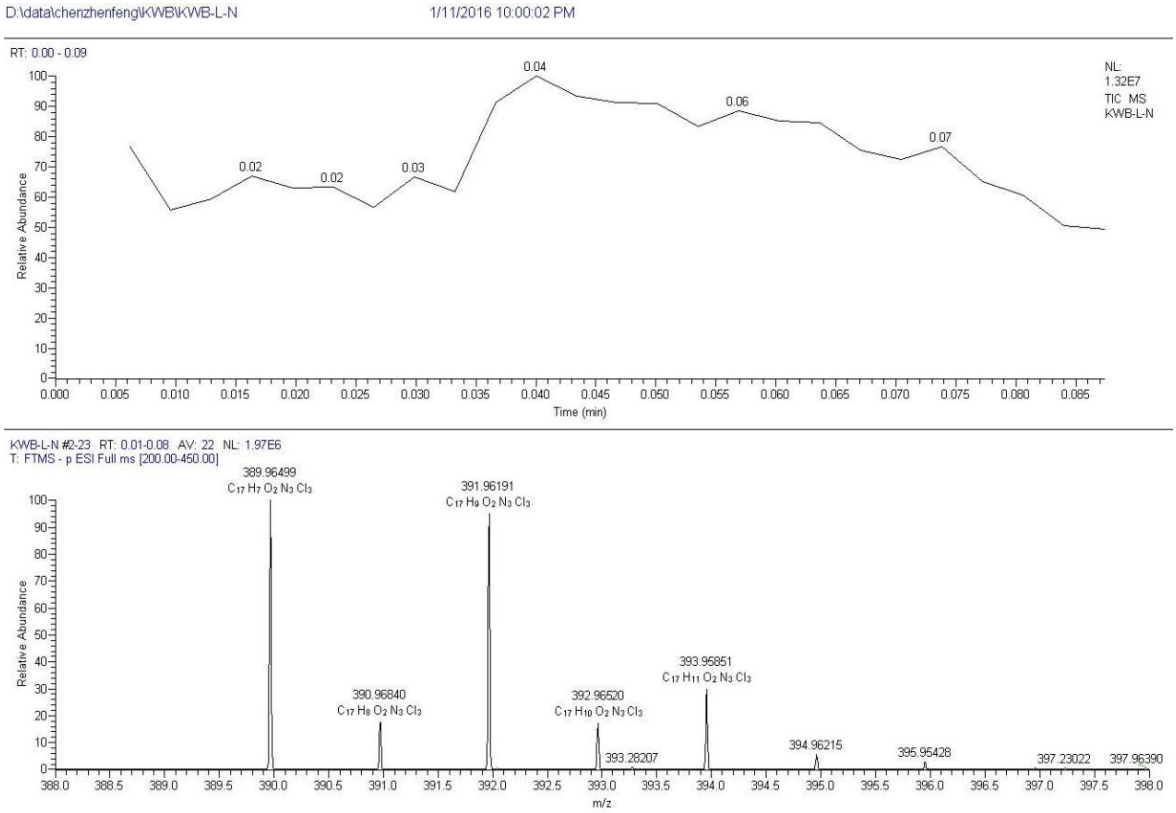

Fig. S2-92. ESI-HRMS of compound 3d$_5$

3d$_6$: Yield, 62.2%; ^{1}H NMR (400 MHz, DMSO-d$_6$) δ 12.96 (s, 1H, NH), 8.78 (s, 1H, HC=C), 7.67 (s, 2H, H-Ar), 7.55 (s, 1H, H-Ar), 7.44 (s, 1H, H-Ar), 7.27 (s, 2H, H-Ar), 6.30 (s, 2H, O-CH$_2$-O); ^{13}C NMR (101 MHz, DMSO-d$_6$) δ 153.07, 149.12, 148.42, 146.10, 145.04, 140.27, 124.14, 122.89, 122.55, 104.55, 103.50, 103.27; ESI-HRMS, calculated *m/z* for $C_{17}H_{10}ClN_3O_2$ $[M+H]^+$: 324.0540, found: 324.0532.

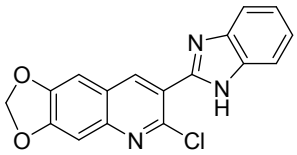

Fig. S2-93. Chemical structure of compound 3d$_6$

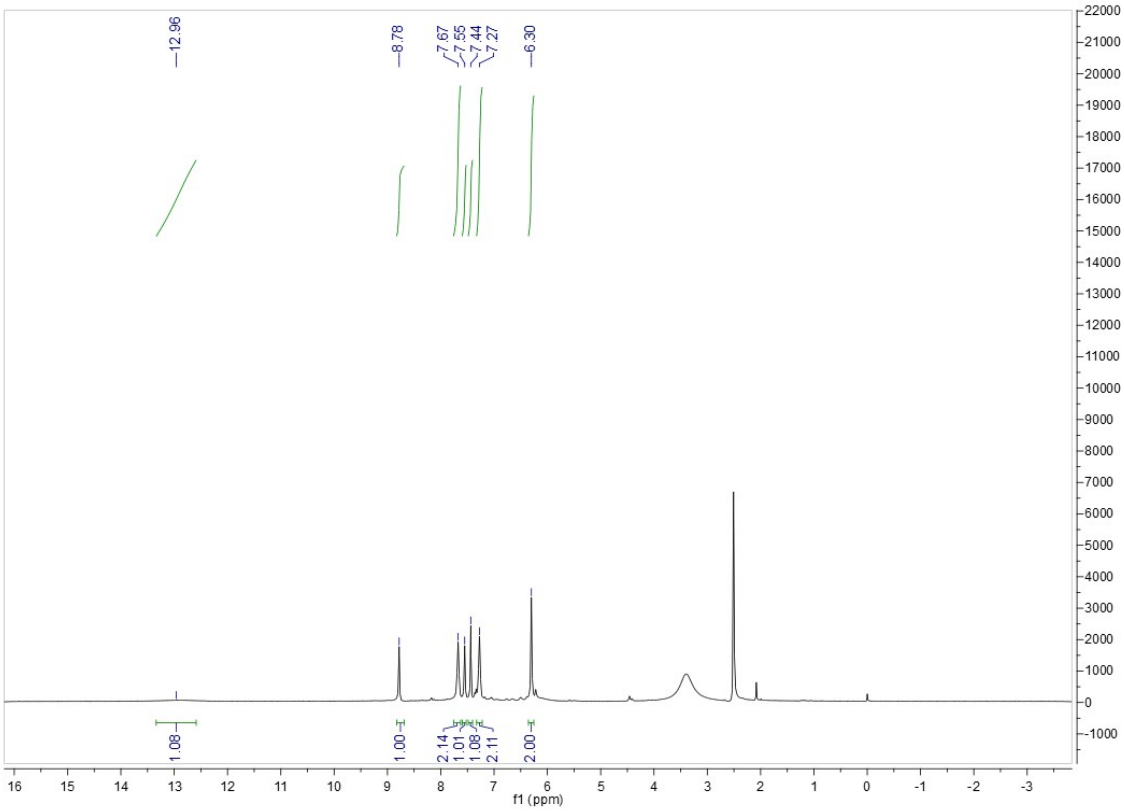

Fig. S2-94. ^{1}H NMR of compound 3d$_6$

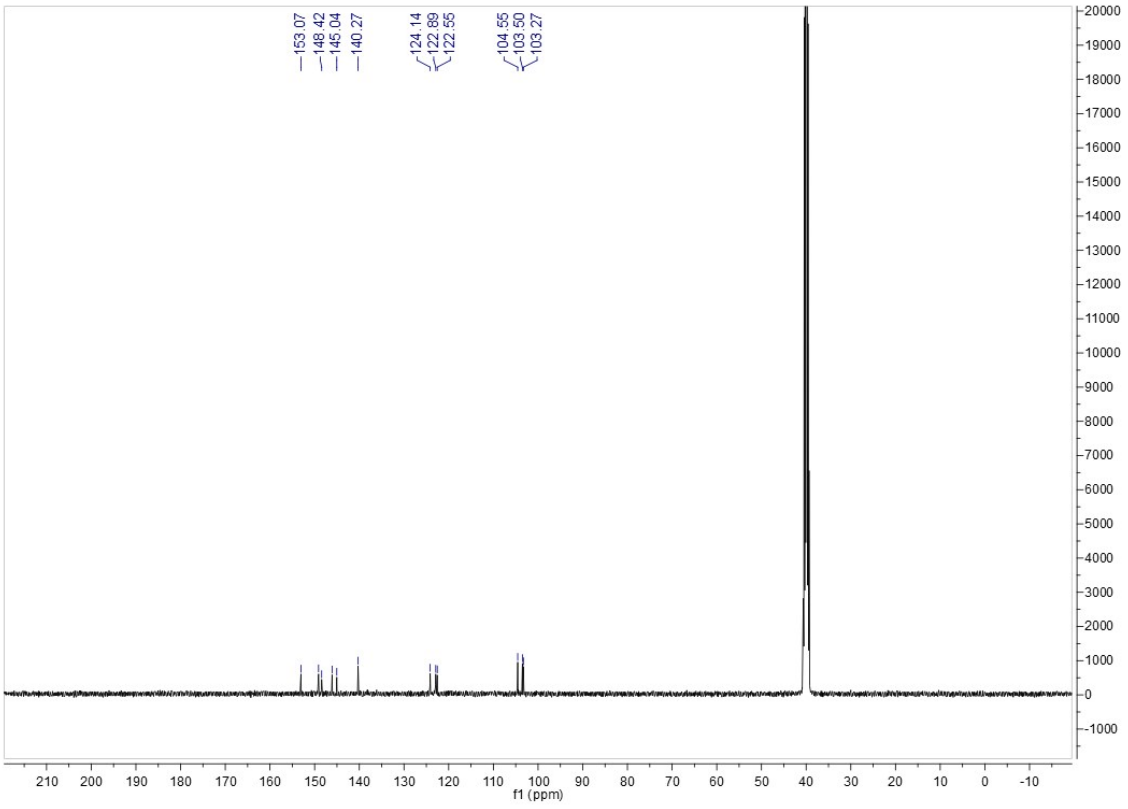

Fig. S2-95. ^{13}C NMR of compound 3d$_6$

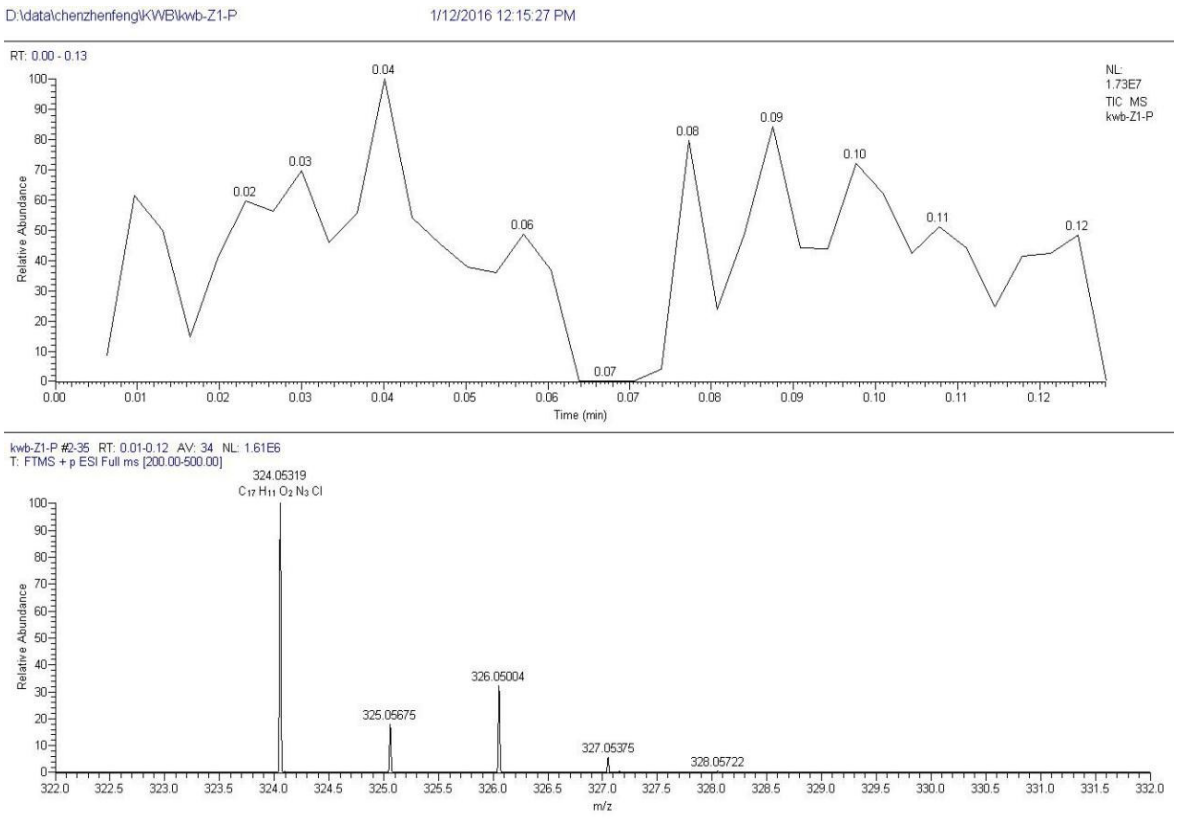

Fig. S2-96. ESI-HRMS of compound 3d$_6$